STUDY of DUALITY IN BOND GRAPH MODELS. APPLICATION TO CONTROL LAW SYNTHESIS

Stefan Lichiardopol

ÉCOLE CENTRALE DE LILLE

Année : 2007 N^0 d'ordre : 54

THÈSE

présentée en vue d'obtenir le grade de

DOCTEUR

en

Spécialité: AUTOMATIQUE ET INFORMATIQUE INDUSTRIELLE

par

Stefan LICHIARDOPOL

DOCTORAT DELIVRE EN COTUTELLE
PAR L'ECOLE CENTRALE DE LILLE ET
L'UNIVERSITÉ "POLITEHNICA" DE BUCAREST

ÉTUDE DE LA DUALITÉ DES MODÈLES BOND GRAPHS. APPLICATION À LA COMMANDE

Soutenue le 23.10.2007 devant le jury d'examen:

M. Joachim Rudolph	Rapporteur	Privatdozent à la TU Dresden Institut für Regelungs- und Steuerungstheorie (RST)
M. Wilfrid Marquis-Favre	Rapporteur	Maitre de Conférerences à l'INSA de Lyon Laboratiore Ampère
Mme. Geneviève Dauphin-Tanguy	Examinateur	Professeur à l'École Centrale de Lille, LAGIS
M. Bogdan Dumitrescu	Examinateur	Professeur à l'Université "Politehnica" de Bucarest, Faculte d'Automatique et des Ordinateurs
M. Nicolas Venuti	Invité	PDG Virtual Dynamics
M. Dumitru POPESCU	Directeur de thèse	Professeur à l'Université "Politehnica" de Bucarest, Faculte d'Automatique et des Ordinateurs
M. Christophe SUEUR	Directeur de thèse	Professeur à l'École Centrale de Lille, LAGIS

Thèse préparée au Laboratoire d'Automatique, de Génie Informatique et Signal, LAGIS, UMR 8146 - École Centrale de Lille

Acknowledgements

This has been an exciting and intense project. During the last three years, I have had the opportunity to work together with some brilliant people who have graciously shared their precious time to introduce me to the world of bond graphs.

My two PhD promotors, Mr. C. Sueur and Mr. D. Popescu provided a sustainable support during the three years of research. The research time, I have spent in France at Ecole Centrale de Lille, has been particularly fruitful. The multitude of questions we have raised during our discussions with Mr. Sueur has provided the road map for this report.

Mr. J. Rudolph and Mr. W. Marquis-Favre reviewed this PhD report before publication and helped me shape the final version of this report. The long discussions we have had helped me refine the more delicate issues and present them from a more comprehensive perspective.

Mr. B. Dumitrescu, who beside Mr. C. Popeea opened my horizons towards research, also accepted to take part in the jury of the PhD defense. If it was not for that first research stage at the Technical University of Tampere, I would probably not have chosen this path.

I also would like to express my reconnaissance to Mrs. G. Dauphin-Tanguy who beside M. Popescu made possible the existence of this joint PhD degree between "Politehnica" University of Bucharest and Ecole Centrale de Lille. During the three years, I have studied at Ecole Centrale de Lille, she was always close to us and gave us strength and showed tons of enthusiasm for our research. Beside the humane touch, she put into our relation, made us forget that we lived away from our families.

For the "Accueil à la française", I would like to thank Marie-Fraçoise, Brigitte and Christine as well as Monique and Virginie who helped us with the administrative matters. I am also grateful to all my PhD students colleagues:

Catalin C., Christophe N., Chafik, Zackaria, Hicham and Farid.
All my gratitude goes to Ms. H. Catsiapis who showed us over three years of discussions the French culture. She made possible all those interesting and unforgettable voyages to Paris, Loire Valley, Versailles, Mont St. Michel and Champagne. My knowledge and interest in the French culture is greatly her work, with her enthusiasm she managed to open our appetite for art, history and cuisine/wine.
In the end, I would like to thank my family, especially my wife, Anca, who was beside me in this quest and who supported me. Also, I am indebted to my family who from Romania provided the link to my roots and kept a close contact during these three years.

Etude de la dualité des modèles bond graphs. Application à la commande

La clé de voute de ce travail de recherche est l'étude de la propriété de dualité. Cette notion a émergé comme concept philosophique et la plupart des systèmes philosophiques et spirituels l'ont adopté. C'est vrai qu'on ne retrouve pas la dualité " homme-femme " ou " bien-mal " ou encore " matériel-spirituel " dans l'automatique, mais différents types de dualité peuvent être définis à partir des concepts mathématiques et pas seulement.

Le concept de dualité a été défini d'un point de vue mathématique et beaucoup de recherches ont été menées en utilisant comme représentation mathématique, pour un système physique, la représentation d'état ou la représentation par un module. L'étude des systèmes dynamiques, en particulier l'étude de lois de commande, est au cœur de notre travail de recherche. Dans ce contexte, notre démarche essaie de développer le concept de dualité à travers les propriétés des systèmes dynamiques et les lois de commande associées en utilisant une approche graphique. Les deux représentations graphiques utilisées dans ce rapport sont les modèles bond graphs et les systèmes structurés. Ces outils, historiquement utilisés comme moyens de modélisation et d'analyse sont aussi employées ici comme outils pour la génération de lois de commande. Cette recherche répond aux besoins des industriels qui exploitent des machines de plus en plus performantes. Les approches proposées exigent une connaissance précise des phénomènes physiques mis en jeu dans ces processus et la possibilité d'adaptabilité à des situations différentes.

L'automatique est une discipline qui regroupe de nombreuses activités, comme la modélisation des systèmes dynamiques, l'analyse des modèles et

la conception des lois de commande. Ce travail de recherche est focalisé sur l'étude d'un point vue graphique de la dualité au niveau de l'analyse et de la conception de lois de commande sur des modèles linéaires, à paramètres invariants ou variables dans le temps, et des extensions pour des modèles non linéaires.

La première étape du notre travail a été de définir d'un point de vue graphique le concept de model dual. En utilisant la définition mathématique proposée par Kalman dans la représentation d'état et généralisée pour des systèmes linéaires à paramètres variant dans le temps (LTV) par van der Schaft (où le modèle dual est appelé " adjoint model "[58]) et la définition introduite par Rudolf en 1996 en utilisant la théorie des modules [50], nous avons reformulé ce concept de model dual pour les modèles bond graphs et les systèmes structurés. Si pour les systèmes structurés la démarche pour obtenir le model dual est très simple, car le lien entre un système structuré et la représentation d'état est évidente, pour les modèles bond graphs la technique d'obtention du model dual est plus complexe. Le modèle bond graph dual est obtenu en trois étapes : transformations graphiques au niveau du model bond graph, inversion du signe des signaux de sortie et changement de variable pour le vecteur d'état. Ces transformations restent néanmoins élémentaires, aussi bien d'un point de vue graphique que mathématique. De plus, contrairement à un modèle d'état quelconque, pour lequel les variables du modèle dual n'ont pas de sens physique, pour un modèle bond graph, les variables du modèle dual sont les variables de co-énergie, c'est à dire des variables d'effort et de flux. De plus, les notions de chemin causal et de boucle causale sont les mêmes pour le bond graph dual, mais pour prendre en compte la modification du vecteur état, de nouvelles procédures de calcul des gains des chemins et boucles causales sont proposées. Elles sont peu différentes des techniques classiques. Le point essentiel est que l'équation d'état du modèle bond graph dual est bien la même que celle obtenue par une approche purement mathématique (Equation d'état ou module).

Au niveau de l'analyse structurelle des modèles linéaires à paramètres variant dans le temps, tous les concepts étaient à définir, aussi bien pour les modèles bond graphs, que pour les modèles structurés. Nous avons introduit le concept de modèle structuré de commandabilité et modèle structuré d'observabilité. Les concepts similaires de bond graph de commandabilité et

bond graph d'observabilité ont été définis. Avec ces nouvelles représentations nous avons pu développer des procédures graphiques de calcul des matrices de commandabilité et d'observabilité. Mais l'objectif était d'étudier graphiquement les propriétés structurelles de commandabilité et d'observabilité, en généralisant les techniques connues pour les modèles LTI. En utilisant le concept de cycle et familles de cycles introduit par Reinschke [47] et les définitions des systèmes structurés LTV, nous avons proposé une technique graphique pour l'analyse des propriétés de commandabilité/observabilité. Grâce à ces nouveaux modèles structurés, obtenus par simples ajouts d'arcs, nous avons pu reformuler les procédures d'analyse en appliquant exactement les mêmes critères graphiques que dans le cas LTI. Pour les modèles bond graph, une extension du cas LTI est aussi possible, elle est présentée dans les travaux de Chalh. Dans ce cas, les travaux démontrent que pour l'analyse de la propriété d'observabilité, le passage par le modèle dual, et ainsi étude de la commandabilité du modèle dual, simplifie considérablement la complexité du problème, car la propriété d'observabilité est plus difficile à étudier dans le cas des modèles bond graphs LTV. Cette complexité n'apparaît dans le cas des systèmes structurés.

L'étude de la dualité des systèmes par une approche graphique nous a ainsi permis de mettre en avant la dualité entre la commandabilité et l'observabilité, aussi bien d'un point de vue graphique, c'est-à-dire sur les modèles de commandabilité et d'observabilité, que sur les propriétés elles-mêmes et que sur les techniques de calcul des matrices de commandabilité et d'observabilité (par approche mathématique ou graphique).

Le dernier stade dans notre travail de recherche a été d'étudier la dualité entre deux lois de commande: le retour d'état et l'injection sortie. La problématique que nous avons abordée est le découplage quasi-statique des modèles LTV. Ce type de problématique nécessite l'étude de la structure à l'infini du modèle (pour la vérification de la propriété de découplabilité) et de la structure finie (pour la vérification de la stabilité du modèle découplé). De plus, pour le calcul de l'expression de la loi de commande, l'approche géométrique utilisant les concepts d'(A,B) et de (C,A)-invariance est exploitée.

Une première étape à permis de mettre en évidence la dualité de la structure à l'infini en ligne (utilisée dans le cadre du retour d'état) et la structure à l'infini en colonne (utilisée dans le cadre de l'injection de sortie). Les pro-

priétés de découplabilité peuvent ainsi être étudiées de manière équivalente sur le modèle initial ou le modèle dual. De la même manière, il a été montré que les espaces invariants sont duaux, et qu'il est donc possible de caractériser ces espaces sur le modèle initial et le modèle dual. Nous en avons conclu que les lois de commande de type retour d'état et injection de sortie sont caractérisées par une formulation duale. Ainsi, les matrices du retour d'état sont obtenues par simple transposition de matrices d'injection de sortie, obtenues sur le modèle dual.

Ces techniques permettent de conclure, que l'utilisateur a le choix de travailler soit sur le modèle initial, soit sur le modèle dual, tout en conservant les techniques classiques d'analyse. Ces méthodes ont été généralisées pour des systèmes non linéaires en utilisant les modèles variationels.

De nombreuses perspectives sont envisagées. La dualité dans les modèles bond graphs a été développée à partir des notions mathématiques connues, en particulier la théorie des modules (ou représentation d'état) et nous avons mis en évidence la dualité entre les variables d'énergie (variables d'état du modèle bond graph initial) et les variables de co-énergie (variables d'état du modèle bond graph dual), ce qui n'est pas le cas dans une représentation d'état classique. Ces aspects physiques permettent d'envisager une possible connexion avec les techniques bond graphs développées autour de la représentation dite " Hamiltonienne ". En effet cette dernière approche s'attache à retrouver des propriétés physiques du système et il serait intéressant de comparer les résultats obtenus par ces deux approches.

Certaines caractéristiques qui définissent le bond graph dual sont aussi communes avec le modèle bond graph adjoint qui est utilisé pour la synthèse de la commande optimale. Même si les procédures actuelle pour la caractérisation de la commande optimale concernent seulement les systèmes LTI, une extension aux modèles LTV est envisagée si nous considérons une procédure similaire à celle de dualisation.

Pour le découplage entrée-sortie des systèmes dynamiques, nous n'avons pas abordé le problème de stabilité, c'est-à-dire l'étude de la structure finie. Pour les systèmes LTI, cette étude consiste à trouver les zéros invariants. Une première question serait de comparer les zéros invariants du modèle initial et ceux du modèle dual. Ces zéros sont obtenus d'un point de vue mathématique par l'analyse de la matrice système, et il est donc assez naturel de dire que le

modèle dual contient les même zéros invariants. Par contre, cette notion est plus complexes dans le cadre des système LTV, et dans ce cas une étude plus approfondie reste à faire. Cette extension permettrait ainsi de caractériser de nouveaux sous-espaces invariants assurant le découplage avec stabilité, lorsque ce découplage avec stabilité est possible.

La dualité entre l'(A,B)-invariance et la (C,A)-invariance doit aussi être généralisée pour les modèles non linéaires. Cette extension permettrait de faciliter le calcul de lois de commande pour le découplage des systèmes LTV et non-linéaires, en exploitant par exemple le modèle variationnel.

En utilisant le concept d'injection sortie, on peut aussi considérer les problèmes de synthèse d'observateur. En effet, la synthèse d'observateur peut être assimilé au problème de commande par injection de sortie. On peut montrer par exemple que l'expression de la loi de commande pour la synthèse d'un observateur avec rejet de perturbation est la même que celle avec injection de sortie. Cette constatation amène à penser que les problèmes de commande par retour d'état, par injection de sortie et le problème de synthèse d'estimateur d'état et peuvent être définis dans un même formalisme. Une extension concerne bien entendu le problème de commande par retour de mesure qui est plus exploitable que le retour d'état, puisqu'il exige la connaissance de moins d'information.

Cette première étude de la dualité en est juste à ses balbutiements, et nous espérons développer des résultats intéressants concernant les problèmes d'observation d'estimation, mais aussi dans le domaine de la surveillance.

Contents

Acknoledgements **v**

Résumé en francais **x**

Table of Contents **xiii**

1 Duality. Theoretic Background **5**

1.1 Mathematical Apparatus 6

1.2 Linear Systems & Modules 7

1.3 Dual System 8

1.3.1 Module Theoretical Approach 9

1.3.2 State Space Representation 10

1.4 Dual Properties in System Analysis 12

1.4.1 Module Theoretical Approach 13

1.4.2 State Space Approach 14

1.5 Duality in Control Laws 15

1.5.1 Controllability and Observability Indices 15

1.5.2 State Feedback and Output Injection 18

1.6 Conclusions 21

2 Graphical Methods in System Analysis and Control Synthesis 23

2.1 Linear Structured Systems 23

2.1.1 Definition 23

2.1.2 Directed Graphs 25

2.2 Bond Graph Modeling 26

2.2.1 Bond Graph Language 27

2.2.2 Vectorial Representation 33

2.3 Graphical Methods in System Analysis 36

2.3.1 System Analysis for Structured Systems 37
2.3.2 System Analysis with a Bond Graph Approach 37
2.4 Decoupling Problem with a Graphical Approach 39
2.4.1 System Analysis 40
2.4.2 Control Synthesis 42
2.5 Decoupling Problem with Stability 44
2.5.1 Graphical Methods for Determining the Control Law . 45
2.6 Conclusions 45

3 Dual Model. Dual Properties 47
3.1 Dual Model. A Graphical Approach 47
3.1.1 A Structured System Procedure 48
3.1.2 Dual Bond graph Model 49
3.1.3 Graphic Computational Rules for the Dual Bond Graph Model 59
3.2 Structural Analysis 65
3.2.1 Definition of new LTV Graphical Models 66
3.2.2 Controllability and Observability Matrices 72
3.2.3 System Analysis using Graphical Procedures 75
3.2.4 Duality in System Analysis 82
3.3 Conclusions 90

4 Duality in Control Synthesis 93
4.1 Infinite Structure 94
4.1.1 Definitions 94
4.1.2 Duality between Row and Column Infinite Structure . 95
4.2 Decoupling Problem for LTV Models 95
4.2.1 State Feedback 96
4.2.2 Output Injection 101
4.2.3 Duality between State Feedback and Output Injection . 106
4.2.4 Application 109
4.3 Decoupling Problem with Pole Placement for LTV Models . . 118
4.3.1 Geometrical Approach 118
4.4 Decoupling and Input-Output Linearization of Nonlinear Systems 123
4.4.1 Variational Model 124
4.4.2 State Feedback 126

4.4.3 Output Injection 127
4.4.4 Application - Nonlinear Structured System 127
4.4.5 Application - Nonlinear Bond Graph Model 129
4.5 Conclusions 134

Conclusions and Perspectives **140**

References **140**

A Appendix **147**
A.1 Some Matrix Definitions 147
A.2 Dualization effects upon the vectorial representation 149

Introduction

This report is mainly focused on the study of the duality in linear systems from a graphic point of view. The two graphical representations which are used through-out this study are the bond graphs and the structured systems.

The concept of duality emerged as a philosophical concept and almost all philosophical systems have discussed the essence of duality, starting from the ancient Chinese duality between Yin and Yang till the classical philosophers of the XIX^{th} century. Engineers have borrowed this concept and have exploited it in system control. First, in the study of linear time-invariant models, where the duality was synonymous with transposing some matrices from the state space representation, some results were developed in [22], [29] and [30]. Later on, some results concerning the linear time-variant models have been introduced. In [29] and [58], the dual (adjoint) model was presented by transposing and changing signs in the state space representation of the linear model.

Beside the state space representation, which sees the duality only as algebraic operation which is applied on the matrices of the state representation, in the mid 1990's, J. Rudolph presented in [50], a study of the duality in linear systems using a module theoretic approach. This approach is based on the module theory introduced by Fliess [20], which may be seen as a more conceptual version of the polynomial perspective. In this approach a system is defined as a left module, while the dual model is defined using the corresponding right module. Therefore, we obtain a simple and elegant way to pass from the presentation matrix of one system to the presentation matrix of its dual. In his study, Rudolph tackled two types of duality which appear in system control: the duality between the controllability and observability from the analysis stage and the duality between two control laws: state feed-

back and output injection.

This study tries to the approach developed in [50]. Firstly, we wanted to use a graphical approach and secondly to give a physical interpretation to the variables of the dual model. The focus was set on the bond graphs, but we also used the structured systems representation to give a global graphical perspective. One of the difficulties of this study was that, the bond graph methodology already had the concept of "duality" [6]. Just like the bond graph models which are mid-way between the physical model and the mathematical system, the concept of "duality" was based on physical concepts. The "dual" model was obtained by interchanging the flow and effort variables on the bond graph model. Unfortunately, this type of duality did not change anything on a mathematical level, i.e. the state space representation of the "dual" was equivalent to those of the given system. This report presents a definition of duality on the bond graph model which introduces in the bond graph methodology the same concept of duality as the ones used in the state space representation or in the module theoretical approach. From this perspective the state variables of the dual model are the co-energy variables of the dynamic elements in integral causality. For the structured systems the scope of action was limited to the linear time-invariant models (see [18] for an in-depth survey of the state of the art on structured systems). Here, we have extended their use to linear models in general, time-invariant or not. The concept of duality has been introduced also for structured systems using the state space representation since the two are closely related.

The next step was to study the duality between the controllability and observability. The graphic procedures developed for the study of these properties for LTI models (in [25], [43], [47] and [51] for structured systems and in [56] for bond graphs) are not valid for LTV systems. In [40], we have introduced some graphic procedures for determining these properties graphically, using the structured systems. In [9], a procedure for determining the controllability of LTV bond graphs has been proposed. We have extended this procedure to observability using the duality and applying the same procedure for the controllability of the dual bond graph model.

After the analysis part, we concentrated on the duality between two control laws: state feedback and output injection (according to [50]). For our study, this duality has been developed via the solution of the static decoupling prob-

lem. Graphical procedures have been proposed for the decoupling of LTV bond graph models and structured systems. A short passage through the geometrical approach allowed us to develop two control laws for decoupling with pole placement. The study of the duality between (A, B) and (C, A)-invariance from [27] gave us the possibility to develop graphical procedures for the graphical synthesis of the two control laws.

The last part of the study was focused on the extension of these procedures for nonlinear models. The solution which we have implemented is based on the use of variational models. The variational (tangential) system is an LTV model and the linear time-varying procedures can be applied.

This report is structured into four chapters. The first one concerns the definition of the concept of duality in the literature. The second chapter presents a discussion of the graphical tools which are used in the sequel. In the third chapter, we introduce the concept of duality in the bond graph and structured systems methodologies. The graphical procedures for obtaining the dual model are developed. In the last part of this chapter, we tackle the system analysis and the duality between controllability and observability. The last chapter is the largest because it concerns the study of duality between control laws. We discuss here the problem of system decoupling by state feedback and by output injection both with and without pole placement. In the end, we extend these procedures to nonlinear models.

The graphical procedures developed in this report are always followed by applied examples on which we show how these methods can be used.

The last part of this report is dedicated to conclusions and perspectives. A vast range of possible developments are presented, from the physical aspects (the use of Hamiltonians with the concept of duality), to the study of geometrical approach for nonlinear models and the design of observers.

Chapter 1

Duality. Theoretic Background

This chapter is focused on the mathematical framework which will be used in the report and the presentation of the concept of duality in linear models as it appears in the system control literature. The duality concept is an old issue, well-known to the control community. This introductory chapter gathers the most important research activities concerning this problem. For time-varying linear systems the question of systems duality has been introduced either by transposing matrices and changing signs in state space representation [58] or by opposed module in the theoretical module approach [50]. Contrary to the time-invariant case, matrices transposing is not satisfactory for defining the dual system in the linear time-varying case (see [30],[29] and [22]). Of course, we can not directly present the duality concept without recalling first the mathematical apparatus used by the two approaches. Moreover, as we shall see in the sequel, the algebraic theory is more adequate to system analysis and control synthesis using graphical approaches.

The structure of this chapter is logically linked to the order of the stages in which the duality concept has been developed. In the first section, the algebraic tool based on the differential modules is recalled. Here, we present the basic concepts of algebraic structures: group, ring, field, module, as well as their differential extensions, i.e. differential field and differential module. For more details on algebraic structures, [10] and [34] are highly recommended. In the second section, we present the relation between the mathematical structures and linear systems using the module theoretical approach. Then using this perspective, we tackle the concept of duality. In the last three sections, we recall the duality concept as it was developed in [50], passing by

definition, dual properties and the duality between control laws.

1.1 Mathematical Apparatus

Differential algebra is the discipline which extends the methods of abstract algebra for the study of linear and nonlinear differential equation systems. The bases of differential algebra have been posed by [33] and [49]. Here, we briefly recall some definitions of differential algebra.

Let k be an ordinary differential field, i.e. a commutative field equipped with a single derivation $\frac{d}{dt}$ (in the sequel denoted also as s) such that, for all $a, b \in k$ properties (1.1) are verified.

$$\begin{cases} \frac{da}{dt} \in k, \\ \frac{d}{dt}(a+b) = \frac{da}{dt} + \frac{db}{dt}, \\ \frac{d}{dt}(ab) = \frac{da}{dt}b + a\frac{db}{dt}. \end{cases} \tag{1.1}$$

For notational convenience $\dot{a}$ denotes $\frac{da}{dt}$. A constant is an element $c \in k$ such that $\dot{c} = 0$. A differential sub-field of k, whose elements are constants, is called a field of constants.

If R is a field, then an R-module is a vector space. Modules are thus generalizations of vector spaces, and much of the theory of modules consists of recovering desirable properties of vector spaces in the realm of modules over certain rings.

A left R-module over the ring R consists of an abelian group $(M, +)$ and an operation $R \times M \to M$ such that: $\forall r, s \in R$ and $\forall x, y \in M$, we have

- $r(x + y) = rx + ry$
- $(r + s)x = rx + sx$
- $(rs)x = r(sx)$
- $1x = x$

A R-module M is called free if it has a basis, i.e. there exists a family e_i such that: M is generated by this family, and the elements e_i are R-linearly independent. This means that any element $m \in M$ can be written, in an

unique manner, in the form: $m = \sum_i \lambda_i e_i$.
Let N be a submodule of an R-module M and $x \in M$. The class of $x(modN)$ is the set of all $y \in M$ such that $x - y \in N$; this class is denoted by $\bar{x} = x + N$. The set of all classes $\bar{x}$, $x \in M$ is also a R-module, called quotient module.
An element $\tau \in M$ is a torsion element if $\exists a \in R,\ a \neq 0$ such that $a\tau = 0$. The set of all torsion elements of a R-module M is a R-module, called the torsion sub-module of M.
The non-commutative ring $k[s]$ of the polynomials of the form (1.2) is denoted as R. Its elements can be understood as linear differential operators.

$$\sum_{finite} \alpha_i s^i,\ \alpha_i \in k \tag{1.2}$$

The multiplication in R is defined by (1.3).

$$sa = as + \dot{a},\ a \in k \tag{1.3}$$

Obviously, $k[s]$ is commutative if and only if k is a field of constants. In general, non-commutative case, $k[s]$ is a principal ideal ring [10].

1.2 Linear Systems & Modules

The module theoretical approach as introduced in [20],[50] is based on finitely generated modules over the ring $R = k[s]$. Given a family $z = (z_1, z_2, \ldots, z_q)$, the module generated by z is denoted by $[z]$. The elements of the (left) R-module $[z]$ are the finite sums of the form $\sum_{i=1}^{q} a_i z_i,\ a_i \in R$.
A linear system $\sum$ is a finitely generated left R-module. The system is called constant, if the field k of the coefficients of the polynomials in $R = k[s]$ is a field of constants. It is called time-varying otherwise. Our interest is mainly in the second case since the first one can be seen as a particular case.
Consider a finite system of linear differential equations in the variables $\omega_1, \omega_2, \ldots, \omega_r$, with coefficients in k. With the differential operators in R, this can be written as (1.4), or, using the matrix notation, as $S\omega = 0$, with $S = (s_{j,i})$ over R and $\omega = (\omega_1, \omega_2, \ldots, \omega_r)^T$. S is the presentation matrix of $\sum$.

$$\sum_{i=1}^{r} s_{j,i}\omega_i = 0,\ j = 1, \ldots, q \tag{1.4}$$

Note that the presentation matrix S is not unique, and it depends on the choice of variables ω used to write the defining equations (1.4) of $\sum$.
A linear dynamics is a finitely generated left R-module $\sum$ containing a finite set $u = (u_1, u_2, \ldots, u_m)$ of elements, called the input, such that the quotient $\sum/[u]$ is a torsion module. This implies that any other element of the module is R-linearly dependent on u, i.e. $\forall \sigma \in \sum,\ \exists a(s), b_i(s) \in R$, with $a(s) \neq 0$ such that (1.5) is verified.

$$a(s)\sigma + \sum_{i=1}^{m} b_i(s)u_i = 0 \tag{1.5}$$

The output of the system is a set $y = (y_1, y_2, \ldots, y_p)$ of elements of $\sum$. According to 1.5, this is equivalent to:

$$a_j(s)y_j + \sum_{i=1}^{m} b_{j,i}(s)u_i = 0 \tag{1.6}$$

for $j = 1, \ldots, p$ and $a_j(s), b_{j,i} \in R$ with $a_j(s) \neq 0$.
A state of a dynamics $\sum$ is a subset of elements of $\sum$ such that their residues in the quotient $\sum/[u]$ form a basis of this quotient, considered as a k-vector space. Let $x = (x_1, x_2, \ldots, x_n)$ be a state. Then the canonical image x^+ being basis of $\sum/[u]$, the derivatives of x^+ satisfies $\dot{x}_l^+ = \sum_{i=1}^{n} a_{l,i}x_i^+$. Therefore, the components of x satisfy differential equations of form:

$$\dot{x}_l = \sum_{i=1}^{n} a_{l,i}x_i + \sum_{j=1}^{m} b_{l,j}(s)u_j \tag{1.7}$$

1.3 Dual System

The aim of this section is to present two approaches to define the dual system, a module theoretical approach and a state space perspective. In the first case, the multiplication rule of the ring of the dual module(=system) is changed, in the second, a new state representation is defined. These two approaches are proven to be equivalent in [50].
In the following, a notation is introduced to distinguish the variables and the parameters related to the given system and to its dual. For instance, if the state variable of the system is x then the state variable of the dual model is $\bar{x}$. The same notational trademark applies also to the matrices in the state space representation.

1.3.1 Module Theoretical Approach

Consider the ring R. An opposite ring R° with a new multiplication rule has been defined in [10] and used by [50] to extend the duality concept in the module theoretical framework.

The opposite ring R° is the ring with the same additive group structure as R but with the reverse multiplication ([10]), i.e. $a \circ b = ba$. From the multiplication rule of R relation (1.8) is obtained.

$$a \circ s = sa = as + \dot{a} = s \circ a + \dot{a} \tag{1.8}$$

Replacing s by $-s$ and $\circ$ by the usual multiplication is equivalent to (1.9), which is the multiplication rule of R.

$$a(-s) = -sa + \dot{a} \tag{1.9}$$

Therefore, passing to the opposite ring R° is equivalent to using the same multiplication rule and replacing s with $-s$.

The multiplication rule can be applied to the product of matrices also. $A(s)B(s)$ over R is mapped to $B^T(-s)A^T(-s)$ over R°, where the elements of the matrices $A(s)$ and $B(s)$ are polynomials in s.

Obviously, the opposite of R° is R. In the commutative case reversing the multiplication does not lead to a new ring. Because of the way the opposite ring R° is introduced, it is easy to observe that any left R-module can be considered as right R°-module ([50]).

The first step is to determine the ring of the dual system, the second is to determine the dual system presentation matrix.

In the previous section, we have seen that a presentation matrix can be associated nonuniquely with the system $\sum$. We will choose a generating family of $\sum$ in such a way that it contains the input u and the output y, if the latter is defined. Let $\omega = (\omega_1, \omega_2, \ldots, \omega_n)$ be a family of elements of $\sum$ such that $(u_1, \ldots, u_m, y_1, \ldots, y_p, \omega_1, \ldots, \omega_n) = (u, y, \omega)$ is generating $\sum$. To such a choice of generators corresponds a presentation matrix S over R such that $S(u, y, \omega)^T = 0$.

Consider the system $\sum = [u, y, \omega]$, with input u and output y, satisfying $S(u, y, \omega)^T = 0$. Let $\bar{\sum}$ be the right R-module generated by the family $\bar{\omega} = (\bar{\omega}_1, \ldots, \bar{\omega}_r)$, where r is the number of rows of matrix S, such that

$$(-\bar{y}, \bar{u}, 0) + \bar{\omega} S = 0 \tag{1.10}$$

Definition 1. *[50] "The equations of the dual system are obtained by passing to the left module over the opposite ring R°, which yields:*

$$(-\bar{y}, \bar{u}, 0)^T + S^T(-s)\bar{\omega}^T = 0, \tag{1.11}$$

where $S^T(-s)$ indicates that s is replaced by $-s$ in the entries of S."

Example 1. *Consider the linear differential equations system $\sum$ as in the equation (1.12).*

$$\begin{cases} \dot{\omega}_1 + \frac{R_r}{L_r}\omega_1 + \frac{K\Phi(t)}{J}\omega_2 - u = 0 \\ \dot{\omega}_2 - \frac{K\Phi(t)}{L_r}\omega_1 + \frac{f}{J}\omega_2 = 0 \\ y = \frac{1}{J}\omega_2 \end{cases} \tag{1.12}$$

The presentation matrix for system $\sum = [u, y, \omega_1, \omega_2]$ in (1.12) is:

$$S = \begin{pmatrix} -1 & 0 & s + \frac{R_r}{L_r} & \frac{K\Phi(t)}{J} \\ 0 & 0 & -\frac{K\Phi(t)}{L_r} & s + \frac{f}{J} \\ 0 & 1 & 0 & -\frac{1}{J} \end{pmatrix} \tag{1.13}$$

To obtain the equations for the dual system $\bar{\sum}$, we apply the procedure from definition 1 which leads to:

$$\begin{pmatrix} -\bar{y} \\ \bar{u} \\ 0 \\ 0 \end{pmatrix} + \begin{pmatrix} -1 & 0 & 0 \\ 0 & 0 & 1 \\ -s + \frac{R_r}{L_r} & -\frac{K\Phi(t)}{L_r} & 0 \\ \frac{K\Phi(t)}{J} & -s + \frac{f}{J} & -\frac{1}{J} \end{pmatrix} \begin{pmatrix} \bar{\omega}_1 \\ \bar{\omega}_2 \\ \bar{\omega}_3 \end{pmatrix} = 0 \tag{1.14}$$

Equation (1.14) is equivalent to:

$$\bar{\sum}: \begin{cases} \dot{\bar{\omega}}_1 - \frac{R_r}{L_r}\bar{\omega}_1 + \frac{K\Phi(t)}{L_r}\bar{\omega}_2 = 0 \\ \dot{\bar{\omega}}_2 - \frac{K\Phi(t)}{J}\bar{\omega}_1 - \frac{f}{J}\bar{\omega}_2 - \frac{1}{J}\bar{u} = 0 \\ \bar{y} = -\bar{\omega}_1 \end{cases} \tag{1.15}$$

1.3.2 State Space Representation

For the state space representation, the concept of dual model is well known in the literature [20],[29],[58]. The relations between the matrix representation of the given system and its dual are recalled (1.16)-(1.19).

$$\bar{A}(t) = -A^T(t) \tag{1.16}$$

$$\bar{B}(t) = C^T(t) \tag{1.17}$$

$$\bar{C}(t) = -B^T(t) \tag{1.18}$$

$$\bar{D}(t) = D^T(t) \tag{1.19}$$

It is easy to prove that the two representations, state representation and module representation, for the dual system are similar. Consider the linear system (1.20), whose presentation matrix in module representation is given by equation (1.21).

$$\begin{cases} \dot{x}(t) = A(t)x(t) + B(t)u(t) + \sum_k B_k(t)u^{(k)}(t) \\ y(t) = C(t)x(t) + D(t)u(t) + \sum_k D_k(t)u^{(k)}(t) \end{cases} \tag{1.20}$$

Remark 1. *In the following, we do not use the derivatives of the inputs since in the graphical representations which are the scope of this report we can not obtain these terms in the state space representation.*

For notational simplicity, the variables in the state space representation are considered as column vectors, while in module representation they are row vectors.

$$\begin{pmatrix} -B(t) & 0 & sI - A(t) \\ -D(t) & I & -C(t) \end{pmatrix} \begin{pmatrix} u & y & x \end{pmatrix}^T = 0 \tag{1.21}$$

Applying the procedure described in definition 1 yields:

$$(-\bar{y}, \bar{u}, 0)^T + \begin{pmatrix} -B^T(t) & -D^T(t) \\ 0 & I \\ -sI - A^T(t) & -C^T(t) \end{pmatrix} \begin{pmatrix} \bar{\omega}_1^T \\ \bar{\omega}_2^T \end{pmatrix} = 0, \tag{1.22}$$

where the row vector $\bar{\omega}$ has been partitioned in $\bar{\omega}_1$ and $\bar{\omega}_2$ according to the number of state variables and inputs, respectively. Rewriting the equations of the dual system, where the input is obviously $\bar{u} = -\bar{\omega}_2$ and a state vector is $\bar{x} = \bar{\omega}_1$, leads to equation (1.23), where the similarity between the two approaches is evident.

$$\begin{cases} \dot{\bar{x}} = -A^T(t)\bar{x} + C^T(t)\bar{u} \\ \bar{y} = -B^T(t)\bar{x} + D^T(t)\bar{u} \end{cases} \tag{1.23}$$

In equation (1.23), if the variable change $\tilde{\bar{x}} = -\bar{x}$ is performed then the following state space representation is obtained:

$$\begin{cases} \dot{\tilde{\bar{x}}} = -A^T(t)\tilde{\bar{x}} - C^T(t)\bar{u} \\ \bar{y} = B^T(t)\tilde{\bar{x}} + D^T(t)\bar{u} \end{cases} \tag{1.24}$$

Relation (1.24) presents a known results to the control community, which in [58] is called adjoint system. In fact in [50], it has been proved that the adjoint system and the dual system are the same.

In the state space representation, dualizing directly according to definition 1 is not reversible, the dualization should be performed on the dual model after the basis change in order to obtain the given system. In figure 1.1, a schema regarding the results of the dualizing procedure on the different state space representations of the system and its dual is reproduced.

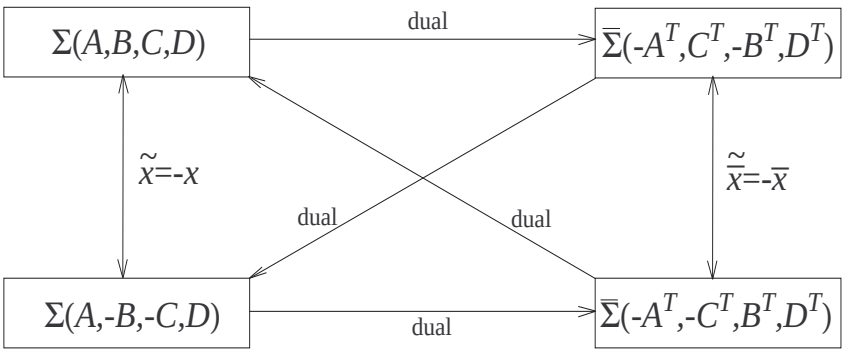

Figure 1.1: Duality in State Space Representation

1.4 Dual Properties in System Analysis

The concept of duality between the controllability property and the observability property is well-known to the control system community. This duality concept between the two structural properties is the aim of this section. In the sequel all the references concerning these two properties mean structural properties.

Even though there are two approaches, the module theoretical approach and the state space representation, for determining this duality there is a theorem which is valid in both cases.

Theorem 1. *[50] The system $\sum$ is observable if and only if the dual system $\bar{\sum}$ is controllable, and vice versa.*

In the following subsections, the concept of duality between the controllability and the observability is reached firstly using the module description and secondly using the state representation.

1.4.1 Module Theoretical Approach

Controllability means there are no variable which are k-linear dependent of the other variables of the module.

Theorem 2. *[20]$\sum$ is controllable if and only if it is free, i.e. T is trivial, where T is the torsion sub-module.*

Observability means that any element in $\sum$ can be computed by a k-linear equation from the output y, the input u and a finite number of their derivatives.

Theorem 3. *[20]$\sum$ is observable if and only if $\sum$ and $[u, y]$ coincide.*

The proof of theorem 1 using the module theoretical approach in [50] is based on the theorems 2 and 3.

Remark 2. *[50] "The controllability of Σ does not depend on the choice of an input. Contrariwise, the observability depends on the choice of the input and of the output. Hence, there is an asymmetry or "lack of duality" between these two structural properties. However, the definition of the dual system depends on the choice of the module generated by the input and the output, too."*

Example 2. *Let us consider the example (1.12) as in the previous section. The properties of controllability and observability are studied for both the system $\sum$ (eq. (1.12)) and its dual $\bar{\sum}$ (eq. (1.15)), using their module representations.*
The R-module $\sum$ is free since ω_2 form a basis, therefore the system $\sum$ is controllable. Analogously one can observe that $\bar{\omega}_1$ form a basis for the R°-module $\bar{\sum}$ and that the system $\bar{\sum}$ is also controllable.
For determining the observability property of system $\sum$, it is sufficient to

express the system variables ω_1 and ω_2 as functions of the input and output and their derivatives.

$$\omega_1 = \frac{L_r}{K\Phi(t)}(J\dot{y} + fy) \tag{1.25}$$

and

$$\omega_2 = Jy \tag{1.26}$$

and therefore the system $\sum$ is observable.
The same technique is applied to determine whether the dual system is observable.

$$\bar{\omega}_1 = -\bar{y} \tag{1.27}$$

and

$$\bar{\omega}_2 = \frac{L_r}{K\Phi(t)}\dot{\bar{y}} - \frac{R_r}{K\Phi(t)}\bar{y} \tag{1.28}$$

and therefore the dual system $\bar{\sum}$ is observable too.
This example illustrates the results obtained by theorem 1 in the module theoretical approach. The system $\sum$ is controllable and its dual system $\bar{\sum}$ is observable and vice-versa.

1.4.2 State Space Approach

The study of controllability and observability has also been performed from the state space perspective (see [52] and [29]). This study is based on the computation of the controllability and observability matrices, on which a rank condition is imposed.
According to [52] and [20], an LTV system is controllable, respectively observable if the rank of the matrices (1.29) and (1.30) respectively is full.

$$R(t) = \begin{pmatrix} B(t) & (A(t) - \frac{d}{dt})B(t) & \cdots & (A(t) - \frac{d}{dt})^{n-1}B(t) \end{pmatrix} \tag{1.29}$$

$$O(t) = \begin{pmatrix} (C(t)^T)^T \\ ((A(t)^T + \frac{d}{dt})C(t)^T)^T \\ \vdots \\ ((A(t)^T + \frac{d}{dt})^{n-1}C(t)^T)^T \end{pmatrix} \tag{1.30}$$

Remark 3. *In the two rank conditions above, we have considered that the functions involved do not present any singularities.*

The differences between the LTI and the LTV case cases concern mostly the derivatives $\pm\frac{d}{dt}$. Therefore in order to extend the procedures designed for LTI models to the LTV models, the use of these derivatives must be emphasized.

1.5 Duality in Control Laws

In this section, we are recalling perhaps one of the most important duality in system control, the duality between state feedback and output injection. This concept is discussed for the static state feedback and its dual the static output injection. In [50], this duality is presented with a module theoretical approach, using Brunovsky forms and filtration (for an in-depth discussion see [8] and [14] respectively). Without presenting the details from [50], we just recall the most important aspects of this duality. In fact we can divide this discussion into two parts: the invariant indices under the state feedback and under output injection and the duality between the two control laws.

1.5.1 Controllability and Observability Indices

1.5.1.1 Definitions

The definition for controllability and observability indices has been provided for LTI systems using the state space representation. Analogously, using the controllability and observability matrices, these definitions have been extended to LTV models in [22] and [29]. First we recall the definitions for these indices and then we prove that they are dual.
As we are going to use the controllability and observability matrices from relations (1.29) and (1.30), let us first define two operators which will make the notation easier. Consider the operator $\mathcal{N} = A - \frac{d}{dt}$ for controllability and $\mathcal{L} = A^T + \frac{d}{dt}$ for observability. The definitions are similar in the two cases, therefore we are going to focus on the controllability indices first.

Theorem 4. *[29] An LTV system $\Sigma(A, B)$ is controllable iff*

$$rk(B, \mathcal{N}B, \ldots, \mathcal{N}^{n-1}B) = n \tag{1.31}$$

where n is the dimension of the state space.

Remark 4. *An LTV system presents parameters which are time-dependent, in our study, we do not consider the case when the value of time is negative or when, for a particular moment of time t, we observe a discontinuity.*

Let us consider the integers l_i, starting with $rk(B) = l_0$ and we may set $rk(B,\mathcal{N}B) = l_0 + l_1$,...,$rk(B,\mathcal{N}B,\ldots,\mathcal{N}^{n-1}B) = l_0 + \ldots + l_{n-1}$.

Definition 2. *The integers* $\lambda_i = card\{k|l_k \geq i\}$, $i = 1,\ldots,m$ *are called controllability indices.*

The observability indices are defined in the same way.
The integers k_i, obtained from the relations $rk(C^T) = k_0$, $rk(C^T,\mathcal{L}C^T) = k_0 + k_1$,...,$rk(C^T,\mathcal{L}C^T,\ldots,\mathcal{L}^{n-1}C^T) = k_0 + \ldots + k_{n-1}$.

Definition 3. *The integers* $\mu_j = card\{i|k_i \geq j\}$, $j = 1,\ldots,p$ *are called observability indices.*

1.5.1.2 Duality between Controllability and Observability Indices

The concept of duality between controllability and observability can be extended to the controllability and observability indices.

Theorem 5. *The set of observability indices of a system* Σ *is equal to the set of controllability indices of the dual system* $\bar{\Sigma}$ *and vice versa.*

Proof:
Given the system

$$\Sigma : \begin{cases} \dot{x}(t) = A(t)x(t) + B(t)u(t) \\ y(t) = C(t)x(t) \end{cases} \tag{1.32}$$

its dual system is:

$$\bar{\Sigma} : \begin{cases} \dot{\bar{x}}(t) = \bar{A}(t)\bar{x}(t) + \bar{B}(t)\bar{u}(t) \\ \bar{y}(t) = \bar{C}(t)\bar{x}(t) \end{cases} \tag{1.33}$$

where $\bar{A}(t) = -A^T(t)$, $\bar{B}(t) = C^T(t)$ and $\bar{C}(t) = -B^T(t)$.
According to definition 3, we know that the observability indices of the system Σ are defined using the integers k_i, from the series $rk(C^T) = k_0$, $rk(C^T,\mathcal{L}C^T) = k_0 + k_1$,..., $rk(C^T,\mathcal{L}C^T,\ldots,\mathcal{L}^{n-1}C^T) = k_0 + \ldots + k_{n-1}$. According to definition 2, the controllability indices of the dual system $\bar{\Sigma}$ are defined using the integers $\bar{l}_i$, from the series $rk(\bar{B}) = \bar{l}_0$, $rk(\bar{B},\bar{\mathcal{N}}\bar{B}) = \bar{l}_0 + \bar{l}_1$,...,

$rk(\bar{B}, \bar{\mathcal{N}}\bar{B}, \ldots, \bar{\mathcal{N}}^{n-1}\bar{B}) = \bar{l}_0 + \ldots + \bar{l}_{n-1}$. This series can also be written in terms of matrices A, B, C of the system Σ as: $rk(C^T) = \bar{l}_0$, $rk(C^T, (-A^T - sI)C^T) = \bar{l}_0 + \bar{l}_1$,..., $rk(C^T, (-A^T - sI)C^T, \ldots, (-A^T - sI)^{n-1}C^T) = \bar{l}_0 + \ldots + \bar{l}_{n-1}$. Multiplying the column vectors of a matrix by a constant scalar does not change the rank of the matrix, therefore the above series is equivalent to the following series: $rk(C^T) = \bar{l}_0$, $rk(C^T, (A^T + sI)C^T) = \bar{l}_0 + \bar{l}_1$,..., $rk(C^T, (A^T + sI)C^T, \ldots, (A^T + sI)^{n-1}C^T) = \bar{l}_0 + \ldots + \bar{l}_{n-1}$, which is the series for determining the observability indices the system Σ. Therefore $k_i = \bar{l}_i$ and $\mu_j = \bar{\lambda}_j$. Analogously, we can prove that the controllability indices λ_j of system Σ are equal to the observability indices $\bar{\mu}_j$ of the dual system $\bar{\Sigma}$.

Example 3. *Let us consider the following system:*

$$\begin{cases} \dot{x}_1 = tx_2 + x_4 \\ \dot{x}_2 = x_3 \\ \dot{x}_3 = x_1 + x_2 + x_3 \\ \dot{x}_4 = t^2 x_1 \\ y_1 = (t+1)x_1 + x_2 \\ y_2 = x_3 \\ y_3 = x_2 \end{cases} \tag{1.34}$$

which means $A = \begin{pmatrix} 0 & t & 0 & 1 \\ 0 & 0 & 1 & 0 \\ 1 & 1 & 1 & 0 \\ t^2 & 0 & 0 & 0 \end{pmatrix}$ *and* $C = \begin{pmatrix} t+1 & 1 & 0 & 0 \\ 0 & 0 & 1 & 0 \\ 0 & 1 & 0 & 0 \end{pmatrix}$. *For calculating the observability indices, definition 3 is used.*

- $k_0 = rk(C^T) = 3$.
- $k_1 = rk(C^T, (A^T + sI)C^T) - k_0 = 4 - 3 = 1$
- $k_2 = 0$
- $k_3 = 0$

Therefore $\mu_1 = 2$, $\mu_2 = 1$ *and* $\mu_3 = 1$.

Let us now consider the dual system of model (1.34).

$$\begin{cases} \dot{\bar{x}}_1 = -\bar{x}_3 - t^2\bar{x}_4 + (t+1)\bar{u}_1 \\ \dot{\bar{x}}_2 = -t\bar{x}_1 - \bar{x}_3 + \bar{u}_1 + \bar{u}_3 \\ \dot{\bar{x}}_3 = -\bar{x}_2 - \bar{x}_3 + \bar{u}_2 \\ \dot{\bar{x}}_4 = -\bar{x}_1 \end{cases} \tag{1.35}$$

with matrices $\bar{A} = -A^T = \begin{pmatrix} 0 & 0 & -1 & -t^2 \\ -t & 0 & -1 & 0 \\ 0 & -1 & -1 & 0 \\ -1 & 0 & 0 & 0 \end{pmatrix}$ *and* $\bar{B} = C^T = \begin{pmatrix} t+1 & 0 & 0 \\ 1 & 0 & 1 \\ 0 & 1 & 0 \\ 0 & 0 & 0 \end{pmatrix}$.
For calculating the controllability indices, definition 2 is used.

- $\bar{l}_0 = rk(\bar{B}) = 3.$
- $\bar{l}_1 = rk(\bar{B}, (\bar{A} - sI)\bar{B}) - \bar{l}_0 = 4 - 3 = 1$
- $\bar{l}_2 = 0$
- $\bar{l}_3 = 0$

Therefore $\bar{\lambda}_1 = 2$, $\bar{\lambda}_2 = 1$ *and* $\bar{\lambda}_3 = 1$.
On this simple example, it is easy to observe that the observability indices of the system Σ *are identical to the controllability indices of the dual system* $\bar{\Sigma}$ *and that the duality between the two sets of indices holds.*

1.5.2 State Feedback and Output Injection

The concept of duality in linear models can be defined not only for the controllability property and the observability property as can be seen in the previous section, but also it can be extended to the control laws. A state feedback control can be considered as the dual of an input injection control law [50]. These concepts are valid for linear and non linear models, in a state space description or in a module theoretical framework.
But let us first define these control laws, and afterwards we continue with the duality between them.

1.5.2.1 Definitions

State feedback and output injection are two well-known control laws. We are recalling here their definitions.

Definition 4. *Given a linear system (in fact these control laws can be defined for any linear or nonlinear system, but for simplicity we have chosen only the linear models):*

$$\begin{cases} \dot{x}(t) = A(t)x(t) + B(t)u(t) \\ y(t) = C(t)x(t) \end{cases} \tag{1.36}$$

a static state feedback control law is defined by

$$u(t) = F(t)x(t) + G(t)v(t) \tag{1.37}$$

where F and G are matrices of appropriate dimensions and $v(t)$ is a new input vector (see figure 1.2).

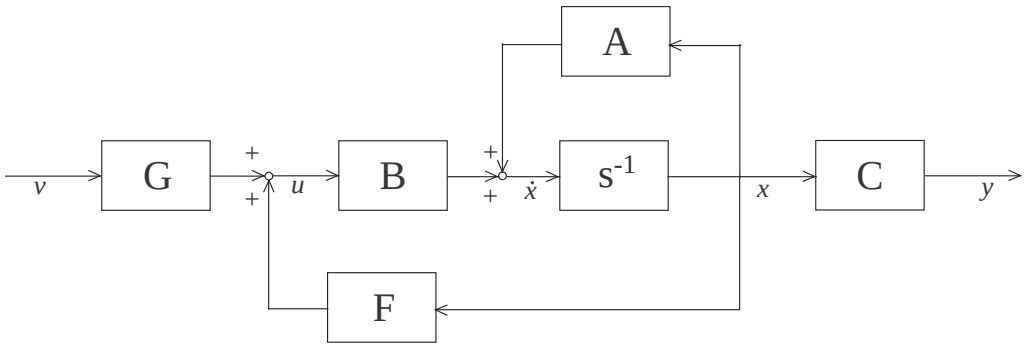

Figure 1.2: Control scheme for state feedback

Output injection was defined in the literature for quite some time, see [4], even though it has not been used. Its expression is:

$$\begin{cases} \dot{x}(t) = A(t)x(t) + B(t)u(t) + K(t)y(t) \\ y(t) = C(t)x(t) \end{cases} \tag{1.38}$$

Equation (1.38) is equivalent to:

$$\begin{cases} \dot{x}(t) = (A(t) + K(t)C(t))x(t) + B(t)u(t) \\ y(t) = C(t)x(t) \end{cases} \tag{1.39}$$

where the state matrix of the global system is $A + KC$.
In [4], this control law has been defined regarding the pole placement problem, while in [50], the control law has been extended by taking into account the duality concept. This way a new output injection control law has been introduced.

Definition 5. *Given a linear system (1.36), the output injection control law is:*

$$\begin{cases} \dot{x}(t) = A(t)x(t) + B(t)u(t) + K(t)y(t) \\ y(t) = C(t)x(t) \\ z(t) = L(t)y(t) \end{cases} \tag{1.40}$$

where $z(t)$ is a new output vector (see figure 1.3).

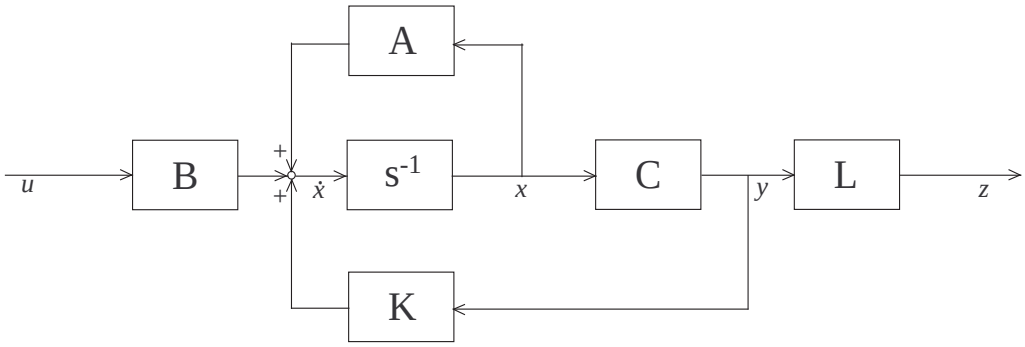

Figure 1.3: Control scheme for output injection

1.5.2.2 Duality between State Feedback and Output Injection

In this section, we recall the approach described in [50] for defining the duality between the two control laws.

Theorem 6. *State feedback control law is the dual of output injection control law.*

Proof:
Let us consider an LTV system:

$$\Sigma : \begin{cases} \dot{x}(t) = A(t)x(t) + B(t)u(t) \\ y(t) = C(t)x(t) \end{cases} \tag{1.41}$$

and its dual system:

$$\bar{\Sigma} : \begin{cases} \dot{\bar{x}}(t) = \bar{A}(t)\bar{x}(t) + \bar{B}(t)\bar{u}(t) \\ \bar{y}(t) = \bar{C}(t)\bar{x}(t) \end{cases} \tag{1.42}$$

where $\bar{A}(t) = -A^T(t)$, $\bar{B}(t) = C^T(t)$ and $\bar{C}(t) = -B^T(t)$.
If we consider the state feedback control for system (1.41) and the output injection control law for system (1.42), then we obtain relations (1.43) and (1.44) respectively.

$$\Sigma_{sf} : \begin{cases} \dot{x}(t) = (A(t) + B(t)F(t))x(t) + B(t)G(t)v(t) \\ y(t) = C(t)x(t) \end{cases} \tag{1.43}$$

$$\bar{\Sigma}_{oi} : \begin{cases} \dot{\bar{x}}(t) = (\bar{A}(t) + \bar{K}(t)\bar{C}(t))\bar{x}(t) + \bar{B}(t)\bar{u}(t) \\ \bar{z}(t) = \bar{L}(t)\bar{C}(t)\bar{x}(t) \end{cases} \tag{1.44}$$

And now, if the duality procedure from definition 1 is applied on system (1.43), we obtain:

$$\bar{\Sigma_{sf}} : \begin{cases} \dot{\tilde{x}}(t) = -(A^T(t) + F^T(t)B^T(t))\tilde{x}(t) + C^T(t)\tilde{u}(t) \\ \tilde{y}(t) = -G^T(t)B^T(t)\tilde{x}(t) \end{cases} \tag{1.45}$$

From confronting equations (1.44) and (1.45), we can easily observe that $\bar{K}(t) = F^T(t)$ and $\bar{L}(t) = G^T(t)$.

1.6 Conclusions

In this chapter, we have recalled a part of the studies on the concept of duality in the control literature, starting with the definition of dual system, then duality between system properties (controllability and observability) and in the end the duality between control laws (state feedback versus output injection).This chapter was focused on linear systems, time-invariant or not. These results will be discussed in detail in the following chapters through graphical representations: the structured systems and the bond graphs.

Chapter 2

Graphical Methods in System Analysis and Control Synthesis

The study of graphical procedures for system analysis and control synthesis needs the definition of graphical representations of systems. Two representations have been considered in this report: the structured systems (introduced by [43]) and the bond graphs (introduced by [45]).
As stated in the title of this chapter, after the definition of these graphical representations, we recall the graphical procedures which have been developed for system analysis and control synthesis. For the control synthesis, we focus mostly on a well-known problem, the decoupling by state feedback problem without and with stability.
All the procedures described in this chapter for LTI models are extended in the following chapters for LTV models.

2.1 Linear Structured Systems

2.1.1 Definition

So far, the study of structured systems concerned only the linear time-invariant systems of type (2.1),

$$\begin{cases} \dot{x}(t) = Ax(t) + Bu(t) \\ y(t) = Cx(t) + Du(t) \end{cases} \tag{2.1}$$

where $x(t) \in \mathbb{R}^n$, $u(t) \in \mathbb{R}^m$ and $y(t) \in \mathbb{R}^p$ denote the state, input and respectively output vectors of the system. The matrices A, B, C and D are

real valued matrices of suitable dimensions.
The basic idea behind the expression "structured systems" is that only the zero/nonzero information in the matrices of the state space representation is kept. The fixed zeros are conserved, while the nonzero entries are replaced by free parameters. If the system has f nonzeros, then it can be parameterized by means of a parameter vector $\lambda \in \Lambda = \mathbb{R}^f$. The set of parameterized system thus obtained is the structured system (2.2).

$$\begin{cases} \dot{x}(t) = A_\lambda x(t) + B_\lambda u(t) \\ y(t) = C_\lambda x(t) + D_\lambda u(t) \end{cases} \tag{2.2}$$

In [18] it is assumed, and we quote, that "the actual value of each of the nonzeros is unknown" and that it "can take any real value". The generic properties can be obtained on a structured based representation, but in order to determine the control laws the actual values are imperiously needed. Therefore even if certain properties are "structurally" determined, we have to choose a $\lambda \in \Lambda$, so that the system (2.2) becomes completely known as in equation (2.1). In the following, we shall consider that the structured systems have the actual parameters instead of λ, this way no confusion is possible. But we keep in mind that we speak about "generical" properties and real control laws.
Structured systems can be represented by means of directed graphs. The set $G = (V, E)$ of a structured system (2.2) is defined by a vertex set V and an edge set E. The vertex set V is given by $V = U \bigcup X \bigcup Y$ with $U = \{u_1, u_2, \ldots, u_m\}$ the set of input vertices, $X = \{x_1, x_2, \ldots, x_n\}$ the set of state vertices and $Y = \{y_1, y_2, \ldots, y_p\}$ the set of output vertices. If (a, b) represents a directed edge from the vertex $a \in V$ to the vertex $b \in V$, the edge set E is composed by $E = E_A \bigcup E_B \bigcup E_C \bigcup E_D$ with $E_A = \{(x_j, x_i) \mid A_{\lambda,ij} \neq 0\}$, $E_B = \{(u_j, x_i) \mid B_{\lambda,ij} \neq 0\}$, $E_C = \{(x_j, y_i) \mid C_{\lambda,ij} \neq 0\}$ and $E_D = \{(u_j, y_i) \mid D_{\lambda,ij} \neq 0\}$.

Example 4. *Let us consider a separately excited direct current motor (SEDCM). The physical system presents a nonlinear behavior, but we consider here a simplified model in which we assimilate the nonlinear behavior of the control circuit with a time-varying modulation of the flux in the stator ([1]). This*

model can be depicted by system (2.3),

$$\begin{cases} L\frac{dI_r(t)}{dt} + RI_r(t) = V_r(t) - K\Phi\Omega_r(t) \\ J\frac{d\Omega(t)}{dt} + f\Omega(t) = K\Phi I_r(t) \end{cases} \tag{2.3}$$

where Φ is the flux induced by the stator, $I_r(t)$ and $V_r(t)$ are the current and the voltage respectively in the rotor (the last variable is the input source) and $\Omega(t)$, the rotational speed of the motor, is the output variable. If the state vector is defined as $x(t)^T = (I_r(t), \Omega(t))^T$, the input variable $u(t) = V_r(t)$ and the output variable $y(t) = \Omega(t)$, then a state space representation (2.1) can be obtained, where

$$A = \begin{bmatrix} -\frac{R}{L} & -\frac{K\Phi}{L} \\ \frac{K\Phi}{J} & -\frac{f}{J} \end{bmatrix} \quad B = \begin{bmatrix} \frac{1}{L} \\ 0 \end{bmatrix} \qquad C = \begin{bmatrix} 0 & 1 \end{bmatrix} \tag{2.4}$$

Figure 2.1 presents the representation in the structured system methodology of the SEDCM.

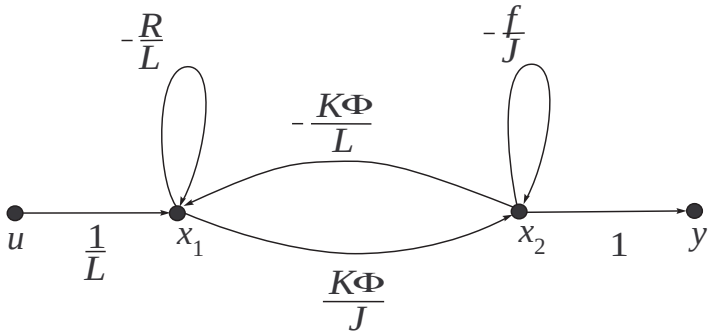

Figure 2.1: Graph of the SEDCM

2.1.2 Directed Graphs

The structured systems are graphically defined by a directed graph. Properties of directed graphs are fundamental for the procedures proposed for dealing with structured systems. Therefore, in the following, we present some of the most important definitions concerning directed graphs and structured systems. These definitions belong to graph theory, but their use in the study

of structured systems imposes that we briefly recall them.

Definition 6. *A path between vertex $v_0 \in V$ and vertex $v_t \in V$ is a sequence of t edges $(v_0, v_1), (v_1, v_2), \ldots, (v_{t-1}, v_t)$, with $v_i \in V$ and $(v_{i-1}, v_i) \in E$*

The vertex $v_0 \in V$ is called the beginning vertex and $v_t \in V$ is called the end vertex. Another way of expressing definition 6, is to say that the path contains the vertices $v_0, v_1, \ldots, v_t$, where it may happen that some vertices occur more than once. In fact the same path can be written as $v_0 \rightarrow v_1 \rightarrow \ldots \rightarrow v_t$. A path is called simple path if each vertex on the path occurs only once.

Definition 7.

1. *Two paths are disjoint if they consist of disjoint sets of vertices.*
   p ($p \geq 2$) paths are disjoint if they are mutually disjoint, i.e. whichever two paths among the p paths are disjoint.
2. *An U-rooted path is a path which has the beginning vertex in the set U.*
3. *The set of mutually disjoint U-rooted paths forms an U-rooted path family.*
4. *An Y-toped path is a path which has the end vertex in the set Y.*
5. *The set of mutually disjoint Y-toped paths forms a Y-toped path family.*
6. *A cycle (loop) is a path where the beginning and the end vertex are identical.*
7. *A cycle family is a set of mutually disjoint cycles.*

2.2 Bond Graph Modeling

As an intermediary representation between the mathematical level and the technical one, the bond graph tool is a graphical framework for modeling physical systems. This methodology has been introduced in 1960's by [45]. In the 1990's, the bond graph methodology has extended its scope. A set

of analysis procedures and even graphical control synthesis methods using bond graph representation have been developed in [56],[23],[5] and [1].
In this section, we present the bond graph elements and the modeling methodology and the vectorial representation which describes the relation between the bond graph model with the physical, power flow linkage and the state space representation.

2.2.1 Bond Graph Language

The first part of this section concerns the presentation of the most important definitions for reading and handling a bond graph model. We recall first different elements which build up a bond graph model and their physical significance as in [31]. Afterwards, we present some graphical rules such as causal path, and the procedures for determining the gains of causal paths and causal loops.
A bond graph consists of subgraphs linked together by half arrows, representing power bonds. They exchange instantaneous energy at places called ports inside or outside the same physical domain. The variables that are forced to be identical when two ports are connected are the power variables, considered as functions of time. The various power variables are classified in a universal scheme, and called either effort $e(t)$ or flow $f(t)$. Their product $P(t) = e(t)f(t)$ is the instantaneous power flowing between the ports. For system characterization, there are two more important variables, called energy variables: the momentum $p(t) = \int e(t)dt$ and the displacement $q(t) = \int f(t)dt$ in generalized notation. Tables 2.1 and 2.2 show power and energy variables for several physical domains.

Table 2.1: Power variables for several physical domains

	Effort e	Flow f
Mechanical(Transl.)	force, F	velocity v
Mechanical(Rot.)	torque, τ	angular velocity, ω
Hydraulic	pressure, P	volume flow rate, Q
Electrical	voltage, u	current, i

Table 2.2: Energy variables for several physical domains

	Momentum p	Displacement q
Mechanical(Transl.)	momentum, p	displacement x
Mechanical(Rot.)	angular momentum, h	angle, θ
Hydraulic	pressure momentum, p_P	volume, V
Electrical	flux linkage, λ	charge, q

2.2.1.1 Bond Graph Elements

A few basic types of elements are required in order to represent models in a variety of energy domains. In the following we regrouped basic 1-port elements. A causal stroke, placed perpendicularly to the bond, shows up the way the constitutive relations in an element have to be written.

1. Resistor Element

An R element is a passive dissipative element. It allows modeling the energy dissipation phenomena, characterized by a relation between the effort and the flow. Regarding the causality imposed on the element, this relation can be $e = \Phi_R(f)$ for figure 2.2.a or $f = \Phi_R^{-1}(e)$ for figure 2.2.b. A few examples of technical components which present a dissipative behavior: electrical resistor, mechanical damper, dashpot, friction, hydraulic restriction.

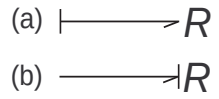

Figure 2.2: Bond Graph Symbol for resistor

2. Capacitor Element

A C element is a dynamic element. It allows modeling the energy storage phenomena, characterized by a relation between the effort and the integrate of the flow. Regarding the causality imposed on the element, this relation can be $e = \Phi_C^{-1}(\int f dt)$ for figure 2.3.a or $f = \frac{d\Phi_C(e)}{dt}$ for figure 2.3.b. A few examples of technical components which are assimilated to a C element: electrical capacitor, mechanical spring, torsion bar, tank, accumulator.

3. Inductance Element

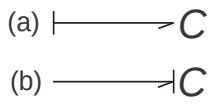

Figure 2.3: Bond Graph Symbol for capacitor

An I element is a dynamic element. It allows modeling the energy storage phenomena, characterized by a relation between the flow and the integrate of the effort. Regarding the causality imposed on the element, this relation can be $f = \Phi_I^{-1}(\int e dt)$ for figure 2.4.a or $e = \frac{d\Phi_I(f)}{dt}$ for figure 2.4.b. A few examples of technical components which are assimilated to an I element: electrical inductance, mass, inertia.

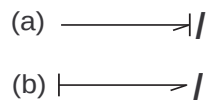

Figure 2.4: Bond Graph Symbol for inductance

4. Source Element

A source element Se, Sf is an active element. It allows modeling the active phenomena, represented by power sources. An Se element is an effort source, such as: voltage supply, pressure supply, gravity. An Sf element is a flow source, such as: current supply, pump. In figure 2.5, the causality for each type of source is presented.

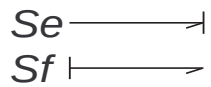

Figure 2.5: Bond Graph Symbol for sources

5. Detector Element

The detectors are used for sensors, supposed to be ideal (no power is dissipated and no power is stored). An De element is an effort detector, such as: voltmeter, force sensor, pressure sensor. An Df element is a flow detec-

tor, such as: ampermeter, flow rate sensor, tachometer. In figure 2.6, the causality for each type of source is presented.

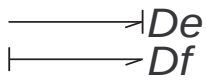

Figure 2.6: Bond Graph Symbol for sources

In a bond graph model the elements are connected by power bonds and junction elements. The junction structure elements with their causality restrictions are presented in the following. They are power conservative.

1. 0-*junction*

An 0-junction is a common effort junction characterized by the following relations $e_1 = e_2 = \ldots = e_n$ and $\sum f_i = 0$.

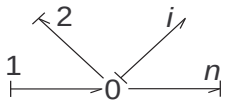

Figure 2.7: 0-junction

2. 1-*junction*

An 1-junction is a common flow junction characterized by the following relations $f_1 = f_2 = \ldots = f_n$ and $\sum e_i = 0$.

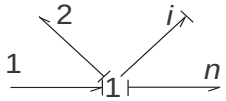

Figure 2.8: 1-junction

3. Transformer

A transformer element TF is a 2-port element. Regarding the causality imposed on the element, this relation can be $\begin{cases} e_2 = \frac{1}{m} e_1 \\ f_1 = \frac{1}{m} f_2 \end{cases}$ for figure 2.9.a or $\begin{cases} e_1 = m e_2 \\ f_2 = m f_1 \end{cases}$ for figure 2.9.b. A few examples of technical components which

present this behavior: electrical transformer, lever, gear pair, hydraulic ram.

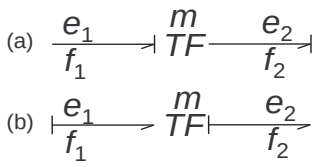

Figure 2.9: Transformer

4. Gyrator

A gyrator element GY is a 2-port element. Regarding the causality imposed on the element, this relation can be $\begin{cases} f_1 = \frac{1}{r} e_2 \\ f_2 = \frac{1}{r} e_1 \end{cases}$ for figure 2.10.a or $\begin{cases} e_1 = r f_2 \\ e_2 = r f_1 \end{cases}$ for figure 2.10.b. A few examples of technical components which which presents this behavior: hall effect sensor, gyroscope, voice coil, DC motor.

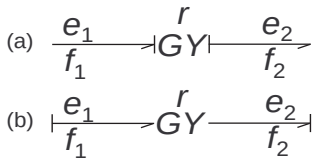

Figure 2.10: Gyrator

2.2.1.2 Causal Analysis

The causal structure of a bond graph provides interesting characteristics through the causal analysis. Among these characteristics are the notions of causal paths, causal loops, very useful in calculating the transfer function, the state space representation and control synthesis [12]. In this part of the section, we recall the most important definitions concerning these characteristics.

Definition 8. *Given two sets J_1 and J_2 composed by the following elements: $J_1 = \{C, I, R, Se, Sf\}$ and $J_2 = \{C, I, R, De, Df\}$. A causal path between*

an element of the set J_1 and an element of the set J_2 is a chain of intercalated power bonds, junctions and elements such that a complete and correct causality is given to all the sequence; two bonds connected to the same node (element) have opposed causalities.

The notion of causal path on a bond graph model is similar to the one of path on an oriented graph model. Nevertheless, on an oriented graph model, a path can not be defined between resistive elements and/or storage elements in derivative causality. Definition 8 allows the introduction of the concept of causal loop.

Definition 9. *A causal loop is a closed causal path between two elements of the set $\{C, I, R\}$. This path starts from the element and returns to the same element without passing any bond more than once, following the same variable.*

Remark 5. *[60] A causal mesh is a causal loop which does not pass through any element (dynamic or dissipative element).*

In this study the concepts of causal loop and causal mesh do not hold an essential place. Nevertheless, the concept of causal path is used a lot, mostly using two characteristics: the length of the path and the gain of the path.

Definition 10. *a. On a bond graph model which presents only dynamic elements in integral causality, the length of a causal path from an element in the set $J_1 = \{C, I, R, Se, Sf\}$ to an element in the set $J_2 = \{C, I, R, De, Df\}$ is equal to the number of dynamic elements I and C on the causal path, $+1$ if the element in J_2 is a dynamic element in integral causality.*
b. On a bond graph model in integral causality, which still presents dynamic elements in derivative causality, the generalized length of a causal path is equal to the difference between the number of dynamic elements in integral causality and the number of dynamic elements in derivative causality along the path, $+1$ if the element in J_2 is a dynamic element.

Definition 11. *The gain of the causal path is defined as being the function which connects the input variable of the element on one end to the output variable of the element on the other end of the causal path. In the LTI case,*

the gain of the causal path is:

$$T_i = (-1)^{n_0+n_1} \prod_i {m_i}^{k_i} \prod_j {r_j}^{l_j} \prod_e g_e \tag{2.5}$$

where:

- n_0*: number of orientation switches in 0 junctions when the flow variable is followed;*
- n_1*: number of orientation switches in 1 junctions when the effort variable is followed;*
- m_i*: gain of the element* TF_i *(transformer) along the causal path, with* $k_i = +1$ *or* $k_i = -1$*, according to the causality on the transformer;*
- r_j*: gain of the element* GY_j *(gyrator) along the causal path, with* $l_j = +1$ *or* $l_j = -1$*, according to the causality on the gyrator;*
- g_e*: gain of the* R*,* I *and* C *elements along the causal path.*

2.2.2 Vectorial Representation

A bond graph model is composed by basic elements, associated to ports, I and C elements for energy storage, R elements for energy dissipation, Se, Sf, MSe and MSf for energy sources and De, Df for detectors. The elements 0, 1 (junctions), MTF, TF (transformers) and MGY, GY (gyrators) compose the junction structure, which exchanges energy with various parts of the dynamic system and which must insure energy conservation. The vectorial representation is presented in figure 2.11. The algebraic representation for linear models is given by equation (2.6).

$$\begin{pmatrix} \dot{x}_i \\ z_d \\ D_{in} \\ y \\ z \end{pmatrix} = \begin{pmatrix} S_{11} & S_{12} & S_{13} & S_{14} & S_{15} \\ S_{21} & S_{22} & S_{23} & S_{24} & S_{25} \\ S_{31} & S_{32} & S_{33} & S_{34} & S_{35} \\ S_{41} & S_{42} & S_{43} & S_{44} & S_{45} \\ S_{51} & S_{52} & S_{53} & S_{54} & S_{55} \end{pmatrix} \begin{pmatrix} z_i \\ \dot{x}_d \\ D_{out} \\ u \\ d \end{pmatrix} \tag{2.6}$$

State vector x_i is composed by energy variables p for I elements and q for C elements in integral causality. x_d is the vector of the variables associated

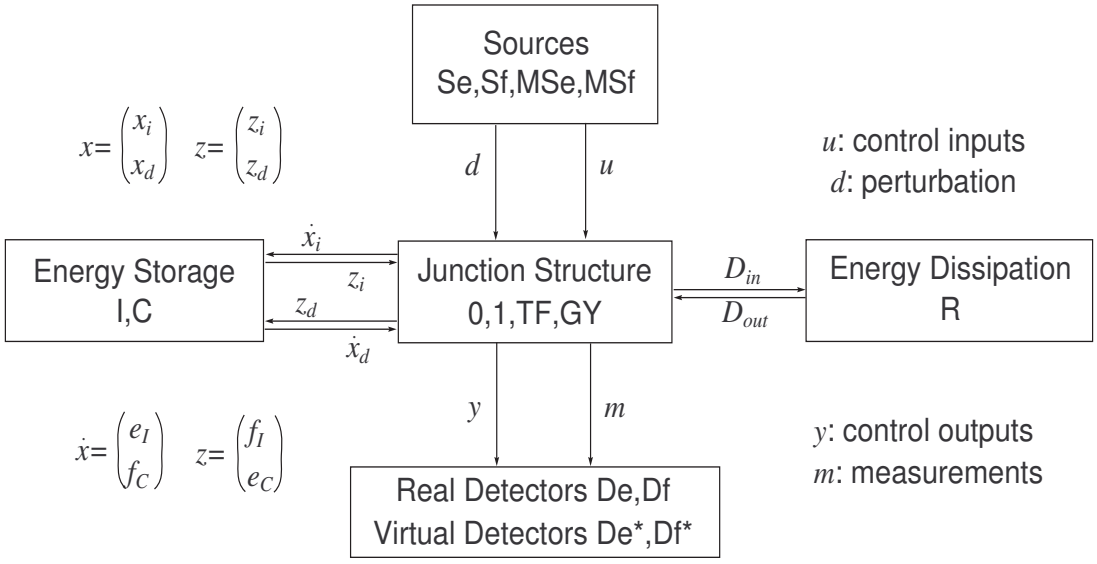

Figure 2.11: Vectorial representation of a bond graph model

to dynamic elements (I and C) in derivative causality. While z_i and z_d are their complementary vectors which contain power variables (f for I elements and e for C elements). D_{in} and D_{out} regroup the efforts and the flows of the dissipative elements R.

For linear bond graph models, S_{ij} are matrices of appropriate dimensions, whose values depend on the junction structure. The matrices S_{11} and S_{33} are skew-symmetric (eq. (2.7)) because the gains of causal paths between dynamic elements in integral causality or between dissipative elements are opposite when the same causal path is considered from each end. Using the same remark concerning the gains of the causal path, equation (2.8) presents the relation between four other matrices.

$$\begin{cases} S_{11} = -S_{11}^T \\ S_{33} = -S_{33}^T \end{cases} \tag{2.7}$$

$$\begin{cases} S_{21} = -S_{12}^T \\ S_{31} = -S_{13}^T \end{cases} \tag{2.8}$$

The elementary laws associated to bond graph elements (R, I and C), also called constitutive laws, are presented for the linear case by equation (2.9),

$$\begin{cases} D_{out} = LD_{in} \\ z_i = F_i x_i \\ z_d = F_d x_d \end{cases} \tag{2.9}$$

where the matrices L, F_i and F_d are diagonal matrices containing the information characterizing the dissipation laws, the relations between the effort and the flow in storage elements in integral and respectively derivative causality.

Remark 6. *In the definition of vectorial representation of linear bond graphs, two hypothesis have been considered:*

- *Two storage elements in derivative causality are not causally linked, i.e.* $S_{22} = 0$. *Otherwise, switching the causality along this causal path brings the two elements in integral causality.*

- *An R element can not be causally linked with a dynamic element in derivative causality , i.e.* $S_{23} = S_{32} = 0$. *Otherwise, changing the causality along this path brings the dynamic element in integral causality ([31]).*

Determining the state space representation (2.10) from the vectorial representation is very easy in the linear case.

$$\begin{cases} \dot{x}_i = Ax_i + B_u u + B_d d \\ y = C_y x_i + D_u u + D_d d \\ z = C_z x_i + R_u u + R_d d \end{cases} \tag{2.10}$$

Equations (2.11)-(2.15) present the relations between state space representation and the vectorial representation supposing that there are no dynamic elements in derivative causality on the bond graph model.

$$A = [S_{11} + S_{13}(I - LS_{33})^{-1} LS_{31}]F_i \tag{2.11}$$

$$\begin{cases} B_u = S_{14} + S_{13}(I - LS_{33})^{-1} LS_{34} \\ B_d = S_{15} + S_{13}(I - LS_{33})^{-1} LS_{35} \end{cases} \tag{2.12}$$

$$\begin{cases} C_y = [S_{41} + S_{43}(I - LS_{33})^{-1}LS_{31}]F_i \\ C_z = [S_{51} + S_{53}(I - LS_{33})^{-1}LS_{31}]F_i \end{cases} \tag{2.13}$$

$$\begin{cases} D_u = S_{44} + S_{43}(I - LS_{33})^{-1}LS_{34} \\ D_d = S_{45} + S_{43}(I - LS_{33})^{-1}LS_{35} \end{cases} \tag{2.14}$$

$$\begin{cases} R_u = S_{54} + S_{53}(I - LS_{33})^{-1}LS_{34} \\ R_d = S_{55} + S_{53}(I - LS_{33})^{-1}LS_{35} \end{cases} \tag{2.15}$$

2.3 Graphical Methods in System Analysis

The graphical procedures developed for structured systems and LTI bond graph models for system analysis are similar. In this section, these methods are presented in the two cases. The focus is mainly on the study of controllability property, while procedures for determining the observability property are tackled only superficially.

Structured system are based on "non-zero" cells in the state space representation, while in the bond graph models the elements are considered without the exact numerical value of the physical components. In both cases, for certain values of the parameters the controllability and observability properties can be easily determined using numerical criterion (rank condition for the controllability/observability matrix). For some values a property may be true, while for other values not. However, it turns out that once a property is true for one parameter value, it is true for almost all parameter values. Therefore, a property which is true for almost all parameter values, is also often said to be true generically ([13]). The aim of this section is to recall the graphical procedures which have been introduced for studying structural properties.

From this point of view, there is a difference between the structural properties for structured systems and bond graphs. On the structured system the parameters are localized on the gains of the arcs, while on the bond graphs the parameters are localized in the elements. This means that on the structured systems some parameters may appear on different arcs, while on the bond graph this problem does not appear. In practice this can generate some erroneous results for the structured systems because a rank condition may

be false due to the connection of parameters. Therefore the results obtained with the bond graph methodology are more reliable than the ones obtained on structured systems.

2.3.1 System Analysis for Structured Systems

Structural properties have been studied since the 1970's. In [25], [43], [47], [48] and [51], some results concerning structural system analysis have been provided. In this section, we recall the most important methods for determining structural properties. Controllability and observability properties can be determined using the following two theorems.

Theorem 7. *[47] An LTI structured system is generically controllable if and only if in the graph G, every state vertex is the end vertex of an U-rooted path and there exists a disjoint union of U-rooted path family and a cycle family that covers all state vertices.*

Theorem 8. *[47] An LTI structured system is generically observable if and only if in the graph G, every state vertex is the start vertex of an Y-toped path and there exists a disjoint union of Y-toped path family and a cycle family that covers all state vertices.*

These theorems allows to check the structural controllability, respectively observability, of the system on the associated graph.

2.3.2 System Analysis with a Bond Graph Approach

The structural controllability and observability properties can be determined for a given LTI system using its bond graph representation and graphical transformations, without calculating the rank of the controllability matrix and of the observability matrix respectively. These results have been introduced in [56].
Consider n as the number of dynamic elements in integral causality on the bond graph model in integral causality.
Prior to giving the procedure for determining whether a bond graph model of an LTI system is controllable/observable or not, a few definitions should be made.

Definition 12. *[56] c is the number of dynamical elements which are still in integral causality after the following transformations are performed:*

- *derivative causality is imposed on the bond graph model.*
- *all the necessary dualisations of the input sources have been made to eliminate the dynamic elements which keep on the integral causality, without introducing unsolvable causal loops.*

Definition 13. *[56] Consider the matrix* $[A\ B]$*, the bond graph rank of this matrix is noted* $bg\_rk[A\ B]$ *and is calculated according to equation (2.16).*

$$bg\_rk[A\ B] = n - c \tag{2.16}$$

Using these definitions the condition for structural controllability of a bond graph model can be expressed as in theorem 9.

Theorem 9. *[56] A bond graph model is structurally controllable iff :*

- $bg\_rk[A\ B] = n$.
- *each dynamic element in integral causality on the bond graph in integral causality is causally linked to an input source.*

Using the same steps, the observability property can be determined based on the bond graph model.

Definition 14. *[56] o is the number of dynamical elements which are still in integral causality after the following transformations are performed:*

- *derivative causality is imposed on the bond graph model.*
- *all the necessary dualisations of the output detectors have been made to eliminate the dynamic elements which keep on the integral causality, without introducing unsolvable causal loops.*

Definition 15. *[56] Consider the matrix* $\begin{bmatrix} C \\ A \end{bmatrix}$*, the bond graph rank of this matrix is noted* $bg\_rk \begin{bmatrix} C \\ A \end{bmatrix}$ *and is calculated according to equation (2.17).*

$$bg\_rk \begin{bmatrix} C \\ A \end{bmatrix} = n - o \tag{2.17}$$

Observability of a bond graph model can be determined using theorem 10.

Theorem 10. *[56] A bond graph model is structurally observable iff :*

- $bg\_rk \begin{bmatrix} C \\ A \end{bmatrix} = n.$
- *each dynamic element in integral causality on the bond graph in integral causality is causally linked to an output detector.*

Remark 7. *The concept of dualization used in definitions 12 and 14 represents the old type of duality (described in [6] and recalled in section 3.1.2.1) which consists of interchanging the flow and the effort variables. In the case of these two definitions, this means that a flow source or a flow detector can be replaced by an effort source or an effort detector and vice versa.*

2.4 Decoupling Problem with a Graphical Approach

The decoupling or noninteracting control problem is one of the most famous problems of control theory. Besides its practical interest, it has also led to a number of fundamental results of general interest in system theory. Let us recall the formulation of the problem (also known as the row-by-row decoupling problem or Morgan's problem) and graphical procedures which were proposed for the decoupling of LTI models.
Given an LTI system of type (2.1), where we assume that the system is square, i.e. the system has the same number of inputs and outputs ($m = p$). The plant described by (2.1) is combined with the feedback law

$$u(t) = Fx(t) + Gv(t) \tag{2.18}$$

where v is an m-tuple and the matrices F and G have appropriate dimensions. The plant is said to be decoupled if the i^{th} input affects only the i^{th} output for $i = 1, 2, \ldots, m$ (of course the renumbering of inputs/outputs is possible).
It has been shown in [15] that this problem has a solution if and only if the

infinite structure of the global system $\Sigma(C, A, B)$ coincides with the union of the infinite structures of the m row subsystems $\Sigma(c_i, A, B)$, $i = 1, 2, \ldots, m$ obtained by focusing on each output component individually as the output of system.
In the following, two graphical approaches, first the structured systems approach and secondly the bond graph approach, are presented for solving the decoupling problem for LTI models. These two perspectives are presented in parallel since they resemble a lot and they are based on the same mathematical background.

2.4.1 System Analysis

This section concerns the system analysis part of the decoupling problem. Graphical procedures exist in both cases, structured systems and bond graphs, for deciding whether an LTI model can be decoupled or not by a static state feedback control law of type (2.18). As stated before, these procedure are based on the global and row infinite structure, therefore they can be reduced to determining these infinite structures. Some definitions concerning the global and row infinite structure are recalled. Then, we are going to focus on graphical methods for the determining the infinite structures of structured systems and afterwards using bond graph models.

2.4.1.1 Infinite Structure. Definitions

Infinite zero orders of a global system are defined using the infinite Smith-McMillan form.

Definition 16. *[26] Given a rational matrix $T(s) \in \mathbb{R}_{rat}^{p\times m}$ of rank r, it is always possible to find two bicausal matrices $U(s)$ and $V(s)$ which verify equations (2.19) and (2.20), where $\Phi(s)$ is called the infinite Smith-McMillan form.*

$$T(s) = U(s)\Phi(s)V(s) \tag{2.19}$$

$$\Phi(s) = \begin{pmatrix} s^{-n'_1} & 0 & \cdots & 0 \\ 0 & \ddots & \ddots & \vdots \\ \vdots & \ddots & s^{-n'_r} & 0 \\ 0 & \cdots & 0 & 0 \end{pmatrix} \tag{2.20}$$

The coefficients n'_1 are ordered decreasingly in the matrix $\Phi(s)$. They characterize the infinite orders of poles or zeros of the matrix $T(s)$, as can be seen from the following theorem.

Theorem 11. *[16] Given a rational matrix $T(s) \in \mathbb{R}_{rat}^{p\times m}$ of rank r, the infinite Smith-McMillan form of $T(s)$ is unique. If n'_i is positive then it is called infinite zero order. If n'_i is negative then it is called infinite pole order.*

Definition 17. *[15] The infinite structure of the global system $\Sigma(C, A, B)$ is composed by the set of orders of zero at infinity of its transfer matrix.*

The relation between the input-output perspective and infinite structure of the global system is given by the following property.

Property 1. *[19] The global orders of zero at infinity are equal to the minimal number of derivatives of each output variable necessary so that the input variables appear explicitly and independently in the equations.*

For each row subsystem $\Sigma(c_i, A, B)$, it is associated an infinite structure, called row infinite structure. This structure characterizes each output variable taken separately.

Definition 18. *The order of zero at infinity of the row subsystem $\Sigma(c_i, A, B)$ is the integer n_i, which verifies equation (2.21).*

$$n_i = min\left\{j \in \mathbb{N} | c_i A^{j-1} B \neq 0\right\} \tag{2.21}$$

Property 2. *The integer n_i is equal to the number of derivatives of the output variable $y_i(t)$ necessary so that an input variable appears explicitly.*

2.4.1.2 Graphical methods for LTI Structured Systems

In this subsection, we recall a graph theoretic characterization of the generic infinite structure of a structured system. These results have been presented in [11],[55] and [59].

Property 3. *The order of zero at infinity for the row sub-system $\Sigma(c_i, A, B)$ is equal to the length of the shortest path between the i^{th} output vertex y_i and the set of input vertices.*

Property 4. *The global orders of zero at infinity of an invertible model are calculated according to equation (2.22), where L_k is the smallest sum of the lengths of k different input-output paths.*

$$\begin{cases} n'_1 = L_1 \\ n'_k = L_k - L_{k-1} \end{cases} \tag{2.22}$$

Using these properties and the result proposed in [15], we can decide graphically whether an LTI system can be decoupled by a state feedback control law.

2.4.1.3 Bond Graph Approach

The results concerning the infinite structure for LTI bond graph models have been developed in [57]. The graphical procedures for determining the infinite structure on a bond graph model are based on the following properties.

Property 5. *[57] The order of the at infinity n_i of the row subsystem $\Sigma(c_i, A, B)$ is equal to the length of the shortest causal path between the output detector and the set of input sources.*

Property 6. *[57] The number of zeros at infinity of the global system represented by a bond graph is equal to the maximal number of different input-output causal paths.*

Property 7. *[57] The orders of zero at infinity n'_i of the global invertible system $\Sigma(C, A, B)$ are determined according to equation (2.23), where L_k is the smallest sum of the lengths of k different input-output causal paths on a bond graph model.*

$$\begin{cases} n'_1 = L_1 \\ n'_k = L_k - L_{k-1} \end{cases} \tag{2.23}$$

2.4.2 Control Synthesis

Theorem 12. *[15] An LTI square system can be decoupled by a regular static state feedback control law if and only if the set of orders of zero at infinity of*

the global system $\Sigma(C, A, B)$ *is equal to the set of orders of zero at infinity of the row sub-systems* $\Sigma(c_i, A, B)$, $i = 1, 2, \ldots, m$.

If the conditions from theorem 12 are fulfilled then the decoupling state feedback law (2.18) has the following expression([19] and [61]):

$$F = -\Omega^{-1} \begin{pmatrix} c_1 A^{n_1} \\ \vdots \\ c_m A^{n_m} \end{pmatrix} \tag{2.24}$$

$$G = \Omega^{-1} diag(g_i)_{i=1,\ldots,m} \tag{2.25}$$

where Ω is given by relation (2.26) and $diag(g_i)$ is a diagonal matrix with parameters g_i influencing the statical gain of each input-output decoupled channel.

$$\Omega = \begin{pmatrix} c_1 A^{n_1-1} B \\ \vdots \\ c_m A^{n_m-1} B \end{pmatrix} \tag{2.26}$$

The graphical methods for control synthesis concern the computation of the matrices Ω and $\begin{pmatrix} c_1 A^{n_1} \\ \vdots \\ c_m A^{n_m} \end{pmatrix}$. In fact this means calculating the vectors $c_i A^{n_i}$ and $c_i A^{n_i-1} B$.

Determining the vectors $c_i A^{n_i}$ and $c_i A^{n_i-1} B$ is similar for the structured systems and for the bond graph models, therefore we present these graphical procedures together.

The vectors $c_i A^{n_i}$ represent the gains of the paths of length n_i between the output vertex y_i and state vertices x_j, $j = 1, \ldots, n$ on a structured system. The gain of each path is obtained by multiplying the gains of the arcs along the path. Analogously, on a bond graph model, the vectors $c_i A^{n_i}$ represent the gains of the causal paths of length n_i between the i^{th} output detector and the dynamic elements in integral causality. These gains can be determined according to definition 11.

For the vectors $c_i A^{n_i-1} B$ we have to take into account the gains of the path of length n_i between the output vertex y_i and the input vertices u_k, $k = 1, \ldots, m$ on the graph representation of the structured system. Similarly, on the bond graph model, we have to determine the gains of the causal path of length n_i

between the i^{th} output detector and the input sources in order to determine the vectors $c_i A^{n_i-1} B$.

Once the matrices Ω and $\begin{pmatrix} c_1 A^{n_1} \\ \vdots \\ c_m A^{n_m} \end{pmatrix}$ are determined graphically, the results are introduced in equations (2.24) and (2.25) and we obtain the decoupling state feedback control law.

2.5 Decoupling Problem with Stability

Supposing that, for a given system, the existence of a solution for the decoupling by static state feedback control problem is proven, we want to find the solution which allows to decouple the system and to insure system stability. This problem has been introduced for LTI systems by [19] and [24] at the end of the 1960's. For square systems, it has been proven that by imposing a decoupled structure by a state feedback control law, some modes of the closed loop system could not be freely assigned. In [61] and [44], these modes are called fixed modes. In this section, we are only interested in the most simple type of system decoupling which does not interfere with the invariant zeros. If the system can be decoupled with stability by a state feedback control law, then the decoupling state feedback control law:

$$u(t) = Fx(t) + Gv(t) \tag{2.27}$$

is given be relations (2.28) and (2.29).

$$F = -\Omega^{-1}(c_i A^{n_i} + \sum_{j=0}^{n_i-1} p_{ij} c_i A^j)_{i=1,\dots,m} \tag{2.28}$$

$$G = \Omega^{-1} diag(g_i)_{i=1,\dots,m} \tag{2.29}$$

where the parameters p_{ij} are used for defining the dynamic behavior of the closed loop decoupled system by pole placement.

If we note by $Z(C, A, B)$ the set of invariant zeros of the global system $\Sigma(C, A, B)$ and by $Z(c_i, A, B)$ the set of invariant zeros of the row subsystem $\Sigma(c_i, A, B)$, the fixed modes are $Z(C, A, B) - \bigcup_i Z(c_i, A, B)$. If they are stable, we can find the control law (2.28), which stabilizes the system. The

control law (2.28) does not allow to make reappear the invariant zeros, which become unassigned poles.

2.5.1 Graphical Methods for Determining the Control Law

Determining the solution for the decoupling with stability problem means that beside calculating the vectors $c_i A^{n_i}$, we have to determine also the vectors $c_i A^j$, with $j < n_i$. Graphical computation is similar in the two cases.
On a structured system graph, the vectors $c_i A^j$ are determined using the gains of the paths of length j between the i^{th} output vertex and all the state vertices.
On a bond graph model, the vectors $c_i A^j$ are determined using the gains of the causal paths of length j between the i^{th} output detector and all the dynamic elements in integral causality.

2.6 Conclusions

In this chapter, we have recalled two of the graphical representations which will be used through this report: the structured systems and the bond graphs. These representations offer a graphical framework on which we have developed different procedures for the study of the duality.
System analysis for LTI models using graphical procedures, both on structured systems and on bond graphs, will be extended in the next chapter for LTV models. The study of controllability and observability properties for LTV models has not been done graphically, yet. In chapter 3, we tackle this problem focusing on the duality between these two structural properties. The different approaches for structured systems and bond graphs will be pointed out in the next chapter.
We have recalled here, the graphical solution for the decoupling problem because, in chapter 4, we are going to discuss the duality between the state feedback and output injection control laws where we consider as application the decoupling problem, both without and with pole placement. As these decoupling procedures do not exist for LTV case, we have presented the LTI

case so that the reader may be familiar with the graphical approach.

Chapter 3

Dual Model. Dual Properties

The concept of duality is one of the cornerstones of this study. We have worked in two research directions: the structured systems and the bond graph models. These results have been published in [40] for the structured systems and in [37] for the bond graphs. In both cases we have developed the concept of dual system introduced in [50] through graphical representations. The natural way for starting a study of duality is by defining the dual system. As our study is divided for the structured systems and bond graphs, we keep the two studies in parallel.
In the second part of this chapter, we focus on the concept of duality in the system analysis. Graphical methods are proposed for the study of the controllability and observability properties.

3.1 Dual Model. A Graphical Approach

The study of the duality in linear systems begins with the definition of a dual model. In chapter 1, we have seen the definition of duality from the state space representation point of view and with the module theoretical approach. This part of chapter 3 presents the dual model from a graphical perspective, using the graph representation of a structured system and of a bond graph model.

3.1.1 A Structured System Procedure

There is a direct link between the state space representation and the structured system, therefore the definition of the dual structured system is obtained from the definition of the dual model in the state space representation. The dual of the system $\Sigma(A, B, C, D)$ is $\bar{\Sigma}(-A^T, C^T, -B^T, D^T)$.

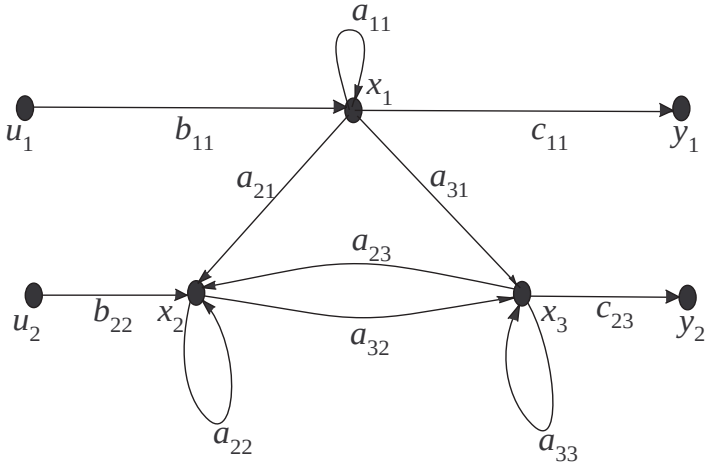

Figure 3.1: Structured system

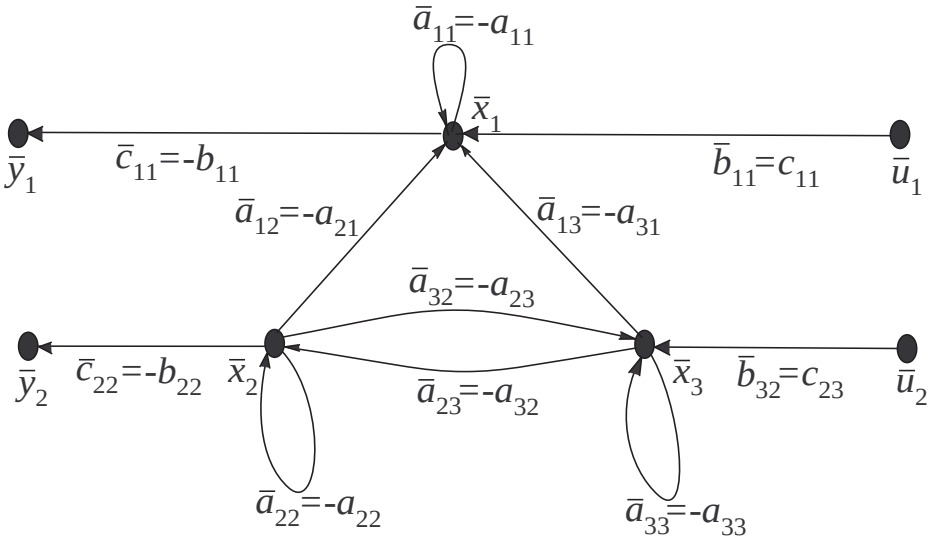

Figure 3.2: Dual Structured System

Procedure

Given a structured system like in figure 3.1. The dual model of the structured system is obtained if the following steps are performed:

1. Draw the graph of the system Σ.

2. Multiply the gains of the arcs between the input vertices and the state vertices by -1: $gain((u_i, x_j)) := -gain((u_i, x_j)), \forall i, j$.

3. Multiply the gains of the arcs between the state vertices by -1: $gain((x_i, x_j)) := -gain((x_i, x_j)), \forall i, j$.

4. Switch the sense of the arcs.

5. Rename the vertices:

   - $u \rightarrow \bar{y}$
   - $y \rightarrow \bar{u}$
   - $x \rightarrow \bar{x}$

Using this procedure, the dual structured system of the model in figure 3.1 is the model in figure 3.2. A remark is nonetheless needed regarding this procedure. The schema of transformations presented in figure 1.1, which concern the duality procedure in the state space representation, is also true in the case of structured systems.

3.1.2 Dual Bond graph Model

Before this study had begun, the bond graph methodology, already contained the concept of duality. This concept of duality, based on physical and graphical considerations, is recalled in the first part of this section. In the second part, we introduce the new concept of dual bond graph model, a definition which is based on the mathematical results from [50]. In fact, this definition of duality is the cornerstone of this report, most of the results are fundamentally linked to it.

3.1.2.1 Duality in Bond graph Methodology

The concept of duality is widely known in the bond graph community. The results concerning this duality have been presented in [6]. This type of duality concern the pair effort-flow. In the following, we recall the most important definitions which have been introduced in [6] and their applications. Of course, we are going to point out some disadvantages of this method, disadvantages which are over-passed with the new type of duality.

Definition 19. *[6] Let B be a bond graph. The dual bond graph of B, denoted by B^*, is the bond graph which is identical to B, except that the labels on the junctions are exactly opposite to those of B.*

By definition, the 0-junctions of B correspond to the 1-junctions of B^* and vice versa. In fact, the dualization procedure consists of the following interchanges:

- 0-junction $\leftrightarrow$ 1-junction
- Effort source $Se \leftrightarrow$ Flow source Sf
- Effort detector $De \leftrightarrow$ Flow detector Df
- C-element $\leftrightarrow$ I-element

But, the most important transformation which occurs is the switch of causality.

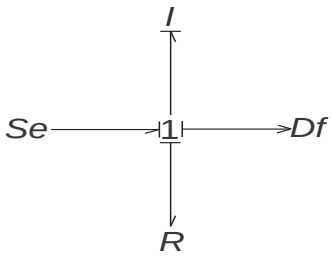

Figure 3.3: Simple bond graph model

Example 5. *In figure 3.3, we have consider an example. The dual bond graph is presented in figure 3.4. The state space representation in the two*

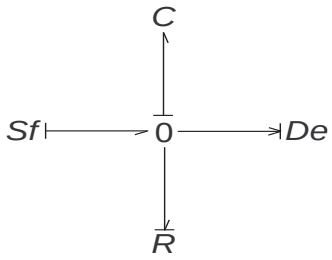

Figure 3.4: Dual bond graph model

case are identical. For the system in figure 3.3, the state space representation (3.1) is obtained, while for its dual bond graph from figure (3.4), we obtain relation (3.2).

$$\begin{cases} \dot{p}_I = -\frac{R}{I} p_I + u \\ y = \frac{1}{I} p_I \end{cases} \tag{3.1}$$

$$\begin{cases} \dot{q}_C = -\frac{1}{RC} q_C + u \\ y = \frac{1}{C} q_C \end{cases} \tag{3.2}$$

Due to the switch of causality the value of the dissipative element on the dual bond graph is inverse. But beside that, the two representations are identical.

Even though from the physical point of view, this type of duality offers an elegant switch between the effort and flow variables, from the mathematical point of view it does not provide any information since the two representations are mathematically equivalent. This is the reason why a new type of duality which offers a physical and mathematical perspective should be introduced. The next section concerns the definition of this new concept of duality.

3.1.2.2 Dual Bond graph Model in the Algebraic Framework

The dualization procedure proposed in [50], and recalled in section 1.3.1, offers a mathematical approach to the study of duality. The aim of this section is to define the dual bond graph model using the same algebraic background. In the following, we present a graphical procedure for determining the dual bond graph and in the end we provide a proof that the model which is obtained offers the same mathematical structure as the procedure from section

1.3.1.

Three steps must be performed for obtaining the dual bond graph model:

1. *Graphic transformations on bond graph model.*
2. *Reverse the outputs.*
3. *State variable change.*

Each step is going to be discussed in the following subsections and in the end a proof is performed to prove that the dual bond graph model respects the definition used in [50], from the module theory point of view, and in [58] with the state space representation.

Graphic Transformations on Bond Graph Model

Using the bond graph of the system $\sum$ the following transformations are performed:

1. The sources become the detectors;
2. The detectors become the sources;
3. The $R:R$ elements have their value changed into $R:(-R)$
4. For each time varying C-element in integral causality, add a dissipative element with the gain $R:-\frac{1}{\frac{dC(t)}{dt}}$ (see figure 3.5).
5. For each time varying I-element in integral causality, add a dissipative element with the gain $R:-\frac{dI(t)}{dt}$ (see figure 3.5).

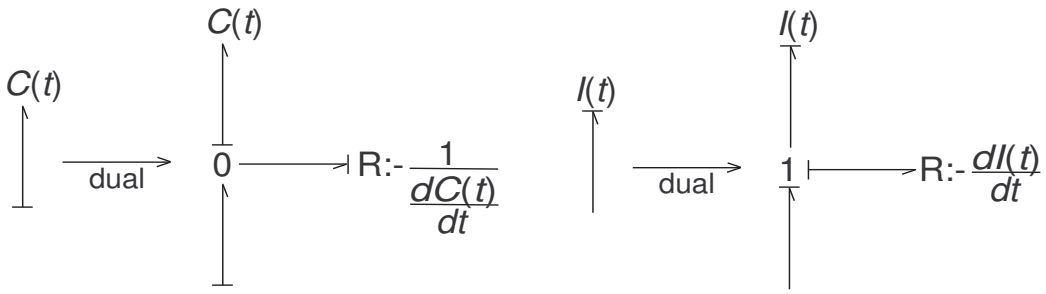

Figure 3.5: Supplementary dissipative elements

These changes affect only some of the matrices in the vectorial representation of the bond-graph (eq. (2.6)). These modifications will be used in the proof which follows the procedure. The modifications are in appendix A.2, due to the repetitive explanations.

Remark 8. *For LTI models, the dualization procedure stops after the step 3; the steps 4 and 5 of the procedure are not considered because there are no dynamic elements with time-varying gains.*

Reverse the outputs

The value of the outputs is considered with a negative value, i.e. $\bar{y} = -y$. This change influences the computations on the matrices $\bar{C}$ and $\bar{D}$, and brings a similar perspective as in the module theoretical approach when the same principle is applied to the outputs.

State variable change

The state variable of the dual system $\bar{\Sigma}$ is $\bar{x} = Fx$, where F is a square diagonal matrix that contains the information about the dynamic elements in the bond graph and is the same as the one used in the vectorial representation of the bond graph, and x is the state vector of the given system Σ.

Remark 9. *If on the bond graph model of the system Σ, the state variables are the energy variables of the storage elements (the generalized momentum p_I for I-elements and the generalized displacement q_C for C-elements), on the dual bond graph model the state variables are the co-energy variables of the storage elements (the flow f_I for I-elements and the effort e_C for C-elements).*

Theorem 13. *If the graphical procedure presented above is performed, then the resulting bond graph model is the dual system, i.e. the state space representation of the dual system is given by equations (1.16-1.19).*

Proof

As the module theoretical approach and the state space representation approach are already proved to be similar in [50], our interest is to prove that the bond graph perspective is similar with only one of them. The state space representation is chosen here because it is more intuitive.

Because of the lack of space only the computation of the matrix $\bar{A}$ is presented. For the others, only the final result is given.
We want to prove that $\bar{A} = -A^T$. The expression of $\bar{A}$ should be calculated on the dual bond graph model $\bar{\sum}$, and the expression of A^T on the bond graph model $\sum$. In both cases the vectorial representation of the bond graph model is used, further information can be found in annexe A.2.
Firstly the matrix $\bar{A}$ has to be calculated. Consider the state vector of the dual bond graph model as x, then

$$\dot{x} = \tilde{A}x + \tilde{B}\bar{u}, \tag{3.3}$$

where

$$\tilde{A} = [\bar{S}_{11} + \bar{S}_{13}(I - \bar{L}\bar{S}_{33})^{-1}\bar{L}\bar{S}_{31}]F. \tag{3.4}$$

If the state variable change $\bar{x} = Fx$ is performed, then

$$(\dot{F^{-1}})\bar{x} + F^{-1}\dot{\bar{x}} = \tilde{A}F^{-1}\bar{x} + \tilde{B}\bar{u}, \tag{3.5}$$

which is equivalent to

$$\dot{\bar{x}} = F(\tilde{A}F^{-1} - (\dot{F^{-1}}))\bar{x} + F\tilde{B}\bar{u}, \tag{3.6}$$

and therefore

$$\bar{A} = F(\tilde{A}F^{-1} - (\dot{F^{-1}})) = F[\bar{S}_{11} + \bar{S}_{13}(I - \bar{L}\bar{S}_{33})^{-1}\bar{L}\bar{S}_{31} - (\dot{F^{-1}})], \tag{3.7}$$

which implies, after the modifications in appendix A.2 and the notations form appendix A.1 that

$$\begin{aligned}\bar{A} = F[S_{11} + \begin{pmatrix} S_{13} & I_{n\times q} \end{pmatrix} (I + \begin{pmatrix} -L & 0_{n_R\times q} \\ 0_{q\times n_R} & -L_d \end{pmatrix} \begin{pmatrix} S_{33} & 0_{n_R\times q} \\ 0_{q\times n_R} & 0_{q\times q} \end{pmatrix})^{-1} \\ \begin{pmatrix} -L & 0_{n_R\times q} \\ 0_{q\times n_R} & -L_d \end{pmatrix} \begin{pmatrix} S_{31} \\ -I_{q\times n} \end{pmatrix} - (\dot{F^{-1}})].\end{aligned} \tag{3.8}$$

After some simple matrix computations we obtain:

$$\bar{A} = F[S_{11} - S_{13}(I + LS_{33})^{-1}LS_{31} + I_{n\times q}L_dI_{q\times n} - (\dot{F^{-1}})]. \tag{3.9}$$

But according to property 37 $I_{n\times q}L_dI_{q\times n} = \frac{d}{dt}(F^{-1})$, which means that the last two terms cancel each other and we obtain:

$$\bar{A} = F[S_{11} - S_{13}(I + LS_{33})^{-1}LS_{31}]. \tag{3.10}$$

Secondly the matrix A^T has to be calculated using the bond graph model $\sum$. Its expression is as follows:

$$\begin{aligned} A^T &= F^T[S_{11}^T + S_{31}^T L^T (I - S_{33}^T L^T)^{-1} S_{13}^T] \\ &= F[-S_{11} + S_{13} L (I + S_{33} L)^{-1} S_{31}]. \end{aligned} \tag{3.11}$$

As matrix L is invertible,

$$L(I + S_{33}L)^{-1} = (I + LS_{33})^{-1}L, \tag{3.12}$$

and therefore

$$\begin{aligned} A^T &= F[-S_{11} + S_{13}(I + LS_{33})^{-1} L S_{31}] \\ &= -F[S_{11} - S_{13}(I + LS_{33})^{-1} L S_{31}]. \end{aligned} \tag{3.13}$$

From the expressions of $\bar{A}$ and A^T we can conclude that

$$\bar{A} = -A^T \tag{3.14}$$

From equation(3.5), we obtain also that $\bar{B} = F\tilde{B}$, which means that:

$$\bar{B} = F(\bar{S}_{14} + \bar{S}_{13}(I - \bar{L}\bar{S}_{33})^{-1}\bar{L}\bar{S}_{34}) \tag{3.15}$$

Let us now consider the transformations which appear on the S-matrices from appendix A.2. This means that:

$$\bar{B} = F^T(S_{41}^T - S_{31}^T(I + LS_{33})^{-1} L S_{43}^T) \tag{3.16}$$

On the other hand, we determine the matrix C^T by transposing the matrix C of the system Σ:

$$C^T = F^T(S_{41}^T + S_{31}^T L(I - S_{33}^T L^T)^{-1} S_{43}^T) \tag{3.17}$$

Using relations (2.8) and (3.12), we obtain:

$$C^T = F^T(S_{41}^T - S_{13}(I + LS_{33})^{-1} L S_{43}^T) \tag{3.18}$$

By comparing expressions (3.16) and (3.18), we observe that

$$\bar{B} = C^T \tag{3.19}$$

The output expression of the dual bond graph is:

$$-\bar{y} = \tilde{C}\tilde{x} + \tilde{D}\bar{u} \tag{3.20}$$

After the variable change $\bar{x} = Fx$, we obtain:

$$-\bar{y} = \tilde{C}F^{-1}\bar{x} + \tilde{D}\bar{u} \tag{3.21}$$

which means that $\bar{C} = -\tilde{C}F^{-1}$ and $\bar{D} = -\tilde{D}$.
Let us determine first the $\bar{C}$.

$$\bar{C} = -\tilde{C}F^{-1} = -(\bar{S}_{41} + \bar{S}_{43}(I - \bar{L}\bar{S}_{33})^{-1}\bar{L}\bar{S}_{31}) \tag{3.22}$$

Using the transformations from appendix A.2, we obtain:

$$\bar{C} = -(S_{14}^T - S_{34}^T(I + LS_{33})^{-1}LS_{31}) \tag{3.23}$$

On the other hand, we determine the matrix B^T by transposing the matrix B of the system Σ:

$$B^T = S_{14}^T + S_{34}^T L(I - S_{33}^T L^T)^{-1}S_{13}^T \tag{3.24}$$

Using relations (2.8) and (3.12), we obtain:

$$B^T = S_{14}^T - S_{34}^T(I + LS_{33})^{-1}LS_{31} \tag{3.25}$$

By comparing expressions (3.23) and (3.25), we observe that

$$\bar{C} = -B^T \tag{3.26}$$

Following the same approach, we continue with the matrix $\bar{D}$.

$$\bar{D} = -(\bar{S}_{44} + \bar{S}_{43}(I - \bar{L}\bar{S}_{33})^{-1}\bar{L}\bar{S}_{34}) \tag{3.27}$$

After the transformations from appendix A.2, this is equivalent to:

$$\bar{D} = -(-S_{44}^T - S_{34}^T(I + LS_{33})^{-1}LS_{43}^T) \tag{3.28}$$

The expression of D^T is:

$$D^T = S_{44}^T + S_{34}^T L^T(I - S_{33}^T L^T)^{-1}S_{43}^T \tag{3.29}$$

By using relations (2.8) and (3.12), this is equivalent to:

$$D^T = S_{44}^T + S_{34}^T(I + LS_{33})^{-1}LS_{43}^T \tag{3.30}$$

By comparing expressions (3.28) and (3.30), we observe that:

$$\bar{D} = D^T \tag{3.31}$$

Even though, as was mentioned before, there are not any relations between the variables in the state representation and in the module representations, the bond graph model offers a lead. It is well known that the state variables of a bond graph model are the energy variables of the dynamic elements in integral causality. For the dual bond graph model, it can be concluded that the state variables are the co-energy variables of the same dynamic elements in integral causality. In the case of physical model, the dual variables can be related to the physical variables.

Remark 10. *In the bond graph literature, the concept of adjoint bond graph has been introduced in [62] for LTI models using a similar procedure.*

Example 6. *Let us consider the separately excited direct current motor (SEDCM). The physical behavior of this motor is nonlinear, but depending on the desired outcome one can use a linear time-varying model instead.*
In this section, the latter case is considered, a SEDCM in which the flux in the stator varies in time. This model can be depicted by relation (3.32),

$$\begin{cases} \frac{d\lambda_{L_r}(t)}{dt} = -\frac{R_r}{L_r}\lambda_{L_r}(t) - \frac{K\Phi(t)}{J}h_J(t) + V_r(t) \\ \frac{dh_J(t)}{dt} = \frac{K\Phi(t)}{L_r}\lambda_{L_r}(t) - \frac{f}{J}h_J(t) \\ y = \frac{1}{J}h_J(t) \end{cases} \tag{3.32}$$

where $\Phi(t)$ is the flux induced by the stator, $\lambda_{L_r}(t)$ and $V_r(t)$ are the flux linkage and the voltage respectively in the rotor (the latter variable is the input source), $h_J(t)$ is the angular momentum of the rotor and the angular velocity is the output variable. The problem is to obtain a constant value for the rotational speed in spite of an induced flux which is under a periodic perturbation of form (3.33).

$$\Phi(t) = \Phi_0(1 + \alpha sin(\omega t)) \tag{3.33}$$

The bond graph model of the SEDCM is presented in figure 3.6, where the state variables are the generalized momenta of the I-elements, $x = \begin{pmatrix} p_{I_1} \\ p_{I_2} \end{pmatrix} = \begin{pmatrix} \lambda_{L_r} \\ h_J \end{pmatrix}$.
The dual model can be constructed using the bond graph in integral causality and the procedure presented above. The dual bond graph model is presented

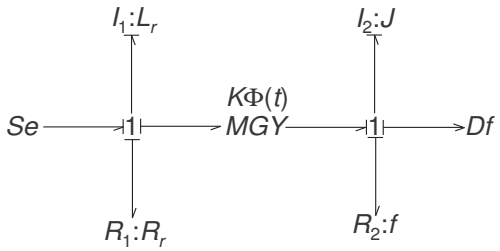

Figure 3.6: Bond Graph of the SEDCM

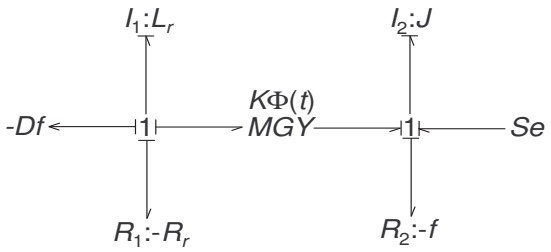

Figure 3.7: Dual Bond Graph Model

in figure 3.7. As one can see, the input and output are reversed and the resistances have negative values. The state space representation of the bond graph in figure 3.7, with the state vector $\tilde{x}(t) = \begin{pmatrix} \tilde{x}_1(t) \\ \tilde{x}_2(t) \end{pmatrix} = \begin{pmatrix} \lambda_{L_r} \\ h_J \end{pmatrix}$ *is:*

$$\begin{cases} \dot{\tilde{x}}_1 = \frac{R_r}{L_r}\tilde{x}_1 - \frac{K\Phi(t)}{J}\tilde{x}_2 \\ \dot{\tilde{x}}_2 = \frac{K\Phi(t)}{L_r}\tilde{x}_1 + \frac{f}{J}\tilde{x}_2 + \bar{u} \\ \bar{y} = -\frac{1}{L_r}\tilde{x}_1 \end{cases} \tag{3.34}$$

The last part of the dualization procedure is the state variable change $\bar{x} = F\tilde{x} = \begin{pmatrix} \frac{1}{L_r} & 0 \\ 0 & \frac{1}{J} \end{pmatrix} \begin{pmatrix} \lambda_{L_r} \\ h_J \end{pmatrix}$. *Therefore, we obtain the state space representation of the dual bond graph model:*

$$\begin{cases} \dot{\bar{x}}_1 = \frac{R_r}{L_r}\bar{x}_1 - \frac{K\Phi(t)}{L_r}\bar{x}_2 \\ \dot{\bar{x}}_2 = \frac{K\Phi(t)}{J}\bar{x}_1 + \frac{f}{J}\bar{x}_2 + \frac{1}{J}\bar{u} \\ \bar{y} = -\bar{x}_1 \end{cases} \tag{3.35}$$

3.1.3 Graphic Computational Rules for the Dual Bond Graph Model

The state vector change $\bar{x} = Fx$, which is synonymous with choosing the power variables as the state variables, causes the modification of the graphical procedures for calculating the gain of a causal path. In this section, we formulate some rules for determining the gain of the causal paths between a dynamic element in integral causality (DE) and a source, a detector and another storage element in integral causality, knowing that the state variables are the flow of the I elements and the effort of the C elements. These computational rules can be used directly on the dual bond graph model and do not require the state variable change. In fact, instead of using the regular bond graph laws and perform the state variable change in the end, these rules can be applied directly. We are going to use these rules for synthesizing control laws for the dual bond graph model in the next chapter. For notational convenience, we have consider that the I and C elements in integral causality present a generic parameter DE.

Property 8. *The gain of the causal path between a source and a dynamic element in integral causality is:*

$$G_{Source \to DE} = (-1)^{n_0+n_1}(\prod_i {m_i}^{k_i})(\prod_j {r_j}^{l_j})(\prod_p {R_p}^{v_p})\frac{1}{DE} \tag{3.36}$$

where:

- n_0*: number of orientation switches in 0 junctions when the flow variable is followed;*
- n_1*: number of orientation switches in 1 junctions when the effort variable is followed;*
- m_i*: gain of the element* TF_i *(transformer) along the causal path, with* $k_i = +1$ *or* $k_i = -1$*, according to the causality on the transformer;*
- r_j*: gain of the element* GY_j *(gyrator) along the causal path, with* $l_j = +1$ *or* $l_j = -1$*, according to the causality on the gyrator;*
- R_p*: gain of the dissipative element* R_p *along the causal path, with* $v_p = +1$ *or* $v_p = -1$*, according to the causality on the* R*-element.*

- *DE: gain of the dynamic element in integral causality at the end of the causal path.*

Property 9. *The gain of the causal path between a dynamic element in integral causality and a detector is:*

$$G_{DE\rightarrow Detector} = (-1)^{n_0+n_1}(\prod_i {m_i}^{k_i})(\prod_j {r_j}^{l_j})(\prod_p {R_p}^{v_p}) \tag{3.37}$$

where:

- n_0*: number of orientation switches in 0 junctions when the flow variable is followed;*
- n_1*: number of orientation switches in 1 junctions when the effort variable is followed;*
- m_i*: gain of the element* TF_i *(transformer) along the causal path, with* $k_i = +1$ *or* $k_i = -1$*, according to the causality on the transformer;*
- r_j*: gain of the element* GY_j *(gyrator) along the causal path, with* $l_j = +1$ *or* $l_j = -1$*, according to the causality on the gyrator.*
- R_p*: gain of the dissipative element* R_p *along the causal path, with* $v_p = +1$ *or* $v_p = -1$*, according to the causality on the R-element.*

Property 10. *The gain of the causal path between a dynamic element in integral causality* DE_i *and another dynamic element in integral causality* DE_j *is:*

$$G_{DE_{in}\rightarrow DE_{out}} = (-1)^{n_0+n_1}(\prod_i {m_i}^{k_i})(\prod_j {r_j}^{l_j})(\prod_p {R_p}^{v_p})\frac{1}{DE_{in}} \tag{3.38}$$

where:

- n_0*: number of orientation switches in 0 junctions when the flow variable is followed;*
- n_1*: number of orientation switches in 1 junctions when the effort variable is followed;*
- m_i*: gain of the element* TF_i *(transformer) along the causal path, with* $k_i = +1$ *or* $k_i = -1$*, according to the causality on the transformer;*

- r_j: *gain of the element* GY_j *(gyrator) along the causal path, with* $l_j = +1$ *or* $l_j = -1$, *according to the causality on the gyrator.*

- R_p: *gain of the dissipative element* R_p *along the causal path, with* $v_p = +1$ *or* $v_p = -1$, *according to the causality on the* R*-element.*

- DE_{in}: *gain of the dynamic element in integral causality at the beginning of the causal path.*

Remark 11. *The gain of the causal loop between a time-varying dynamic element and the corresponding dissipative element which is added on the dual bond graph model is 0.*

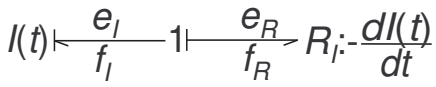

Figure 3.8: Causal loop between dynamic element and its dissipative element

Consider the case of an I-element with its dissipative element on the bond graph model from figure 3.8. For this causal loop, we calculate the gain between the state derivative and the state variable. The state variable of the dual bond graph model is the flow in the I-element $x_i = f_I$. The state derivative is $\dot{x}_i = \dot{f}_I = \frac{d}{dt}\left(\frac{p_I}{I(t)}\right) = \frac{d}{dt}\left(\frac{1}{I(t)}\right) p_I + \frac{1}{I(t)}\frac{dp_I}{dt} = -\frac{\dot{I}(t)}{I^2(t)} I(t) f_I + \frac{1}{I(t)} e_I = -\frac{\dot{I}(t)}{I(t)} f_I + \frac{1}{I(t)}\dot{I}(t) f_R = -\frac{\dot{I}(t)}{I(t)} f_I + \frac{\dot{I}(t)}{I(t)} f_I = 0$. The gain of the causal loop between a time-varying dynamic element and its dissipative element on the dual bond graph model is null because the goal for introducing this dissipative element is to compensate the derivative element which appears when we use a time-varying variable change.
In the sequel, we consider an example and we make a comparative discussion concerning the gains of the causal path if the state variables are the energy variables and if the state variables are the power variables.

Example 7. *Let us consider the electric circuit from figure 3.9, where the gain of the inductance is time-varying. The bond graph model of this circuit is presented in figure 3.10. The state space representation of this bond graph*

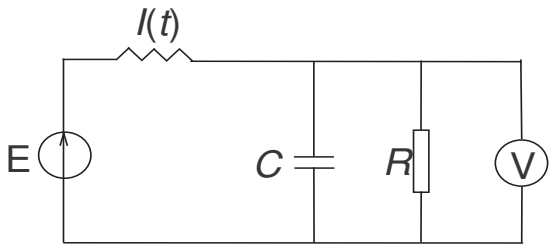

Figure 3.9: Electric circuit

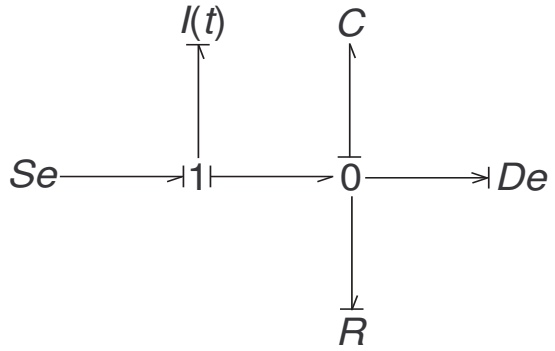

Figure 3.10: Bond Graph Model

model is:

$$A(t) = \begin{pmatrix} 0 & -\frac{1}{C} \\ \frac{1}{I(t)} & -\frac{1}{RC} \end{pmatrix} \quad B = \begin{pmatrix} 1 \\ 0 \end{pmatrix} \qquad C = \begin{pmatrix} 0 & \frac{1}{C} \end{pmatrix} \tag{3.39}$$

The dual bond graph model is obtained following the procedure presented in the previous section. In figure 3.11, the dual bond graph model is pictured. Using this model, we illustrate each type of causal path and the way of computing its gain in the two cases, when the state vector contains the energy variables and when the state vector is composed by the power variables.

In figure 3.12, the causal path between the source Sf and the dynamic C element is presented. This gain g represents the connection between the state derivative and the input $\dot{x} = gu$. Here the input u is the flow of the source. In the first case, the regular computational bond graph methodology, the state variable is the generalized displacement of the C-element q_C and the gain of

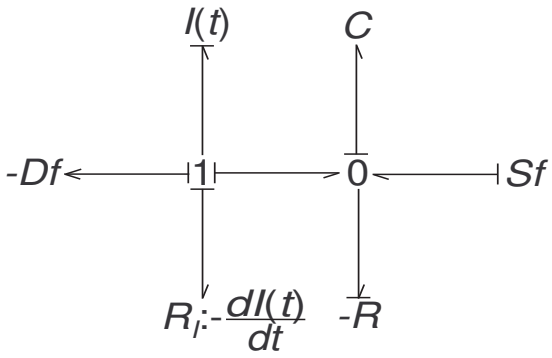

Figure 3.11: Dual Bond Graph Model

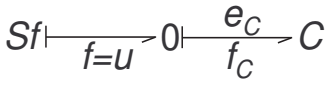

Figure 3.12: Causal path between source and dynamic element

the causal path can be obtained from equation:

$$\dot{x} = \dot{q_C} = f_C = f = u \tag{3.40}$$

therefore the gain is 1*. In the second case, when the state variable is the effort on the* C*-element* e_C*, the gain of the causal path is determined from relation:*

$$\dot{x} = \dot{e_C} = \frac{1}{C} f_C = \frac{1}{C} f = \frac{1}{C} u \tag{3.41}$$

The gain of the causal path in this case is $\frac{1}{C}$*, which is the same results which is obtained with property 8.*

In figure 3.13, the causal path between the detector Df *and the dynamic*

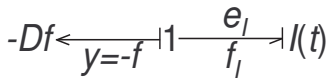

Figure 3.13: Causal path between a detector and a dynamic element

I element is presented. This gain g *represents the connection between the output and the state variable* $y = gx$*. Here the output* y *is the flow of the* 1*-junction. In the first case, the regular computational bond graph methodology,*

the state variable is the generalized momentum of the I-element p_I and the gain of the causal path can be obtained from equation:

$$y = -f = -f_I = -\frac{1}{I}p_I = -\frac{1}{I}x \tag{3.42}$$

therefore the gain is $-\frac{1}{I}$. In the second case, when the state variable is the flow on the I-element f_I, the gain of the causal path is determined from relation:

$$y = -f = -f_I = -x \tag{3.43}$$

The gain of the causal path in this case is -1, which is the same results which is obtained with property 9.

In figure 3.14, the causal path between the C-element and the I element is

Figure 3.14: Causal path between two dynamic elements

presented. This gain g represents the connection between the state derivative and the state variable $\dot{x}_{in} = gx_{out}$. In the first case, the regular computational bond graph methodology, the state variables are the generalized momentum of the I-element p_I and the generalized displacement of the C-element q_C and the gain of the causal path can be obtained from equation:

$$\dot{x}_{in} = \dot{q}_C = f_C = f_I = \frac{1}{I}p_I = \frac{1}{I}x_{out} \tag{3.44}$$

therefore the gain is $\frac{1}{I}$. In the second case, when the state variables are the flow on the I-element f_I and the effort on the C-element e_C, the gain of the causal path is determined from relation:

$$\dot{x}_{in} = \dot{e}_C = \frac{1}{C}f_C = \frac{1}{C}f_I = \frac{1}{C}x_{out} \tag{3.45}$$

The gain of the causal path in this case is $\frac{1}{C}$, which is the same results which is obtained with property 10.

Using these results, we can graphically obtain the state space representation in the two cases.

- *when the state variables are the generalized momentum of the I-element p_I and the generalized displacement of the C-element q_C, the state space representation is:*

$$\tilde{A} = \begin{pmatrix} -\frac{R_I}{I} & -\frac{1}{C} \\ \frac{1}{I} & \frac{1}{RC} \end{pmatrix} \quad \tilde{B} = \begin{pmatrix} 0 \\ 1 \end{pmatrix} \qquad \tilde{C} = \begin{pmatrix} -\frac{1}{I} & 0 \end{pmatrix} \tag{3.46}$$

But, for passing to the dual system, we have to perform the state change $\bar{x} = F\tilde{x} = \begin{pmatrix} \frac{1}{I} & 0 \\ 0 & \frac{1}{C} \end{pmatrix} \tilde{x}$, which leads to the following Kalman representation:

$$\bar{A} = F\tilde{A}F^{-1} - F(\dot{F^{-1}}) = \begin{pmatrix} 0 & -\frac{1}{I(t)} \\ \frac{1}{C} & \frac{1}{RC} \end{pmatrix} \tag{3.47}$$

$$\bar{B} = F\tilde{B} = \begin{pmatrix} 0 \\ \frac{1}{C} \end{pmatrix} \tag{3.48}$$

$$\bar{C} = \tilde{C}F^{-1} = \begin{pmatrix} -1 & 0 \end{pmatrix} \tag{3.49}$$

- *when the state variables are the flows of the I-elements f_I and the efforts of the C-elements e_C, by using properties 8-10, we can directly obtain the state space representation of the dual bond graph model:*

$$\bar{A} = \begin{pmatrix} 0 & -\frac{1}{I(t)} \\ \frac{1}{C} & \frac{1}{RC} \end{pmatrix} \quad \bar{B} = \begin{pmatrix} 0 \\ \frac{1}{C} \end{pmatrix} \qquad \bar{C} = \begin{pmatrix} -1 & 0 \end{pmatrix} \tag{3.50}$$

Remark 12. *The term $-F(\dot{F^{-1}})$ in the expression of $\bar{A}$ is compensated using the dissipative elements which are added on the dual bond graph model. Without the dissipative elements $R(t)$, the time-varying state variable change $\bar{x} = F(t)\tilde{x}$ is not mathematically correct.*

3.2 Structural Analysis

In this section, the focus is mainly on the duality between the structural controllability and observability properties. The rank conditions imposed on the controllability (equation (1.29)) and observability matrices (equation

(1.30)) are one of the possibilities for determining these properties. As the two relations recalled before are expressed in the temporal domain, the entire section deals with a temporal approach. Without getting into further details, we pass to defining the LTV structured systems and the bond graph representations which allows computation of the controllability and observability matrices. In fact, there are two graphical models, one for the controllability (input perspective) and one for the observability (output perspective) for each of graphical representations (structured systems and bond graphs).

Remark 13. *For notational simplicity, we denote by n the number of state vertices of the structured system graph and the number of dynamic elements in integral causality on the bond graph model.*

3.2.1 Definition of new LTV Graphical Models

The new LTV graphical models which are proposed in this section are built up for computational reasons. The controllability and observability matrices present some supplementary time-derivatives which should be taken into account. In order to preserve the graphical procedures developed for LTI models and to use them in the LTV case, we are going to alter the representation of LTV models. In practice, we still use the LTV model, but we add some extra-elements which emulate the action of the derivatives.

3.2.1.1 Structured Systems

Controllability Structured Graph

A graphical representation called the Controllability Structured Graph (CSG) is drawn for the LTV model (3.51).

$$\begin{cases} \frac{d}{dt}x(t) = A(t)x(t) + B(t)u(t) \\ y(t) = C(t)x(t) \end{cases} \tag{3.51}$$

Definition 20. *A differential arc is an arc (x, x), with $x \in X$, X-the set of state vertices, and the gain $g((x, x)) = \pm\frac{d}{dt}$.*

Definition 21. *The length of a path is equal to the number of state vertices on the path.*

Definition 22. *A CSG is a graph $G = (V, E)$ defined in section 2.1.1, with some new differential arcs defined with the following procedure.*

Procedure

1. For each state vertex determine the paths which start from an input vertex and end at that vertex, with length smaller than n and with at least one arc with time-dependent gain.

2. For each of the paths determined on the previous step:

   - Check the first apparition of an arc with a time-dependent gain along the path.
   - For each of the vertices following this arc along the path, add a differential arc with the gain $-\frac{d}{dt}$ (maximum one $-\frac{d}{dt}$ for a vertex).

This new graph is similar to the graph $G = (V, E)$ defined in the LTI or LTV case, but with some arcs defined by $g((x_i, x_i)) = A_{ii} - \frac{d}{dt}$. The procedure is presented on an example.

Let us consider the system in figure 3.15. This is the classical representation

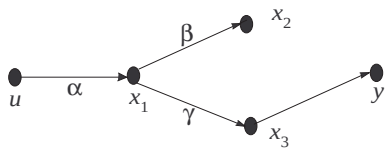

Figure 3.15: LTI Structured System

where the parameters α, β and γ are constants. Let us now consider that at least one parameter(let that be γ) is time dependent. The CSG is presented in figure 3.16. A new arc is drawn, with gain $-\frac{d}{dt}$ on the vertex x_3 because

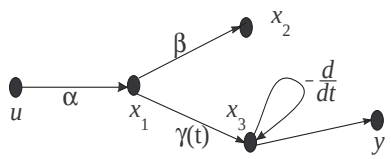

Figure 3.16: CSG of the LTV model

on the path $u \to x_1 \to x_3$, parameter $\gamma(t)$ is time-dependent.

Observability Structured Graph

Using a similar approach with the CSG case, but considering as the starting point the observability matrix, we define the OSG (Observability Structured Graph).

Definition 23. *The OSG of an LTV model (3.51) is a graph $G = (V, E)$ defined as in the LTI case (beside that the gains of the arcs are time-dependent), with some new differential arcs defined by the following procedure.*

Procedure

1. For each state vertex determine the paths which start from that vertex and end in an output vertex, with a length smaller than n and at least one arc with a time-varying gain.

2. For each of the paths determined on the previous step:

   - Check the last apparition of an arc with a time-dependent gain along the path.
   - For each of the vertices before this arc along the path, add a differential arc with the gain $\frac{d}{dt}$ (maximum one $\frac{d}{dt}$ for a vertex).

This new graph is similar to the usual structured system representation, but with some arcs defined by $g((x_i, x_i)) = A_{ii} + \frac{d}{dt}$.
The differences between the CSG and OSG concern the position of the differential arcs relative to the arcs with time-dependent gains and the gains of these arcs.

3.2.1.2 Bond graph models

The procedures defined for computing the controllability and observability matrices for LTI case can not be directly applied on the LTV bond graphs. The existence of the time derivatives in the expression of the controllability and observability matrices provokes this problem. In order to preserve the same procedures, we have to alter the bond graph representation. The solution is to emulate the use of the time-derivatives on the bond graph model.

In the following, we define two types of LTV bond graph models, one for controllability and one for observability.

Controllability Bond Graph

A graphical representation called the Controllability Bond Graph (CBG) is drawn.

Definition 24. *A differential loop is the transformation of a storage element on the bond graph in integral casuality (BGI) like in figure 3.17, where the dissipative element R has a value so that the gain of the differential loop is* $-\frac{d}{dt}$.

When a differential path is part of a causal path, the gain of the path is taken into consideration for calculating the gain of the causal path. This means that the product of all the gains which appear after the differential loop on the path are derived. For simplification, we introduce a dissipative element, whose value can be assigned so that the user can use the same techniques as in the LTI case. When transforming a C-element, the R-element which is added has the value $R : \frac{1}{\frac{d}{dt}(C*)}$. For an I-element, the supplementary R-element has the value $R : \frac{d}{dt}(I*)$. $C*$ and $I*$ mean that the product of the gains which follow should be derived. This way $-\frac{1}{RC}$ and $-\frac{R}{I}$, which are the gains of the differential loops, are equal to $-\frac{d}{dt}$.

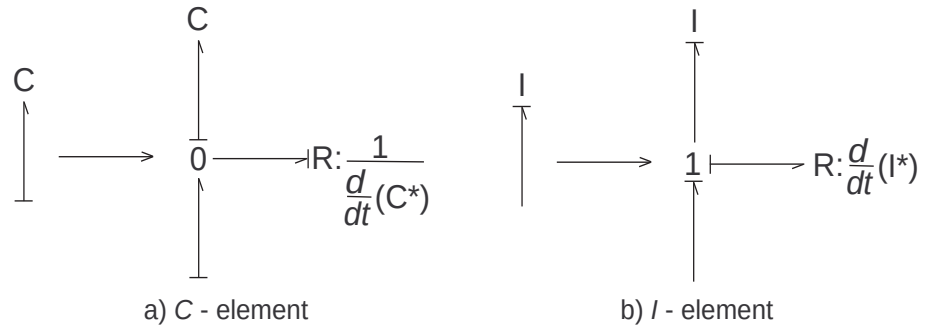

Figure 3.17: Differential Loop Transformation

Definition 25. *A CBG is a bond graph, with some new differential loops defined with the following procedure.*

Procedure

1. For each dynamic element in integral causality on the BGI, determine all the causal paths of length smaller than n, which start from a source and end in that element.

2. For each of the causal paths determined on the previous step:

   - Check the first apparition of an element with a time-dependent gain along the causal path.
   - For each of the dynamical element following this time-dependent gain along the causal path, add a differential loop with the gain $-\frac{d}{dt}$ (maximum one $-\frac{d}{dt}$ for each storage element).

Observability Bond Graph

A graphical representation called the Observability Bond Graph (OBG) is drawn.

Definition 26. *An OBG is a bond graph, with some new differential loops with the gain $\frac{d}{dt}$ defined with the following procedure. The dissipative elements which are added are similar to the ones designed for CBG, but with a negative gain (see figure 3.18).*

Procedure

1. For each dynamic element in integral causality on the BGI, determine all the causal paths of length smaller than $n-1$, which start from an output detector and end in that element.

2. For each of the causal paths determined on the previous step:

   - Check the first apparition of an element with a time-dependent gain along the causal path.
   - For each of the dynamical element following this time-dependent element along the causal path, add a differential loop with the gain $\frac{d}{dt}$ (maximum one $\frac{d}{dt}$ for each storage element).

These new bond graph models are similar to the normal model, but with some supplementary dissipative elements.

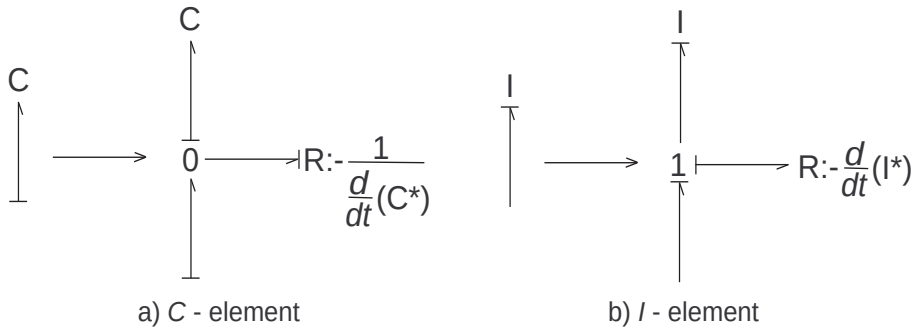

Figure 3.18: Differential Loop Transformation

3.2.1.3 Example

A simple electric circuit has been chosen to exemplify the techniques introduced above. The system is composed by three capacitors and two inductances linked by a transformer like in figure 3.19. Let us now consider that

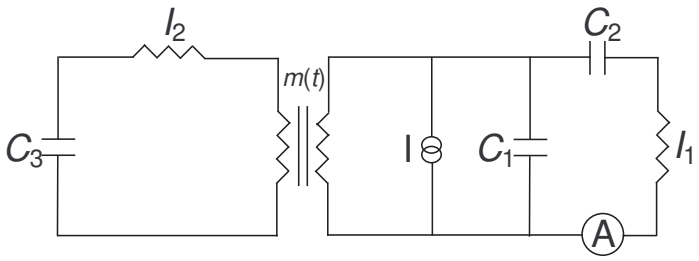

Figure 3.19: System proposed for analysis

the gain of the transformer is time-varying. We propose to represent the Observability Bond Graph so that we can exemplify the use of the design techniques described above. The bond graph model of this system is presented in figure 3.20.

The causal paths of length 4, which start from the output detector and pass through the time-varying transformer are: $Df \rightarrow I_1 \rightarrow C_1 \rightarrow TF \rightarrow I_2 \rightarrow C_3$ and $Df \rightarrow I_1 \rightarrow C_1 \rightarrow TF \rightarrow I_2 \rightarrow TF \rightarrow C_1$. This means that we have to add differential loops on the dynamic elements which appear after the time-dependent transformer on the causal path presented above, i.e. I_2, C_3 and C_1. In figure 3.21, we present the observability bond graph (OBG) associated to the LTV bond graph model from figure 3.20.

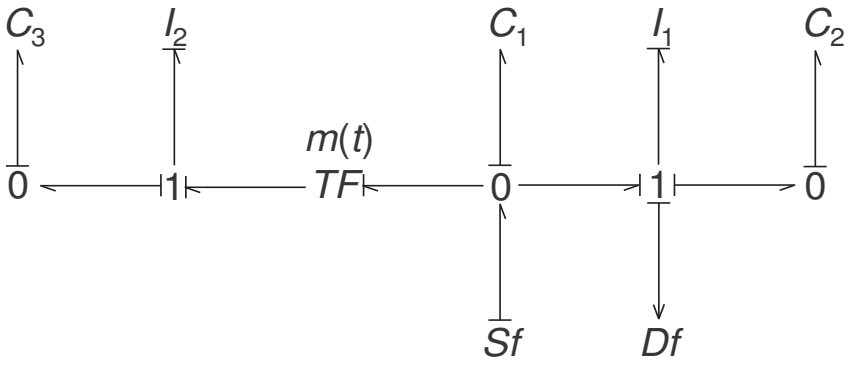

Figure 3.20: Bond Graph in Integral Causality of the LTV model

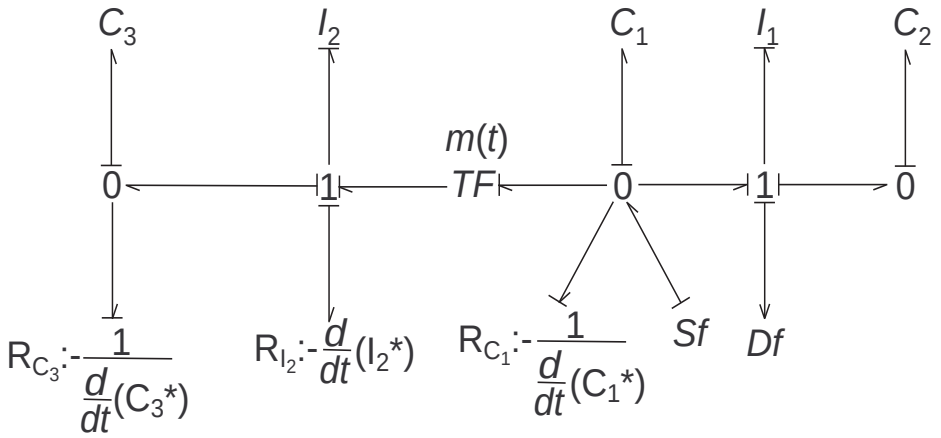

Figure 3.21: Observability Bond Graph Model

3.2.2 Controllability and Observability Matrices

3.2.2.1 Computational Methods using the Graph Representation

The controllability and observability matrices can be deduced graphically from the CSG and OSG (Observability Structured Graph) respectively. If the matrix $B(t)$ is partitioned by columns, the vectors $b_i(t)$ are obtained. Therefore the problem is reduced to the calculation of the vectors $(A(t) - \frac{d}{dt})^{k-1} b_i(t)$.

Property 11. *The vectors* $(A(t) - \frac{d}{dt})^{k-1} b_i(t)$ *are determined according to the formula (3.52), where* p_{ij}^k *is the number of paths of length* k *between the*

i^{th} input and the j^{th} state variable and $G_\alpha(u_i, x_j)$ is the product of the gains of the arcs along the considered path in the order from the top toward the root of the path.

$$[(A(t) - \frac{d}{dt})^{k-1} b_i(t)]_j = \sum_{\alpha=1}^{p_{ij}^k} G_\alpha(u_i, x_j) \tag{3.52}$$

For the observability matrix, the matrix $C(t)$ is partitioned by rows, the vectors $c_i(t)$ are obtained. Property 12 is used for calculating the vectors $(A^T(t) + \frac{d}{dt})^{k-1} c_i^T(t)$, which compose the observability matrix.

Property 12. *The vectors $(A^T(t) + \frac{d}{dt})^{k-1} c_i^T(t)$ are determined on the OSG according to the formula (3.53), where p_{ij}^k is the number of paths of length $k-1$ between the i^{th} output vertex and the j^{th} state variable vertex and $G_\alpha(x_j, y_i)$ is the product of the gains of the elements along the considered path in the order from the state vertex toward the output vertex.*

$$[(A^T(t) + \frac{d}{dt})^{k-1} c_i^T(t)]_j = \sum_{\alpha=1}^{p_{ij}^k} G_\alpha(x_j, y_i) \tag{3.53}$$

Remark 14. *For the differential arcs, the gains which follow have to be derived, except for this particularity, the procedure is the same as for the LTI case, due to the definition of the CSG/OSG.*

Example 8. *Let us consider the model from figure 3.15. In the LTI case the controllability matrix $[\ B \quad AB \quad A^2B\ ]$ is not of full rank and the model is not controllable.*
In the LTV case, the paths of the CSG (figure 3.16) are gathered in table 3.1. Therefore the controllability matrix is:

Table 3.1: Gains and paths on the CSG

Path	Length	Gain
$u \rightarrow x_1$	1	α
$u \rightarrow x_1 \rightarrow x_2$	2	$\beta\alpha$
$u \rightarrow x_1 \rightarrow x_3$	2	$\gamma(t)\alpha$
$u \rightarrow x_1 \rightarrow x_3 \rightarrow x_3$	3	$-\frac{d}{dt}(\gamma(t)\alpha) = -\dot{\gamma}(t)\alpha$

$$R = \begin{pmatrix} \alpha & 0 & 0 \\ 0 & \beta\alpha & 0 \\ 0 & \gamma(t)\alpha & -\dot{\gamma}(t)\alpha \end{pmatrix} \tag{3.54}$$

The $rank(R) = 3$*, which means that the LTV structured system is controllable.*

3.2.2.2 Computational Methods using the Bond Graph Representation

The controllability matrix can be deduced graphically from the CBG. If the matrix $B(t)$ is partitioned by columns, the vectors $b_i(t)$ are obtained. Therefore the problem is reduced to the calculation of the vectors $(A(t)-\frac{d}{dt})^{k-1}b_i(t)$.

Property 13. *The vectors* $(A(t)-\frac{d}{dt})^{k-1}b_i(t)$ *are determined according to the formula (3.55), where* p_{ij}^k *is the number of causal paths of length* k *between the* i^{th} *input source and the* j^{th} *state variable and* $G_\alpha(u_i, x_j)$ *is the product of the gains of the elements (*R*,* I*,* C*,* TF*,* GY*) along the considered path in the order from the dynamic element toward the input source with the sign given by the passage of the* 0 *and* 1*-junctions by the flow or the effort variables.*

$$[(A(t) - \frac{d}{dt})^{k-1}b_i(t)]_j = \sum_{\alpha=1}^{p_{ij}^k} G_\alpha(u_i, x_j) \tag{3.55}$$

Similarly, we can determine the observability matrix using the same procedure, but with the matrices $C(t)$ and $A(t)$ on the OBG. If the matrix $C(t)$ is partitioned by rows, the vectors $c_i(t)$ are obtained. Therefore the problem is reduced to the calculation of the vectors $(A^T(t) + \frac{d}{dt})^{k-1}c_i^T(t)$.

Property 14. *The vectors* $(A^T(t) + \frac{d}{dt})^{k-1}c_i^T(t)$ *are determined according to the formula (3.56), where* p_{ij}^k *is the number of causal paths of length* $k-1$ *between the* i^{th} *output source and the* j^{th} *state variable and* $G_\alpha(x_j, y_i)$ *is the product of the gains of the elements along the considered path in the order from the dynamic element toward the output detector with the sign given by the passage of the* 0 *and* 1*-junctions by the flow or the effort variables.*

$$[(A^T(t) + \frac{d}{dt})^{k-1}c_i^T(t)]_j = \sum_{\alpha=1}^{p_{ij}^k} G_\alpha(x_j, y_i) \tag{3.56}$$

Remark 15. *For the differential loops, the gains which follow have to be derived, except for this particularity, the procedure is the same as for the LTI case, due to the definition of the CBG/OBG.*

Remark 16. *The controllability and observability matrices are calculated on the CBG and OBG respectively, which are associated to the same bond graph model. Even though, we represent transpose matrices (for the observability matrix), it is just a matter of writing the relations and it is not related to the dual bond graph model. In the last part of this section, we discuss the duality between the CBG and the OBG.*

Example 9. *We are going to continue with the example from figure 3.21, for which we propose to determine the observability matrix. In table 3.2, we have determined all the causal paths and their gains. Using these information for building up observability matrix is obvious.*

3.2.3 System Analysis using Graphical Procedures

Graphical methods for determining the structural properties have been developed, both for LTV structured systems and for LTV bond graphs. These results have been published in [40] and [9]. In this section, we discuss each of these approaches.

3.2.3.1 Structured Systems

In order to determine the controllability and observability properties, it is not necessary to calculate the controllability and observability matrices and check a rank condition.
The controllability property for an LTV structured system can be obtained according to the theorem 14 proposed in [43],[48],[18] just like for LTI models, but they should be applied on the CSG.

Theorem 14. *An LTV structured system is generically controllable if on the CSG every state vertex is the end of a U-rooted path and there exists a disjoint union of a U-rooted path family and a cycle family that covers all state vertices.*

The same extension can be used for observability, this time theorem 15 should be applied on the OSG.

Table 3.2: Gains and paths on the OBG

Path	Length	Gain
$Df \leftarrow I_1$	0	$\frac{1}{I_1}$
$Df \leftarrow I_1 \leftarrow C_1$	1	$\frac{1}{C_1}\frac{1}{I_1}$
$Df \leftarrow I_1 \leftarrow C_2$	1	$-\frac{1}{C_2}\frac{1}{I_1}$
$Df \leftarrow I_1 \leftarrow C_1 \leftarrow I_1$	2	$-\frac{1}{I_1}\frac{1}{C_1}\frac{1}{I_1}$
$Df \leftarrow I_1 \leftarrow C_2 \leftarrow I_1$	2	$-\frac{1}{I_1}\frac{1}{C_2}\frac{1}{I_1}$
$Df \leftarrow I_1 \leftarrow C_1 \leftarrow R_{C_1} \leftarrow C_1$	2	0
$Df \leftarrow I_1 \leftarrow C_1 \leftarrow TF \leftarrow I_2$	2	$-\frac{1}{I_2}m\frac{1}{C_1}\frac{1}{I_1}$
$Df \leftarrow I_1 \leftarrow C_1 \leftarrow R_{C_1} \leftarrow C_1 \leftarrow R_{C_1} \leftarrow C_1$	3	0
$Df \leftarrow I_1 \leftarrow C_1 \leftarrow R_{C_1} \leftarrow C_1 \leftarrow TF \leftarrow I_2$	3	0
$Df \leftarrow I_1 \leftarrow C_1 \leftarrow TF \leftarrow I_2 \leftarrow TF \leftarrow C_1$	3	$-\frac{1}{C_1}m\frac{1}{I_2}m\frac{1}{C_1}\frac{1}{I_1}$
$Df \leftarrow I_1 \leftarrow C_1 \leftarrow TF \leftarrow I_2 \leftarrow R_{I_2} \leftarrow I_2$	3	$\frac{d}{dt}\frac{1}{I_2}m\frac{1}{C_1}\frac{1}{I_1}$
$Df \leftarrow I_1 \leftarrow C_1 \leftarrow TF \leftarrow I_2 \leftarrow C_3$	3	$\frac{1}{C_3}\frac{1}{I_2}m\frac{1}{C_1}\frac{1}{I_1}$
$Df \leftarrow I_1 \leftarrow C_1 \leftarrow I_1 \leftarrow C_1$	3	$-\frac{1}{C_1}\frac{1}{I_1}\frac{1}{C_1}\frac{1}{I_1}$
$Df \leftarrow I_1 \leftarrow C_1 \leftarrow I_1 \leftarrow C_2$	3	$\frac{1}{C_2}\frac{1}{I_1}\frac{1}{C_1}\frac{1}{I_1}$
$Df \leftarrow I_1 \leftarrow C_2 \leftarrow I_1 \leftarrow C_1$	3	$-\frac{1}{C_1}\frac{1}{I_1}\frac{1}{C_2}\frac{1}{I_1}$
$Df \leftarrow I_1 \leftarrow C_2 \leftarrow I_1 \leftarrow C_2$	3	$\frac{1}{C_2}\frac{1}{I_1}\frac{1}{C_2}\frac{1}{I_1}$
$Df \leftarrow I_1 \leftarrow C_1 \leftarrow R_{C_1} \leftarrow C_1 \leftarrow R_{C_1} \leftarrow C_1 \leftarrow TF \leftarrow I_2$	4	0
$Df \leftarrow I_1 \leftarrow C_1 \leftarrow R_{C_1} \leftarrow C_1 \leftarrow R_{C_1} \leftarrow C_1 \leftarrow R_{C_1} \leftarrow C_1$	4	0
$Df \leftarrow I_1 \leftarrow C_1 \leftarrow R_{C_1} \leftarrow C_1 \leftarrow R_{C_1} \leftarrow C_1 \leftarrow I_1$	4	0
$Df \leftarrow I_1 \leftarrow C_1 \leftarrow R_{C_1} \leftarrow C_1 \leftarrow TF \leftarrow I_2 \leftarrow R_{I_2} \leftarrow I_2$	4	0
$Df \leftarrow I_1 \leftarrow C_1 \leftarrow R_{C_1} \leftarrow C_1 \leftarrow TF \leftarrow I_2 \leftarrow C_3$	4	0
$Df \leftarrow I_1 \leftarrow C_1 \leftarrow R_{C_1} \leftarrow C_1 \leftarrow TF \leftarrow I_2 \leftarrow TF \leftarrow C_1$	4	0
$Df \leftarrow I_1 \leftarrow C_1 \leftarrow TF \leftarrow I_2 \leftarrow TF \leftarrow C_1 \leftarrow TF \leftarrow I_2$	4	$\frac{1}{I_2}m\frac{1}{C_1}m\frac{1}{I_2}m\frac{1}{C_1}\frac{1}{I_1}$
$Df \leftarrow I_1 \leftarrow C_1 \leftarrow TF \leftarrow I_2 \leftarrow TF \leftarrow C_1 \leftarrow R_{C_1} \leftarrow C_1$	4	$-\frac{d}{dt}\frac{1}{C_1}m\frac{1}{I_2}m\frac{1}{C_1}\frac{1}{I_1}$
$Df \leftarrow I_1 \leftarrow C_1 \leftarrow TF \leftarrow I_2 \leftarrow TF \leftarrow C_1 \leftarrow I_1$	4	$\frac{1}{I_1}\frac{1}{C_1}m\frac{1}{I_2}m\frac{1}{C_1}\frac{1}{I_1}$
$Df \leftarrow I_1 \leftarrow C_1 \leftarrow TF \leftarrow I_2 \leftarrow R_{I_2} \leftarrow I_2 \leftarrow R_{I_2} \leftarrow I_2$	4	$\frac{d}{dt}\frac{d}{dt}\frac{1}{I_2}m\frac{1}{C_1}\frac{1}{I_1}$
$Df \leftarrow I_1 \leftarrow C_1 \leftarrow TF \leftarrow I_2 \leftarrow R_{I_2} \leftarrow I_2 \leftarrow C_3$	4	$-\frac{1}{C_3}\frac{d}{dt}\frac{1}{I_2}m\frac{1}{C_1}\frac{1}{I_1}$
$Df \leftarrow I_1 \leftarrow C_1 \leftarrow TF \leftarrow I_2 \leftarrow R_{I_2} \leftarrow I_2 \leftarrow TF \leftarrow C_1$	4	$\frac{1}{C_1}m\frac{d}{dt}\frac{1}{I_2}m\frac{1}{C_1}\frac{1}{I_1}$
$Df \leftarrow I_1 \leftarrow C_1 \leftarrow TF \leftarrow I_2 \leftarrow C_3 \leftarrow I_2$	4	$\frac{1}{I_2}\frac{1}{C_3}\frac{1}{I_2}m\frac{1}{C_1}\frac{1}{I_1}$
$Df \leftarrow I_1 \leftarrow C_1 \leftarrow TF \leftarrow I_2 \leftarrow C_3 \leftarrow R_{C_3} \leftarrow C_3$	4	$\frac{d}{dt}\frac{1}{C_3}\frac{1}{I_2}m\frac{1}{C_1}\frac{1}{I_1}$

Table 3.3: Gains and paths on the OBG

Path	Length	Gain
$Df \leftarrow I_1 \leftarrow C_1 \leftarrow I_1 \leftarrow C_1 \leftarrow TF \leftarrow I_2$	4	$\frac{1}{I_2} m \frac{1}{C_1} \frac{1}{I_1} \frac{1}{C_1} \frac{1}{I_1}$
$Df \leftarrow I_1 \leftarrow C_1 \leftarrow I_1 \leftarrow C_1 \leftarrow R_{C_1} \leftarrow C_1$	4	$-\frac{d}{dt} \frac{1}{C_1} \frac{1}{I_1} \frac{1}{C_1} \frac{1}{I_1}$
$Df \leftarrow I_1 \leftarrow C_1 \leftarrow I_1 \leftarrow C_1 \leftarrow I_1$	4	$\frac{1}{I_1} \frac{1}{C_1} \frac{1}{I_1} \frac{1}{C_1} \frac{1}{I_1}$
$Df \leftarrow I_1 \leftarrow C_1 \leftarrow I_1 \leftarrow C_2 \leftarrow I_1$	4	$\frac{1}{I_1} \frac{1}{C_2} \frac{1}{I_1} \frac{1}{C_1} \frac{1}{I_1}$
$Df \leftarrow I_1 \leftarrow C_2 \leftarrow I_1 \leftarrow C_1 \leftarrow TF \leftarrow I_2$	4	$\frac{1}{I_2} m \frac{1}{C_1} \frac{1}{I_1} \frac{1}{C_2} \frac{1}{I_1}$
$Df \leftarrow I_1 \leftarrow C_2 \leftarrow I_1 \leftarrow C_1 \leftarrow R_{C_1} \leftarrow C_1$	4	$-\frac{d}{dt} \frac{1}{C_1} \frac{1}{I_1} \frac{1}{C_2} \frac{1}{I_1}$
$Df \leftarrow I_1 \leftarrow C_2 \leftarrow I_1 \leftarrow C_1 \leftarrow I_1$	4	$\frac{1}{I_1} \frac{1}{C_1} \frac{1}{I_1} \frac{1}{C_2} \frac{1}{I_1}$
$Df \leftarrow I_1 \leftarrow C_2 \leftarrow I_1 \leftarrow C_2 \leftarrow I_1$	4	$\frac{1}{I_1} \frac{1}{C_2} \frac{1}{I_1} \frac{1}{C_2} \frac{1}{I_1}$

Theorem 15. *An LTV structured system is generically observable if on the OSG every state vertex is the start of a Y-topped path and there exists a disjoint union of a Y-topped path family and a cycle family that covers all state vertices.*

The LTI model from figure 3.15 does not contain a cycle family that covers all the states. On the contrary, the CSG model (figure 3.16) has this property. The LTV structured system is structurally controllable.

Remark 17. *If the structured system is structurally controllable/observable using the structured graph, without adding the differential arcs, then it is also structurally controllable/observable after adding the differential arcs. The inverse is not always true.*

3.2.3.2 Bond Graph Approach

As the structured systems and the bond graph resembles, one might think that a simple translation of the LTI procedures for system analysis in the LTV case would be enough. Unfortunately, applying theorem 9 on the CBG does not provide a reliable result all the time. Even though in practice, most of the times, this is true, the counterexample in figure 3.22, shows that the bond graphs provide more information through the connectivity and causality than the structured systems.

Let us first present this counterexample for the study of the controllability

property, which shows why the theorem 9 does not work on the CBG, when the equivalent theorem for structured systems, theorem 14 provides an acceptable (even though false) response.

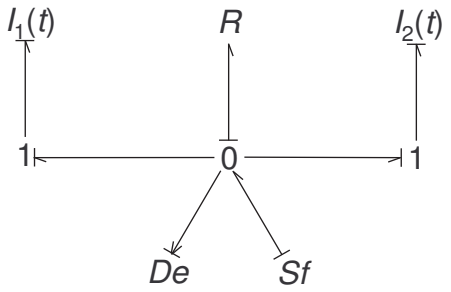

Figure 3.22: Counterexample

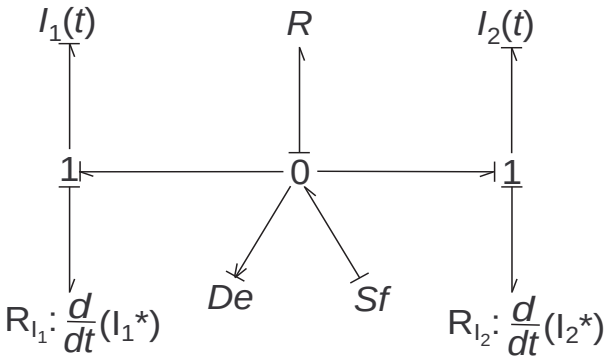

Figure 3.23: CBG in integral causality

Example 10. *The CBG of the bond graph model from figure 3.22 is presented in figure 3.23, where we have considered that the dissipative element R is time-dependent. Applying the theorem 9 on the CBG means passing to derivative causality (figure 3.24) and verifying whether all the dynamic elements pass to derivative causality. It can easily be seen that apparently all the conditions for the controllability property are met.*
On the other hand, if we determine the controllability matrix on the CBG, we obtain:

$$R_{(A,B)}(t) = \begin{pmatrix} R & -\frac{R^2}{I_1} - \frac{R^2}{I_2} - \frac{dR}{dt} \\ R & -\frac{R^2}{I_1} - \frac{R^2}{I_2} - \frac{dR}{dt} \end{pmatrix} \tag{3.57}$$

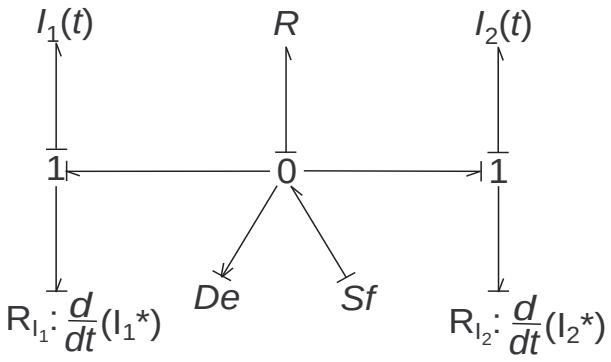

Figure 3.24: CBG in derivative causality

But $rank(R_{(A,B)}(t)) = 1$*, therefore the system is not controllable, which means that the supposed procedure is not valid.*

Theorem 9 on the CBG does not provide a correct answer because contrary to the LTI case where passing to derivative causality is a method for determining the inverse of the state matrix A, here we would determine the inverse of the matrix $A(t) - I\frac{d}{dt}$*.*

If we consider the structured system associated to the bond graph from figure 3.22, we obtain the graph from figure 3.25. In the structured systems methodology, this model is equivalent with the one from figure 3.26, which in

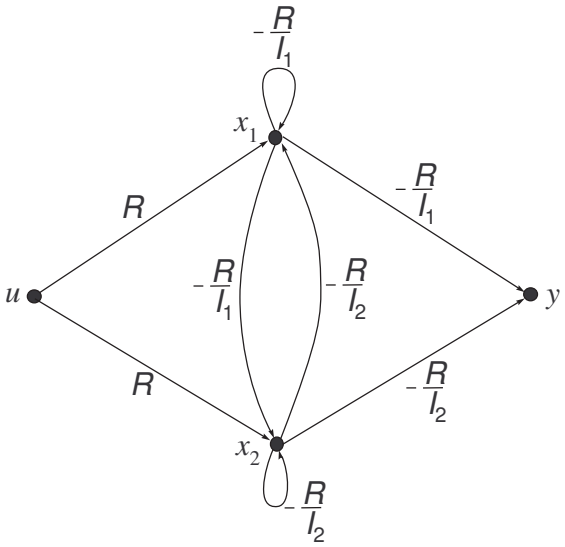

Figure 3.25: Structured system for the same bond graph model

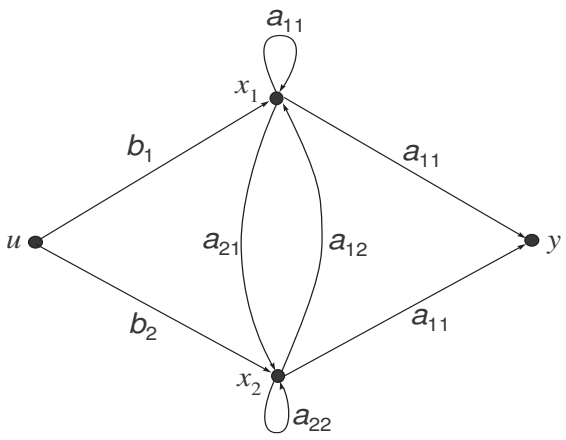

Figure 3.26: Equivalent Structured System

fact is controllable. The problem is that the gains of the arcs are not independent. And according to the definition of "structural" properties this is an "acceptable" fault for the structured systems methodology.

The main difference between the structured systems representation and the bond graph representation is that on the bond graph model the parameters are localized in the elements, while for the structured systems the parameters are on the gains of the edges. Due to this draw-back, the structured systems procedures are less accurate than the bond graph methods.
Retracing the approach proposed for LTI bond graph models for studying the controllability, we can find the right method for the LTV models. The study of structural controllability for an LTI bond graph model consists of determining the rank of matrix $\begin{pmatrix} A & B \end{pmatrix}$. If the rank of this matrix is smaller than n, then there are some linear relation between the rows of this matrix, which means, according to the state space equation $\dot{x}(t) = Ax(t) + Bu(t)$, that there are the same relations between variables $\dot{x}_i$. Thanks to these relations, it is possible to find the orthogonal complement of the controllable part in the LTI models. In [9], it has been proven that it is possible to obtain the same result for LTV bond graph models using the modules.
The particularity of bond graph models (LTI or LTV) is that the same linear relations between the variables $\dot{x}_i$ are obtained directly on the model after

applying the derivative causality ([56]). The dynamic elements which keep the integral causality are causally linked with dynamic elements in derivative causality. For an I-element in integral causality, for example, the unknown variable is the effort, therefore the derivative of state variable. This variable can be represented as a linear combination of known variables of the I-elements (effort e_I) and C-elements (flows f_C) in derivative causality which are derivatives of the state variables. This way, we can find graphically all the linear relations (with constant coefficients for the LTI case and with time-dependent coefficients for the LTV case) between the derivatives of state variables. These linear relations define the torsion submodule. According to theorem 2, an LTV system is controllable if the torsion submodule of the module associated to the system is trivial.
In [9], a graphical method for determining the controllability for LTV models using the bond graph representation is proposed. The aim of the method proposed in [9] is to determine the equations of the torsion submodule. For that we transform the bond graph according to the following procedure:

- Implement a derivative causality on the bond graph model.
- Dualize the maximum number of input sources (switch $Se \leftrightarrow Sf$) in order to eliminate, if possible, the elements remaining in integral causality.

Afterwards, we consider the variables g_i, which are either the effort variable e_I of the I-elements in derivative causality or the flow variable f_C of the C-elements in derivative causality. We can write the relation:

$$g_k - \sum_i \alpha_i^k(t) g_i = 0 \tag{3.58}$$

where $\alpha_i^k(t)$ is the gain of the causal path between the corresponding dynamic elements.
The relations (3.58) represent the equations candidate for the torsion submodule. If the parameters α are constant then relation (3.58) define the torsion submodule and therefore the torsion submodule is not trivial, i.e. the system is not controllable.

Using the same example as in figure 3.22, we get first the LTV bond graph

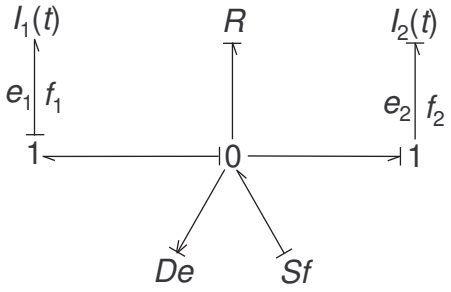

Figure 3.27: Bond graph in derivative causality

in derivative causality (figure 3.27). The only dynamic element which remains in integral causality is I_2. Therefore we can write an equation similar to (3.58):

$$e_1 - e_2 = 0 \tag{3.59}$$

In terms of state variables, it is equivalent with $sx_1 - sx_2 = 0$, which defines the torsion submodule $s(x_1 - x_2) = 0$. Therefore the system is not controllable as we have also seen with the rank condition on the controllability matrix. Concerning the observability property, there is no specific graphical method for determining this property for LTV bond graph models, since obtaining the quotient submodule $\Sigma/[u, y]$ graphically is not very simple. Yet we propose to use the duality between controllability and observability to determine via the dual bond graph model the observability property. The next section is dedicated to the study of duality in system analysis, both in structured systems and bond graphs. The study of observability through the study of the controllability of the dual bond graph model is discussed in the next section.

3.2.4 Duality in System Analysis

The study of duality in system analysis is divided in two parts. First we discuss the duality which appear in the study of structured systems. Secondly, we concentrate on the study of the observability property through the study of the controllability property of the dual bond graph model.

3.2.4.1 Duality between CSG and OSG

The aim of this part of the section is to present the duality which can be observed between the two graphical representations which have been introduced, the Controllability Structured Graph and the Observability Structured Graph. The problem can be put in terms of the duality procedure which has been presented in the previous section.

If the CSG of a system Σ is considered, then what is the representation which is obtained after the dualizing procedure is applied? Is it the OSG of the dual system $\bar{\Sigma}$?

The answer to this question is positive and the proof is intuitive. As the main difference between the CSG and the OSG are the derivatives $\pm\frac{d}{dt}$ which appear on the diagonal of the matrix $A(t)$, we are going to concentrate on the expression of state matrix. If $A(t)$ is the state matrix of the system Σ, then the state matrix of the dual system $\bar{\Sigma}$ is, according to the dualization procedure, $\bar{A}(t) = -A^T$. On the other hand, if we consider the CSG of the system Σ, we obtain the matrix $A(t)-\frac{d}{dt}I$. Applying the graphical dualization procedure on the CSG means to switch the arcs on the CSG and to multiply the gains of inner arcs by -1. In algebraic terms, this means that on the dual graph, we obtain the matrix $-(A(t) - \frac{d}{dt}I)^T = -A^T(t) + \frac{d}{dt}I$. But the OSG of the dual system $\bar{\Sigma}$ presents also the matrix $\bar{A}(t) + \frac{d}{dt}I = -A^T(t) + \frac{d}{dt}I$. Therefore we can conclude that the dual system of the CSG is the OSG of the dual system.

Using the same approach as in figure 1.1, in figure 3.28 we present the duality between the CSG and OSG.

Example 11. *Let us consider the LTV structured system from figure 3.29. For constructing the CSG, we need to determine the paths which start in the vertex u and have a length smaller than 3, the number of state vertices. The only path with a time-varying gain is $u \to x_1 \to x_3$. Therefore, we must add a differential loop on vertex x_3 and we obtain the CSG form figure 3.30. On the other hand, if we dualize the structured system from figure 3.29, we obtain the dual model from figure 3.31. For the dual model, we want to construct the OSG. The only path which starts from $\bar{y}$, has the length smaller than 3 and a time-varying gain is $\bar{y} \leftarrow \bar{x}_1 \leftarrow \bar{x}_3$, and therefore we have to put a differential loop on the vertex $\bar{x}_3$. In figure 3.32, we have pictured the OSG*

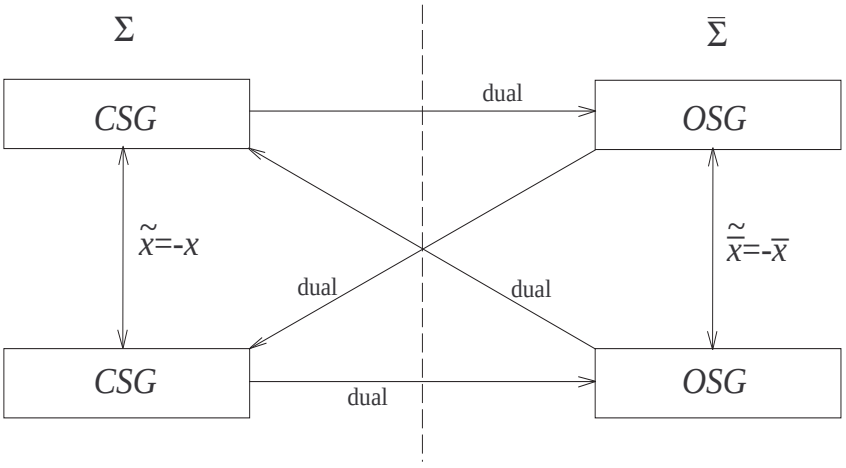

Figure 3.28: Duality between CSG and OSG

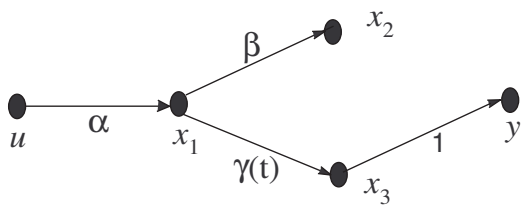

Figure 3.29: Structured System

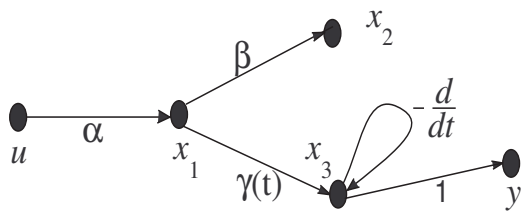

Figure 3.30: CSG of the Structured System

of the dual model.

Performing the dualization procedure directly on the CSG of the structured system can lead also to a graph representation. By inspection, we observe that the dual of the CSG is exactly the OSG of the dual model from figure 3.32.

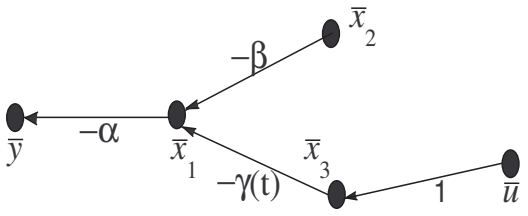

Figure 3.31: Dual of the Structured System

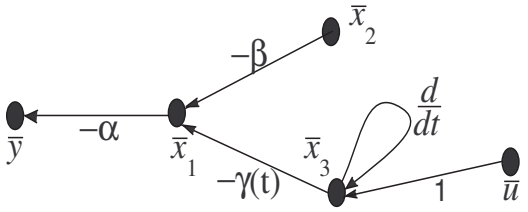

Figure 3.32: OSG of the dual structured system

3.2.4.2 Duality between CBG and OBG

Similarly to the relation of duality between the CSG and the OSG for the structured systems, we can develop the duality between the CBG and the OBG in the bond graph representation. The mathematical foundation is the same as in the structured systems case and the proof is analogous. In the following, we consider an example on which we perform the same duality transformations.

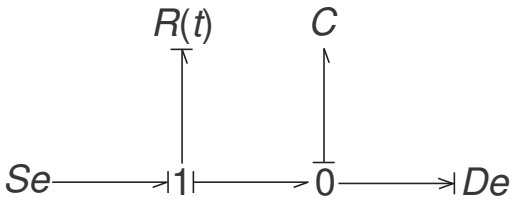

Figure 3.33: Bond graph model

Example 12. *Let us consider the LTV bond graph model from figure 3.33. For constructing the CBG, we need to determine the causal paths which start in the source Se and have a length smaller than* 1*, the number of dynamic*

elements. The only path with a time-varying gain is $Se \rightarrow R \rightarrow C$. Therefore, we must add a differential loop for the C-element and we obtain the CBG form figure 3.34. On the other hand, if we dualize the bond graph from

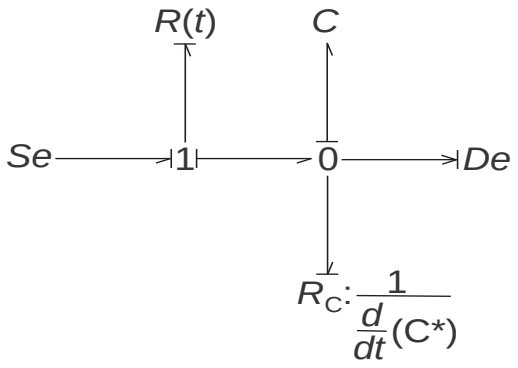

Figure 3.34: CBG of the LTV bond graph model

figure 3.33, we obtain the dual model from figure 3.35. For the dual model, we want to construct the OBG. The only path which starts from $-Df$, has the length smaller than 1 and a time-varying gain is $-Df \leftarrow R \leftarrow C$, and therefore we have to put a differential loop for the C element. In figure 3.36, we have pictured the OBG of the dual model.

Performing the dualization procedure directly on the CBG (figure 3.34) can

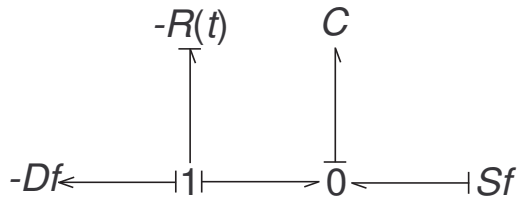

Figure 3.35: Dual bond graph model

lead also to a dual bond graph representation. By inspection, we observe that the dual of the CBG is exactly the OBG of the dual model from figure 3.36.

3.2.4.3 Duality. Key for determining the observability property

Using the duality property of LTV systems, we can obtain the solution for determining the observability property. The aim of this section is to deter-

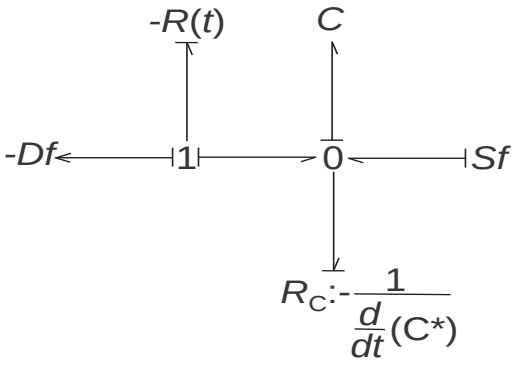

Figure 3.36: OBG of the dual bond graph model

mine whether a bond graph is observable by studying the controllability of the dual model.
The procedure for determining the observability property can be defined as follows:

1. Draw the bond graph.
2. Dualize the bond graph model.
3. Apply the controllability procedure and decide whether the dual bond graph model is controllable or not.
4. Dualize the solution. If the dual system is controllable then the system is observable, if not then the model is not observable.

Two examples are considered here, to show how does this procedure work on bond graph models.

Example 13. *Let us consider the bond graph model from figure 3.37, where the I-elements are time-dependent. For determining the observability, we follow the procedure presented above. The dual bond graph model is presented in figure 3.38. On the dual bond graph model in derivative causality (figure 3.39), we observe there are no dynamic elements in integral causality. Therefore the dual bond graph model is controllable. Through the duality between the controllability and the observability, we conclude that the bond graph from figure 3.37 is observable. Of course, if we calculate the observability matrix, we obtain that it is full rank and that the system is observable.*

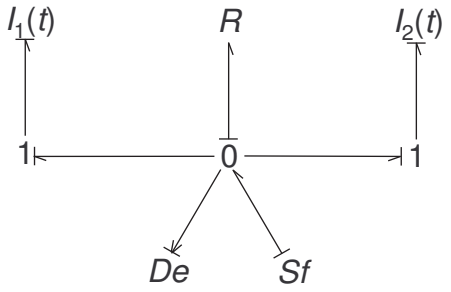

Figure 3.37: LTV Bond Graph Model

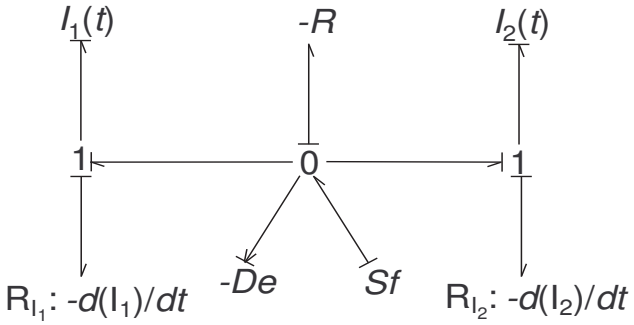

Figure 3.38: Dual Bond Graph

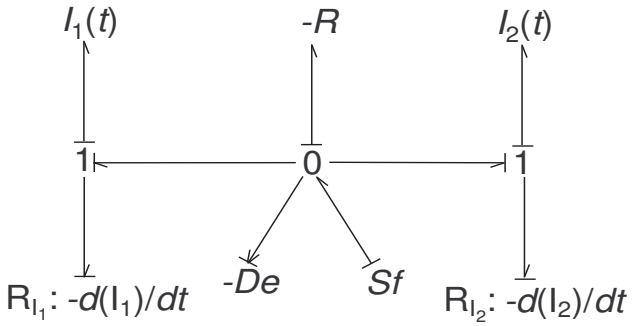

Figure 3.39: Dual Bond Graph in Derivative Causality

Example 14. *Let us consider another example, the one form figure 3.40, where the only time-dependent element is the dissipative element R. Using the same procedure, we have pictured in figure 3.41, the dual bond graph model and in figure 3.42, the dual bond graph model in derivative causality. This time, we observe that the element I_2 remains in integral causality and there is*

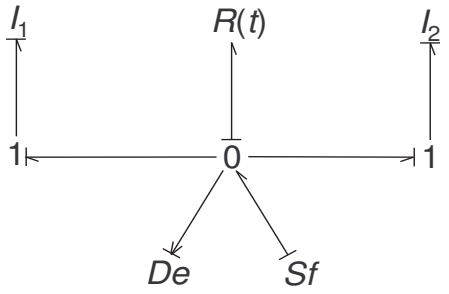

Figure 3.40: LTV Bond Graph Model

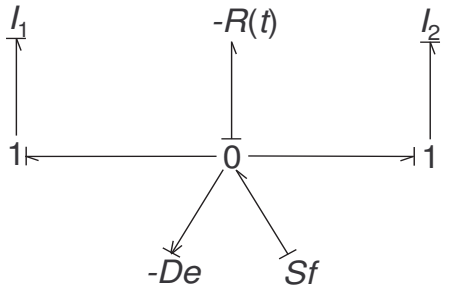

Figure 3.41: Dual Bond Graph

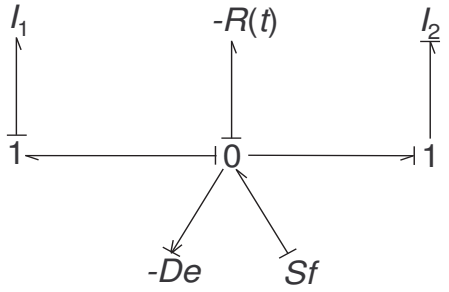

Figure 3.42: Dual Bond Graph in Derivative Causality

a causal path between I_2 and I_1. Therefore we obtain the relation $e_{I_2} - e_{I_1} = 0$, which is equivalent with $\frac{d}{dt}p_{I_2} - \frac{d}{dt}p_{I_1} = 0$. It results that $\frac{d}{dt}I_2 f_{I_2} - \frac{d}{dt}I_1 f_{I_1} = 0$. As I_1 and I_2 have constant gains and the state variables are $x_1 = f_{I_1}$ and $x_2 = f_{I_2}$, we obtain $I_2\frac{dx_2}{dt} - I_1\frac{dx_1}{dt} = 0$. This equation defines the torsion submodule and therefore the dual system is not controllable. By duality, we obtain that the bond graph from figure 3.40 is not observable.

3.3 Conclusions

In this chapter, we have introduced a methodology for studying the duality in system analysis for LTV models. Our study of duality begun by defining the dual graphical representations for the structured systems and for the bond graphs. For structured systems, defining the dual model is easy due to the relation between the state space representation and the graph representation. On the other hand, for bond graph model, defining the dual model presents a more complicated procedure. The most important point of this procedure is the time-dependent state variable change $\bar{x} = F(t)x$. Contrary to the mathematical approach, either state space representation or module theoretical approach, or even the graphical structured systems approach, on the dual bond graph model the state variables have a physical meaning, they are the efforts of the C elements in integral causality and the flows of the I elements in integral causality. With the state variable change on the dual bond graph model, we had to develop some new rules for calculating the gains of the causal loops and causal paths.

In the second part of the chapter, we tackled the system analysis prob-

Table 3.4: System Analysis Methodology

	SS	Bond graph
Computational method → Controllability	CSG	CBG
Computational method → Observability	OSG	OBG
Graphical method → Controllability	CSG	LTV BG
Graphical method → Observability	OSG	Dual BG + Controllability procedure

lem. In order to study the duality between controllability and observability, we have introduced some graphical methods for studying these properties. Firstly, we provide some graphical computational methods for calculating the controllability and observability matrices. These procedures are applied on the Controllability/Observability Structured Graph and the Controllability/Observability Bond Graph, respectively. Secondly, we present some graphical direct methods for determining these structural properties. For the structured systems these procedures are also applied on the CSG/OSG. But, for the bond graphs we have to use a different approach because of the

localization of the time-dependent parameters on the elements. The controllability procedure applied in an LTV bond graph model introduced in [9] is reused here. For the observability procedure, we use the dual bond graph model on which we apply the controllability procedure. In table 3.4, we have gathered the graphical procedures which have been introduced in this chapter for system analysis of LTV models.

Chapter 4

Duality in Control Synthesis

The concept of duality in linear models can be defined not only for the controllability property and the observability property as can be seen in the previous chapter, but also it can be extended to the control laws. A state feedback control can be considered as the dual of an input injection control law [50]. These concepts are valid for linear and non linear models, in a state space description or in a module theoretical framework. Our interest is the study of the duality for linear and non linear models.
The focus of this section is on a graphical procedure, which may offer a more global perspective for the decoupling by state feedback and output injection problems using the structured systems and the bond graph representations. The solution of the decoupling problem by state feedback for LTI models is based on the infinite structure of the model. This study proposes similar procedure for LTV models and therefore we have to explore the infinite structure of LTV systems first. Then, in the second section, we pass to solving a well-known problem, the decoupling problem for LTV models. This problem is studied through the concept of duality between the state feedback and output injection. The decoupling by output injection problem has not been tackled so far in the control literature. Even though the application of this problem on a physical system is impossible, considering the definition of output injection, our approach is a first step towards solving the decoupling by output feedback problem and the construction of observers. The duality between state feedback and output injection is discussed both mathematically and graphically. In the third part of this chapter, we tackle the decoupling with pole placement problem. For this, we use the geometrical approach

introduced by [27] for LTV systems. In the last part, we provide a nonlinear extension for the input-output and linearization of nonlinear models, using the variational model.

4.1 Infinite Structure

The infinite structure of LTV multivariable models is characterized by three sets: $\{n_i'\}$ the set of infinite zero orders of the global model $\Sigma(C, A, B)$, $\{n_i\}$ the set of row infinite zero orders of the row sub-system $\Sigma(c_i, A, B)$ and $\{n^j\}$ the set of column infinite zero orders of the column sub-system $\Sigma(C, A, B^j)$. In the following, when using the underscript index i, we refer to characteristics of the row system $\Sigma(c_i, A, B)$, when using the upperscript index j, we refer to characteristics of the column sub-system $\Sigma(C, A, B^j)$ and when we do not use these indices we refer to the global system $\Sigma(C, A, B)$.

4.1.1 Definitions

Definition 27. *[7] The orders of zero at infinity of a global LTV model are characterized by the Smith-McMillan matrix of the input-output relation $T(\sigma, t)$, where $\sigma = s^{-1}$.*

Property 15. *[19] The global orders of zero at infinity are equal to the minimal number of derivations of each output variable necessary so that the input variables appear explicitly and independently in the equations.*

Definition 28. *The row order of zero at infinity for the row sub-system $\Sigma(c_i, A, B)$ is the integer n_i, which verifies condition (4.1).*

$$n_i = min\left\{k | B^T(t)((A^T(t) + I\frac{d}{dt})^{(k-1)}c_i^T)(t) \neq 0\right\} \tag{4.1}$$

Property 16. *n_i is equal to the number of derivations of the output variable $y_i(t)$ necessary for at least one of the input variables to appear explicitly.*

Definition 29. *The column order of zero at infinity for the column sub-system $\Sigma(C, A, B^j)$ is the integer n^j, which verifies condition (4.2).*

$$n^j = min\left\{k | C(t)((A(t) - I\frac{d}{dt})^{(k-1)}B^j)(t) \neq 0\right\} \tag{4.2}$$

Property 17. *n^j is equal to the number of integrations of the input variable $u_j(t)$ necessary for at least one output variable to appear explicitly.*

4.1.2 Duality between Row and Column Infinite Structure

The aim of this subsection is to show the relation between the row infinite structure and the column infinite structure of the dual system. This duality is presented by the following theorem.

Theorem 16. *The set of the infinite zero orders of the column subsystems* $\Sigma(C, A, B^j)$ *is equal to the set of the infinite zero orders of the dual row subsystems* $\bar{\Sigma}(\bar{c}_i, \bar{A}, \bar{B})$ *and vice versa.*

Proof:

If condition (4.1) is written for the dual row subsystem $\bar{\Sigma}(\bar{c}_i, \bar{A}, \bar{B})$, then we obtain:

$$\bar{B}^T(t)((\bar{A}^T(t) + I\frac{d}{dt})^{(k-1)}\bar{c}_i^T)(t) \neq 0 \tag{4.3}$$

Equation (4.3) is equivalent to relation (4.4), if the substitutions (1.16)-(1.18) are applied.

$$(C^T)^T(t)(((-A^T)^T(t) + I\frac{d}{dt})^{(k-1)}(-B^T)_i^T)(t) \neq 0 \tag{4.4}$$

But as we know that transpose of the row of a matrix is the column of the transposed matrix, equation (4.4) is equivalent to:

$$(-1)^k C(t)((A(t) - I\frac{d}{dt})^{(k-1)}B^i)(t) \neq 0 \tag{4.5}$$

Multiplying equation (4.5) by $(-1)^k$ leads to condition (4.2), which is the condition for obtaining the infinite zero orders of the column subsystems $\Sigma(C, A, B^j)$. This means that the same condition applies for obtaining the two sets.

The proof for the equality between the infinite zero orders of the row subsystem $\Sigma(c_i, A, B)$ and the infinite zero orders of the dual column subsystem $\bar{\Sigma}(\bar{C}, \bar{A}, \bar{B}^j)$ is similar and is not detailed here.

4.2 Decoupling Problem for LTV Models

The decoupling problem, or non-interacting control problem is a well-known issue in system control literature. A square system is called decoupled if the

i^{th} output is influenced only by the i^{th} input.
Here this problem has been solved by the two control laws: state feedback and output injection. Not only, the proposed procedures are similar for system decoupling by the two control laws, but also, as is presented in the last part of this section, the obtained control laws are dual.

4.2.1 State Feedback

4.2.1.1 Analytical procedure

The procedure proposed by [46] for input-output decoupling of linear time-varying systems is recalled. The algorithm is defined for numerical purposes, but it offers a lead over the steps to be followed.
The problem is to determine whether the LTV system (3.51) can be decoupled using a state feedback control law as in relation (4.6), where $\bar{u}$ is an m-tuple which represents the new input of the system and the matrices $F(t)$ and $G(t)$ have compatible dimensions. The plant is said to be decoupled if the i^{th} input affects only the i^{th} output, for $i = 1, 2, \ldots, m$.

$$u(t) = F(t)x(t) + G(t)\bar{u}(t) \tag{4.6}$$

The differential operator $\mathcal{L} = A^T + I\frac{d}{dt}$ is defined. It can be applied to the state vector as defined in (4.7).

$$(\mathcal{L}x)(t) = \frac{d}{dt}x(t) + A^T(t)x(t) \tag{4.7}$$

Indices n_i can be defined as in equation (4.8).

$$n_i = min\left\{j | B^T(t)(\mathcal{L}^{(j-1)}c_i^T)(t) \neq 0\right\} \tag{4.8}$$

Using the differential operator and the indices defined above, the matrices $\tilde{A}$ and $\tilde{B}$ are defined like in equations (4.9) and (4.10) respectively.

$$\tilde{A}(t) = \begin{pmatrix} (\mathcal{L}^{(n_1-1)}c_1^T)^T(t) \\ \vdots \\ (\mathcal{L}^{(n_m-1)}c_m^T)^T(t) \end{pmatrix} \tag{4.9}$$

$$\tilde{B}(t) = \tilde{A}(t)B(t) \tag{4.10}$$

Property 18. *[46] The LTV model defined by (3.51) can be decoupled by a static feedback (4.6) if and only if matrix $\tilde{B}(t)$ is non-singular.*

The relations (4.11) and (4.12) give the expression of matrices $F(t)$ and $G(t)$, where $\Lambda(t)$ is an arbitrary diagonal matrix which may impose a desired behavior to the decoupled system [46].

$$F(t) = -\tilde{B}^{-1}(t)[\tilde{A}(t)A(t) + \frac{d}{dt}\tilde{A}(t)] \tag{4.11}$$

$$G(t) = \tilde{B}^{-1}(t)\Lambda(t) \tag{4.12}$$

The steps taken for the decoupling of linear time-varying systems in [46] are:

1. Determine the indices n_i for each output;
2. Calculate the matrices $\tilde{A}(t)$ and $\tilde{B}(t)$;
3. Verify whether proposition 18 is true, if not the procedure stops;
4. Calculate the inverse matrix for $\tilde{B}(t)$;
5. Determine matrices $F(t)$ and $G(t)$ according to the relations (4.11) and (4.12).

The algorithm can be split into two separated parts: the first three steps represent the analysis part and the last two the synthesis of the decoupling law.
In [15], the analysis part has been solved using the infinite structure of LTI models and here an extension for LTV systems is proposed.

Theorem 17. *An LTV square system can be decoupled by a regular static state feedback control law if and only if the set of infinite zero orders of the global system $\Sigma(C, A, B)$ is equal to the set of infinite zero orders of the row sub-systems $\Sigma(c_i, A, B)$, $i = 1, 2, \ldots, m$.*

The result for LTI models from [15] is based on the Smith-McMillan factorization at infinity of rational matrix functions ([16]), while a study of the infinite structure of time-varying systems ([7]) presents the same approach but on LTV models. The generalization of theorem 17 from the LTI case to the LTV case is straight-forward using these previous results.

4.2.1.2 Graphical procedure

Even though in [17], a structured system approach has been proposed for the decoupling of LTI systems, this perspective has it is limitations and it can not be applied for the linear time-varying models. Similar procedures have been proposed in [5], for decoupling of LTI bond graph models, unfortunately this approach is also not appropriate for LTV models. These algorithms have to be generalized to fit the new mathematical specifications.
The aim of this section is to offer a graphical technique, by means of the graph representation to determine whether the structured system can be decoupled and, if so, to calculate the state feedback control law which decouples the LTV system.

A. System Analysis

Using theorem 17, the analysis part consists of determining the infinite structure, the orders of infinite zeros of the global and row subsystems. In the sequel, we consider the two graphical representations and for each case we define graphical procedure for calculating the infinite structures.

Structured Systems

Property 19. *The orders of the infinite zeros of a global invertible structured system are calculated according to equation (4.13), where L_k is the sum of the lengths of the k shortest different input-output paths.*

$$\begin{cases} n'_1 = L_1 \\ n'_k = L_k - L_{k-1} \end{cases} \tag{4.13}$$

Property 20. *The order of the infinite zero for the row sub-system $\Sigma(c_i, A, B)$ is equal to the length of the shortest path between the i^{th} output vertex y_i and the set of input vertices.*

According to properties 19 and 20 and theorem 17, it is then possible to conclude on the decoupling property of the structured system only with a graphical approach.
This algorithm is identical to the one proposed by [17] for the LTI structured models. Either calculating the shortest paths on the graph with the time-dependent coefficients or on the OSG leads to the same result, because for

the shortest path the loops on the same state vertex are useless (or the path is no more the shortest).

Bond Graph Models

Generalizing a result which was introduced in [56] for LTI bond graph models, in [3] and [35], it has been proposed the following property which allows computation of infinite structure for global system and for row subsystems.

Property 21. *[3],[35] The orders of infinite zero of a global invertible bond graph model are calculated according to equation (4.14), where L_k is the sum of the lengths of the k shortest different input-output causal paths.*

$$\begin{cases} n'_1 = L_1 \\ n'_k = L_k - L_{k-1} \end{cases} \tag{4.14}$$

Property 22. *[3],[35] The order of infinite zero for the row sub-system $\Sigma(c_i, A, B)$ is equal to the length of the shortest causal path between the i^{th} output detector D_i and the set of input sources.*

Properties 21 and 22 and theorem 17 provide a graphical procedure for determining the infinite structure of the global system and its row subsystems using the bond graph representation.
This algorithm is identical to the one proposed by [56] for the LTI structured models. Either calculating the shortest causal paths on the bond graph graph with the time-dependent coefficients or on the OBG (with the differential loops) leads to the same result, because for the shortest causal path the differential loops are not taken into account.

B. Control Synthesis

Once the indices n_i are determined and if the decoupling problem has a solution, the next step is to determine the matrices $\tilde{A}(t)$ and $\tilde{B}(t)$, which consists in calculating the vectors $(A^T + I\frac{d}{dt})^{n_i-1}c_i^T$ and $B^T(A^T + I\frac{d}{dt})^{n_i-1}c_i^T$ respectively. The procedure is similar for determining the two matrices, therefore we focus on $\tilde{A}(t)$, afterwards the differences for calculating $\tilde{B}(t)$ will be pointed out. Just as for system analysis, we present first the procedure for structured systems and afterwards the one for bond graph models.

Structured Systems Procedure

We have presented this graphical result in [41] for the synthesis of the state feedback decoupling control law for LTV structured systems.

Property 23. *[41] The vectors* $(A^T(t)+I\frac{d}{dt})^{n_i-1}c_i^T(t)$ *are determined on the OSG according to the formula (4.15), where* $p_{ij}^{n_i-1}$ *is the number of paths of length* n_i-1 *between the* i^{th} *output vertex and the* j^{th} *state variable vertex and* $G_\alpha(x_j,y_i)$ *is the product of the gains of the arcs along the considered path in the order from the root toward the top of the path.*

$$[(A^T(t)+I\frac{d}{dt})^{n_i-1}c_i^T(t)]_j=\sum_{\alpha=1}^{p_{ij}^{n_i-1}}G_\alpha(x_j,y_i) \tag{4.15}$$

Using proposition 23, we determine the formal expression of the vectors directly using a graphical technique.

Matrix $\tilde{B}(t)$ can be determined by considering the paths between the input vertices and the output vertices. With the matrices $\tilde{A}(t)$ and $\tilde{B}(t)$ calculated, matrices $F(t)$ and $G(t)$ are determined according to relations (4.11) and (4.12) respectively.

Bond Graph Approach

In [35], we have proposed a graphical solution for LTV system decoupling by state feedback using a bond graph approach. The control synthesis of this procedure, which consists of determining the matrices $\tilde{A}(t)$ and $\tilde{B}(t)$, is presented here.

Property 24. *The vectors* $(A^T(t)+I\frac{d}{dt})^{n_i-1}c_i^T(t)$ *are determined on the OBG according to the formula (4.16), where* $p_{ij}^{n_i-1}$ *is the number of causal paths of length* n_i-1 *between the* i^{th} *output detector and the* j^{th} *dynamic element in integral causality and* $G_\alpha(x_j,y_i)$ *is the product of the gains elements along the considered causal path in the order from the dynamic element toward the output detector.*

$$[(A^T(t)+I\frac{d}{dt})^{n_i-1}c_i^T(t)]_j=\sum_{\alpha=1}^{p_{ij}^{n_i-1}}G_\alpha(x_j,y_i) \tag{4.16}$$

Proposition 24 allows calculating the formal expression of the vectors directly using a graphical technique on the bond graph model. A multiplication

of time-varying coefficients and derivation operators is needed for obtaining the result.

For determining the matrix $\tilde{B}(t)$ the only difference which should be added is that instead of using the causal paths between the storage elements in integral causality and the output detectors, the causal paths between the input sources and the output detectors have to be used. Once the matrices $\tilde{A}(t)$ and $\tilde{B}(t)$ are calculated, matrices $F(t)$ and $G(t)$ are obtained, according to relations (4.11) and (4.12) respectively.

4.2.2 Output Injection

The decoupling by static output injection problem has not been tackled before this study begun. In fact, we have begun exploring this possibility keeping in mind the duality which might appear. We considered first the decoupling by output injection problem for LTI models. In [42], we have publish some results concerning a graphical procedure for solving this problem for LTI bond graph problems. In the following, we concentrated on LTV models, both structured system representation and bond graph models. The results from the LTV case are a generalization of the results form LTI case, therefore we present here directly the LTV procedures. Most of these procedures can be further simplified for LTI case, but our interest is mostly in linear systems in general and into possible extensions for nonlinear models.

4.2.2.1 Analytical procedure

The procedure proposed by [46] for input-output decoupling of linear time-varying systems by state feedback has been used to extend the numerical solution to output injection case.

The differential operator $\mathcal{N} = A - \frac{d}{dt}I$ is defined. It can be applied to the state vector as defined in (4.17).

$$(\mathcal{N}x)(t) = A(t)x(t) - \frac{d}{dt}x(t) \tag{4.17}$$

If B^j, $j = 1, 2, \ldots, m$ denotes the j^{th} column of the matrix B, then indices n^j can be defined as in equation (4.18).

$$n^j = min\left\{i | C(t)(\mathcal{N}^{(i-1)}B^j(t)) \neq 0\right\} \tag{4.18}$$

It is also interesting to examine the mapping Z, which is computed by the equation:

$$(Zx)(t) = (\mathcal{N}x)(t) + K(t)C(t) \tag{4.19}$$

Concerning Z, we have property 25.

Property 25. $(Z^{(i)}B^j)(t) = \begin{cases} (\mathcal{N}^{(i)}B^j)(t), i = 0, 1, \ldots, n^j - 1 \\ (Z^{(i-n^j+1)}\mathcal{N}^{(n^j-1)}B^j)(t), i \geq n^j \end{cases}$

This property may be established by direct examination, and for brevity the details are omitted here. Similarly, the following two corollaries are stated without proof. The results are analogous to the ones obtained in [46] for the state feedback decoupling problem.

Corollary 1. $(CZ^{(i)}B^j)(t) = \begin{cases} 0, i = 0, 1, \ldots, n^j - 2 \\ (CZ^{(i-n^j+1)}\mathcal{N}^{(n^j-1)}B^j)(t), i \geq n^j - 1 \end{cases}$

This corollary also follows from property 25 and the definition of indices n^j.

The definition of output injection control law (1.40) can be rewritten as (4.20) to show the presence of the mapping Z.

$$\begin{cases} [A(t) - \frac{d}{dt}]x(t) + K(t)C(t)x(t) + B(t)u(t) = 0 \\ z(t) = L(t)C(t)x(t) \end{cases} \tag{4.20}$$

The state equation can be expressed as $(Zx)(t) + B(t)u(t) = 0$ or $(Zx)(t) + \sum_{j=1}^{m} B^j(t)u_j(t) = 0$. And, if we consider only one input at the time, the equation becomes:

$$(Zx)(t) + B^j(t)u_j(t) = 0 \tag{4.21}$$

Multiplying relation (4.21) by CZ^{n^j-1} leads to:

$$(CZ^{n^j}x)(t) + CZ^{n^j-1}B^j(t)u_j(t) = 0 \tag{4.22}$$

If $(C\mathcal{N}^{n^j-1}B^j(t))_{j=1,\ldots,m}$ is nonsingular, then

$$u(t) = -((C\mathcal{N}^{n^j-1}B^j(t))_{j=1,\ldots,m})^{-1}(CZ^{n^j}x)(t) \tag{4.23}$$

which is equivalent to:

$$u_j(t) = -(C\mathcal{N}^{n^j-1}B^j(t))^{-1}(CZ^{n^j}x)(t) \tag{4.24}$$

Let us now define the matrices $\tilde{A}$ and $\tilde{C}$ like in equations (4.25) and (4.26) respectively.

$$\tilde{A}(t) = \begin{pmatrix} (\mathcal{N}^{(n^1-1)}B^1)(t) & \dots & (\mathcal{N}^{(n^m-1)}B^m)(t) \end{pmatrix} \tag{4.25}$$

$$\tilde{C}(t) = C(t)\tilde{A}(t) \tag{4.26}$$

In order to obtain the decoupling by output injection, we have to integrate equation 4.24 n^j times, which should lead to the expression of z, the new output vector, from relation 4.20. The solution of this problem is offered by the following property.

Property 26. *The LTV model defined by relation (1.40) is decoupled by an output injection control law if and only if matrix $\tilde{C}$ is non-singular.*

The relations (4.27) and (4.28) give the expression of matrices $K(t)$ and $L(t)$, where Λ is an arbitrary diagonal matrix which may impose the static gain to the decoupled system.

$$K(t) = -[A(t)\tilde{A}(t) - \frac{d}{dt}\tilde{A}(t)]\tilde{C}^{-1}(t) \tag{4.27}$$

$$L(t) = \Lambda\tilde{C}^{-1}(t) \tag{4.28}$$

Replacing the expression of $K(t)$ in equation 4.24 in the expression of the operator Z and $L(t)$ in the output equation of system (4.20) and performing the n^j times integration leads to identity with the expression of the new output vector.
The steps taken for the decoupling of linear time-varying systems by output injection are:

1. Determine the indices n^j for each input;
2. Calculate the matrices $\tilde{A}(t)$ and $\tilde{C}(t)$;
3. Verify whether property 26 is true, if not the procedure stops;
4. Calculate the inverse matrix for $\tilde{C}(t)$;
5. Determine matrices $K(t)$ and $L(t)$ according to the relations (4.27) and (4.28).

4.2.2.2 Graphical Procedure

Just like in the state feedback decoupling case, the problem is split into two parts: the analysis which determines whether the decoupling by output injection is possible and the control synthesis which consists of calculating the decoupling matrices.

A. System Analysis

For analysis, the following theorem is used:

Theorem 18. *[38], [41] The LTV square system $\Sigma(C(t), A(t), B(t))$ can be decoupled by a static regular output injection control law if and only if the set of global infinite zero orders is equal to the set of infinite zero orders of the column sub-systems $\Sigma(C(t), A(t), B^j(t))$, $j = 1, 2, \ldots, m$.*

Structured Systems Procedure

Theorem 18 can be graphically implemented on LTV structured systems by using properties 19 and 27.

Property 27. *[41] The column infinite zero order for the column sub-system $\Sigma(C, A, B^j)$ is equal to the length of the shortest path between the j^{th} input vertex u_j and the set of output vertices.*

Remark 18. *The properties concerning the graphical computation of infinite zero orders for the row and column subsystems can be applied on CSG, on OSG or on the graph without the differential arcs, because they take into consideration only the shortest paths and therefore all the paths which contain differential arcs are discarded.*

Bond Graph Models

The bond graph procedure for implementing graphically theorem 18 is based on properties 21 and 28.

Property 28. *[38] The column infinite zero order of the column subsystem $\Sigma(C, A, B^j)$ is equal to the length of the shortest causal path between the j^{th} input source and the set of output detectors.*

Remark 19. *Similarly to the structured system case, the properties concerning the graphical computation of orders of infinite zero for the row and*

column subsystems can be applied on CBG, on OBG or on bond graph without differential loops, because they take into consideration only the shortest causal paths and therefore all the causal paths which contain differential loops are discarded (passing through a differential loop once means increasing the length of the pass by one).

B. Control Synthesis

The second part of the algorithm concerns the synthesis of the control law. In the sequel, we present two graphical computation methods for determining the matrices $\tilde{A}(t)$ and $\tilde{C}(t)$ using the structured systems representation and then the bond graph representation.

Structured Systems

The matrices $\tilde{A}(t)$ and $\tilde{C}(t)$ consist in calculating the vectors $(A-I\frac{d}{dt})^{n^j-1}B^j$ and $C(A-I\frac{d}{dt})^{n^j-1}B^j$ respectively. Therefore this graphical procedure has to be performed on the CSG, which presents the differential arcs with gains $-\frac{d}{dt}$. The procedure is similar for determining the two matrices, therefore we focus on $\tilde{A}(t)$.

Property 29. *[41] The vectors $(A-I\frac{d}{dt})^{n^j-1}B^j$ are determined on the CSG according to the formula (4.29), where $p_{ij}^{n^j-1}$ is the number of paths of length n^j between the j^{th} input vertex and the i^{th} state variable vertex and $G_\alpha(u_j, x_i)$ is the product of the gains of the arcs along the considered path in the order from the top toward the root of the path.*

$$[(A-I\frac{d}{dt})^{n^j-1}B^j]_i = \sum_{\alpha=1}^{p_{ij}^{n^j-1}} G_\alpha(u_j, x_i) \tag{4.29}$$

Property 29 allows calculating the formal expression of the vectors directly using a graphical technique. The expression determined for these vectors after the procedure presented above represents a multiplication of time-varying coefficients and time-derivative operators.

For determining the matrix $\tilde{C}(t)$ the only difference which should be added is that instead of using the paths between the input and the state vertices, the paths between the input and the output have to be used. Once the matrices $\tilde{A}(t)$ and $\tilde{C}(t)$ are calculated, matrices $K(t)$ and $L(t)$ are obtained, according

to relation (4.27) and (4.28) respectively.

Bond Graph Procedure

For calculating the vectors $(A-I\frac{d}{dt})^{n^j-1}B^j$ and $C(A-I\frac{d}{dt})^{n^j-1}B^j$ respectively, we need to use the CBG because we have to pass by the differential loops with the gain $-\frac{d}{dt}$.

Property 30. *The vectors $(A - I\frac{d}{dt})^{n^j-1}B^j$ are determined on the CBG according to the formula (4.30), where $p_{ij}^{n^j-1}$ is the number of causal paths of length n^j between the j^{th} input source and the i^{th} dynamic element in integral causality and $G_\alpha(u_j, x_i)$ is the product of the gains of the elements along the considered causal path in the order from the dynamic elements toward the source.*

$$[(A - I\frac{d}{dt})^{n^j-1}B^j]_i = \sum_{\alpha=1}^{p_{ij}^{n^j-1}} G_\alpha(u_j, x_i) \tag{4.30}$$

The formal expression for vectors $(A-I\frac{d}{dt})^{n^j-1}B^j$ is obtained graphically using property 30. For determining the matrix $\tilde{C}(t)$ the only difference which should be added is that instead of using the causal paths between the input source and the dynamic elements in integral causality, we have to take into account the causal paths between the input source and the output detectors. The last step of this algorithm is to use relations (4.27) and (4.28) to calculate matrices $K(t)$ and $L(t)$.

4.2.3 Duality between State Feedback and Output Injection

The main part of this section is focused on the duality between the two control laws presented above. More specifically, we are interested in the duality between the solutions of the decoupling problem in the two cases.

Theorem 19. *The decoupling State Feedback and Output Injection control laws are dual.(i.e. there is a direct relation between the two control laws which permits calculating one from the other and vice-versa).*

Proof:

In order to observe this duality the following steps are performed:

1. Given the system $\Sigma(A, B, C)$, determine the dual system $\bar{\Sigma}(\bar{A}, \bar{B}, \bar{C})$.

2. Apply the decoupling by output injection procedure for the dual model $\bar{\Sigma}(\bar{A}, -\bar{B}, -\bar{C})$ after the state variable change $\tilde{\bar{x}} = -\bar{x}$ has been performed.

3. Apply the dualization procedure for decoupled system $\bar{\Sigma}(\bar{A}+\bar{K}\bar{C}, -\bar{B}, -\bar{L}\bar{C})$.

4. Apply the decoupling by state feedback procedure for the system $\Sigma(A, B, C)$.

5. Verify that the decoupled systems obtained in the two previous steps are identical.

For the first step, the same procedure as in section 1.3.2 is used. This leads to equation (4.31).

$$\begin{cases} \bar{A} = -A^T \\ \bar{B} = C^T \\ \bar{C} = -B^T \end{cases} \tag{4.31}$$

The dual adjoint system for the model in equation (4.31) is obtained after the state variable change $\bar{\tilde{x}} = -\bar{x}$, (see model (4.32)).

$$\begin{cases} \bar{\tilde{A}} = \bar{A} = -A^T \\ \bar{\tilde{B}} = -\bar{B} = -C^T \\ \bar{\tilde{C}} = -\bar{C} = B^T \end{cases} \tag{4.32}$$

On system (4.32), the output injection procedure is applied. The matrices $\bar{K}$ and $\bar{L}$ are calculated according to equations (4.27) and (4.28) respectively. After using the substitutions (4.32), the following expressions are obtained for $\bar{K}$ and $\bar{L}$.

$$\bar{K}(t) = -((-A^T - \frac{d}{dt})^{n^j}(-c_j)^T)_{j=1,\ldots,m}) * (B^T(-A^T - \frac{d}{dt})^{n^j-1}(-c_j)^T)_{j=1,\ldots,m})^{-1} \tag{4.33}$$

$$\bar{L}(t) = \Lambda(B^T(-A^T - \frac{d}{dt})^{n^j-1}(-c_j)^T)_{j=1,\ldots,m})^{-1} \tag{4.34}$$

In equation (4.33), for the expression of $\bar{K}$ the multiplication of two matrices build up by column vectors are used. In expression (4.34), $\bar{L}$ is the inverse of a matrix composed by column vectors. We can easily remark that for each

column vectors we can pass a factor $(-1)^{n^j}$. Therefore relations (4.33) and (4.34) can be rewritten as:

$$\bar{K}(t) = -(-(-1)^{n^j}(A^T+\frac{d}{dt})^{n^j}(c_j)^T)_{j=1,\dots,m})*((-1)^{n^j}B^T(A^T+\frac{d}{dt})^{n^j-1}(c_j)^T)_{j=1,\dots,m})^{-1} \tag{4.35}$$

$$\bar{L}(t) = \Lambda((-1)^{n^j}B^T(A^T+\frac{d}{dt})^{n^j-1}(c_j)^T)_{j=1,\dots,m})^{-1} \tag{4.36}$$

As each column of the matrices is multiplied by $(-1)^{n^j}$, then the matrix can be written as a product of a matrix which contains the vector columns without the factor $(-1)^{n^j}$ and a diagonal matrix which contains in the corresponding cell the factor $(-1)^{n^j}$. If we consider that $U = diag((-1)^{n^j})$, then equations (4.35) and (4.36) become:

$$\bar{K}(t) = -(-(A^T+\frac{d}{dt})^{n^j}(c_j)^T)_{j=1,\dots,m})*U*(B^T(A^T+\frac{d}{dt})^{n^j-1}(c_j)^T)_{j=1,\dots,m}*U)^{-1} \tag{4.37}$$

$$\bar{L}(t) = \Lambda(B^T(A^T+\frac{d}{dt})^{n^j-1}(c_j)^T)_{j=1,\dots,m}*U)^{-1} \tag{4.38}$$

Knowing that $(M*N)^{-1} = N^{-1}*M^{-1}$ and that $U^{-1} = U$, we obtain:

$$\bar{K}(t) = ((A^T+\frac{d}{dt})^{n^j}(c_j)^T)_{j=1,\dots,m})*(B^T(A^T+\frac{d}{dt})^{n^j-1}(c_j)^T)_{j=1,\dots,m})^{-1} \tag{4.39}$$

$$\bar{L}(t) = \Lambda U*(B^T(A^T+\frac{d}{dt})^{n^j-1}(c_j)^T)_{j=1,\dots,m})^{-1} \tag{4.40}$$

The dual of system $\bar{\Sigma}(\bar{A}+\bar{K}\bar{C}, -\bar{B}, -\bar{L}\bar{C})$ is $\Sigma(A+B\bar{K}^T, B\bar{L}^T, C)$. On the other hand, if the procedure for state feedback decoupling is applied on model $\Sigma(A,B,C)$, then the decoupled system is $\Sigma(A+BF, BG, C)$, with F and G from equations (4.11) and (4.12) respectively. By simple inspection, it can be concluded that:

$$F = \bar{K}^T \tag{4.41}$$

$$G = \bar{L}^T * diag((-1)^{n^j})_{j=1,\dots,m} \tag{4.42}$$

The last step is to confront equations (4.11) and (4.39) and (4.12) and (4.40) respectively to prove that the two relations above are true. After simple algebraic operations we obtain the validation of equations (4.41) and (4.42).

4.2.4 Application

The procedures presented in this section concerning system decoupling by state feedback and output injection are used on two simple applications. First, we consider a structured system and then a bond graph model. All the procedures described in this section are tested on these examples.

4.2.4.1 Decoupling of LTV Structured Systems

In order to prove that the inverse statement of theorem 19 is also valid, we are going to consider an LTV system application and determine the output injection control law for system decoupling. Then using the adjoint of the dual system, we calculate the state feedback control law for system decoupling. In the end, we should verify that relations (4.41) and (4.42) are validated by our computations on this example.
Let us consider the system (4.43), where a and b are time-dependent functions, $u = (u_1, u_2)^T$ is the input vector, $x = (x_1, x_2, x_3)^T$ is the state variable vector and $y = (y_1, y_2)^T$ is the output vector. Obviously, system (4.43) is a linear time-dependent system. We have chosen to represent directly the controllability structured graph associated to this model in figure 4.1 because we want to determine the output injection control law which decouples this model and as presented above the graphical procedures are applied on the CSG.

$$\begin{cases} \dot{x}_1 = a(t)u_1 \\ \dot{x}_2 = b(t)u_2 \\ \dot{x}_3 = x_1 + x_2 \\ y_1 = x_1 \\ y_2 = x_3 \end{cases} \tag{4.43}$$

Just like in the above procedure concerning the decoupling by output injection problem, the first step is to verify whether the decoupling problem can be solved. For the analysis stage, we have to determine the infinite zero orders of the column systems $\Sigma(C, A, B^j)$ and the infinite zero orders of the global system $\Sigma(C, A, B)$. Using propositions 19 and 27 provides the solution for this stage of the problem. The shortest path for u_1 is $u_1 \rightarrow x_1 \rightarrow y_1$, which has the length 1 and therefore $n^1 = 1$. Analogously, the shortest path for u_2 is $u_2 \rightarrow x_2 \rightarrow x_3 \rightarrow y_2$ and $n^2 = 2$. For the infinite zero orders of the global

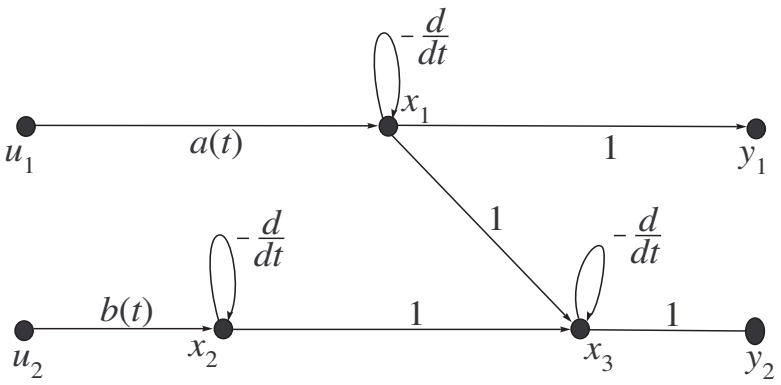

Figure 4.1: CSG for output injection decoupling

system we observe that the shortest input-output path is $u_1 \rightarrow x_1 \rightarrow y_1$ and has a length of 1, therefore $L_1 = n_1' = 1$. The two shortest disjoint paths are $u_1 \rightarrow x_1 \rightarrow y_1$ and $u_2 \rightarrow x_2 \rightarrow x_3 \rightarrow y_2$, therefore $L_2 = 3$ and $n_2' = L_2 - L_1 = 2$. The orders of the infinite zeros of the column sub-systems are $\{1, 2\}$ and the orders of the infinite zeros of the global system are $\{1, 2\}$. According to theorem 18, this model can be decoupled by a regular static output injection control law.

The next step is to determine the output injection control law, i.e. the matrices $K(t)$ and $L(t)$. For this, we must determine first the vectors $C(A - I\frac{d}{dt})^{n^j-1}B^j$ for $\tilde{C}(t)$ and $(A - I\frac{d}{dt})^{n^j}B^j$ for $K(t)$. In table 4.1, the paths and the gains for calculating the vectors $C(A - I\frac{d}{dt})^{n^j-1}B^j$ are presented. For the

Table 4.1: I/O paths

Path	Length	Gain
$u_1 \rightarrow x_1 \rightarrow y_1$	1	a
$u_2 \rightarrow x_2 \rightarrow x_3 \rightarrow y_2$	2	b

vectors $(A - I\frac{d}{dt})^{n^j}B^j$, we take into consideration the paths of length $n^j + 1$ between the state nodes and the input nodes. The results are collected in table 4.2. Using the results from tables 4.1 and 4.2 we obtain $\tilde{C}(t) = \begin{pmatrix} a & 0 \\ 0 & b \end{pmatrix}$

Table 4.2: Input/State paths

Path	Length	Gain
$u_1 \rightarrow x_1 \rightarrow x_1$	2	$-\frac{d}{dt}a$
$u_1 \rightarrow x_1 \rightarrow x_3$	2	a
$u_2 \rightarrow x_2 \rightarrow x_2 \rightarrow x_2$	3	$\frac{d^2}{dt^2}b$
$u_2 \rightarrow x_2 \rightarrow x_2 \rightarrow x_3$	3	$-\frac{d}{dt}b$
$u_2 \rightarrow x_2 \rightarrow x_3 \rightarrow x_3$	3	$-\frac{d}{dt}b$

and $(A - \frac{d}{dt})^{n^j} B^j = \begin{pmatrix} -\frac{da}{dt} & 0 \\ 0 & \frac{d^2b}{dt^2} \\ a & -2\frac{db}{dt} \end{pmatrix}$. This means that, according to relations (4.27) and (4.28), the control law is defined by:

$$K(t) = \begin{pmatrix} \frac{\dot{a}}{a} & 0 \\ 0 & -\frac{\ddot{b}}{b} \\ -1 & \frac{2\dot{b}}{b} \end{pmatrix} \tag{4.44}$$

$$L(t) = \begin{pmatrix} \frac{1}{a} & 0 \\ 0 & \frac{1}{b} \end{pmatrix} \tag{4.45}$$

Let us now consider the adjoint of the dual system for the model (4.43). This dual model is defined by equation (4.46) and the associated structured system is represented in figure 4.1. We have chosen the observability structured graph because the procedure for the decoupling by state feedback is applied on the OSG.

$$\begin{cases} \dot{\bar{x}}_1 = -\bar{x}_3 - \bar{u}_1 \\ \dot{\bar{x}}_2 = -\bar{x}_3 \\ \dot{\bar{x}}_3 = -\bar{u}_2 \\ \bar{y}_1 = a\bar{x}_1 \\ \bar{y}_2 = b\bar{x}_2 \end{cases} \tag{4.46}$$

For the decoupling problem by static state feedback, we have also two stages, firstly the analysis and secondly the control synthesis. For the analysis stage, we must determine the infinite structure for the global and row sub-systems and then apply theorem 17. The shortest input-output path for $\bar{y}_1$ is $\bar{u}_1 \rightarrow \bar{x}_1 \rightarrow \bar{y}_1$ of length 1, therefore $n_1 = 1$. The shortest path for $\bar{y}_2$ is $\bar{u}_2 \rightarrow \bar{x}_3 \rightarrow$

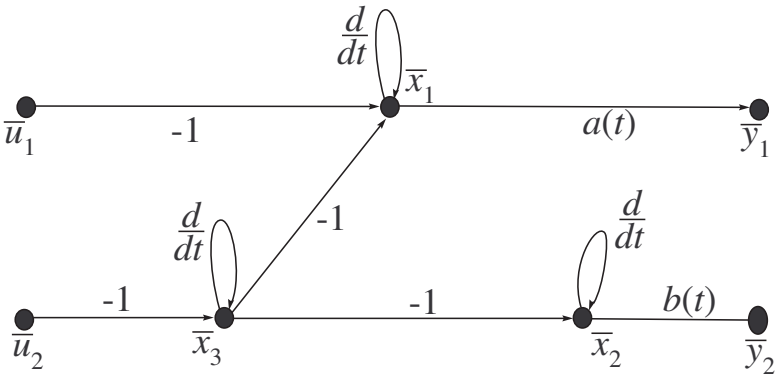

Figure 4.2: OSG for state feedback decoupling

$\bar{x}_2 \rightarrow \bar{y}_2$ of length 2, therefore $n_2 = 2$. The shortest input-output path of the system is $\bar{u}_1 \rightarrow \bar{x}_1 \rightarrow \bar{y}_1$ and therefore $L_1 = n'_1 = 1$. The two shortest disjoint paths are $\bar{u}_1 \rightarrow \bar{x}_1 \rightarrow \bar{y}_1$ and $\bar{u}_2 \rightarrow \bar{x}_3 \rightarrow \bar{x}_2 \rightarrow \bar{y}_2$, therefore $L_2 = 3$ and $n'_2 = L_2 - L_1 = 2$. The orders of the infinite zeros of the row sub-systems are $\{1, 2\}$ and the orders of the infinite zeros of the global system are $\{1, 2\}$. According to theorem 17, this model can be decoupled by a regular static state feedback control law.

Control synthesis is based on the computation of the vectors $(A^T + I\frac{d}{dt})^{n_i} c_i^T$ and $B^T(A^T + I\frac{d}{dt})^{n_i - 1} c_i^T$. In tables 4.3 and 4.4, we present each path and its gain. Using these results, we can conclude that $\tilde{B}(t) = \begin{pmatrix} a & 0 \\ 0 & b \end{pmatrix}$

Table 4.3: I/O paths

Path	Length	Gain
$\bar{u}_1 \rightarrow \bar{x}_1 \rightarrow \bar{y}_1$	1	a
$\bar{u}_2 \rightarrow \bar{x}_3 \rightarrow \bar{x}_2 \rightarrow \bar{y}_2$	2	b

and $(A^T + \frac{d}{dt})^{n_i} c_i^T = \begin{pmatrix} -\frac{da}{dt} & 0 & -a \\ 0 & \frac{d^2 b}{dt^2} & -2\frac{db}{dt} \end{pmatrix}$. This means that, according to relations (4.11) and (4.12), the decoupling matrices are:

$$F(t) = \begin{pmatrix} \frac{\dot{a}}{a} & 0 & -1 \\ 0 & -\frac{\ddot{b}}{b} & \frac{2\dot{b}}{b} \end{pmatrix} \tag{4.47}$$

Table 4.4: State/Output paths

Path	Length	Gain
$\bar{x}_1 \to \bar{x}_1 \to \bar{y}_1$	2	$-\frac{d}{dt}a$
$\bar{x}_3 \to \bar{x}_1 \to \bar{y}_1$	2	$-a$
$\bar{x}_2 \to \bar{x}_2 \to \bar{x}_2 \to \bar{y}_2$	3	$\frac{d^2}{dt^2}b$
$\bar{x}_3 \to \bar{x}_2 \to \bar{x}_2 \to \bar{y}_2$	3	$-\frac{d}{dt}b$
$\bar{x}_3 \to \bar{x}_3 \to \bar{x}_2 \to \bar{y}_2$	3	$-\frac{d}{dt}b$

$$G(t) = \begin{pmatrix} -\frac{1}{a} & 0 \\ 0 & \frac{1}{b} \end{pmatrix} \tag{4.48}$$

A simple inspection of relations (4.44) and (4.53), as well as (4.45) and (4.54) prove that the relations (4.41) and (4.42) are validated for this example.

4.2.4.2 Decoupling of LTV Bond Graph Models

The graphical procedures which were developed in this section are applied on a bond graph model. Just like for the structured system, we consider a LTV bond graph example and we determine the decoupling output injection control law. Then, we dualize the bond graph model and we calculate the state feedback control law which decouples the dual bond graph. In the end we compare the two solutions.

Let us consider the system from figure 4.3, where the dissipative elements R_1 and R_2 have time-dependent values. Our primary aim is to determine the decoupling output injection control law. For this, we need to construct the CBG. For obtaining the CBG, we need the causal paths which start from the input sources and end in dynamic elements in integral causality. The causal paths which present time-varying gains are: $E_1 \to R_1 \to C_1 \to I$ and $E_2 \to R_2 \to C_2 \to I$. Therefore each one of the dynamic elements receive a differential loop. In figure 4.4, we represented the CBG. Now, we have to check whether the LTV bond graph model can be decoupled by static output injection. For this, we must determine the infinite zero orders of the global system and of the column subsystems. Properties 21 and 28 offer a graphical procedure for calculating the infinite structure of the global system

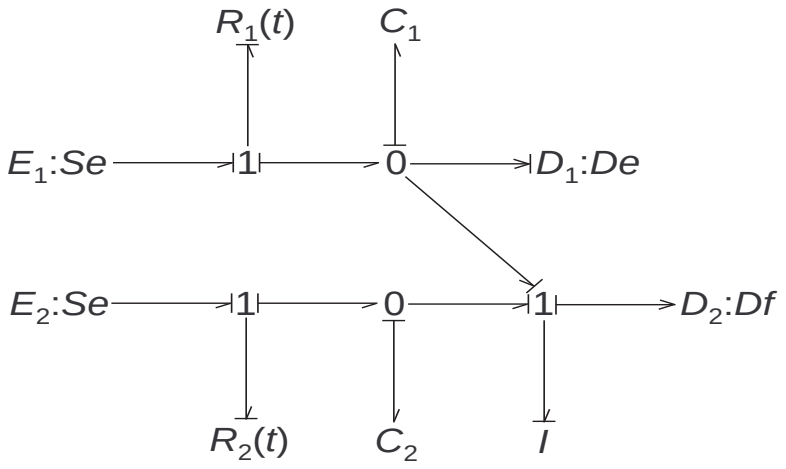

Figure 4.3: Bond Graph Model

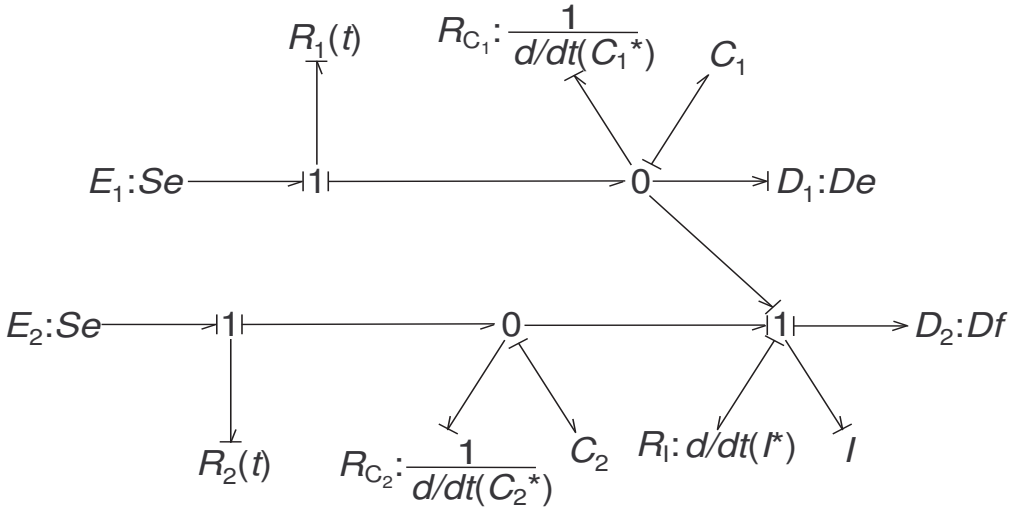

Figure 4.4: Bond Graph Model

and of the column subsystems respectively. The shortest input-output causal path which begins with source $E_1 : De$ is $E_1 \rightarrow R_1 \rightarrow C_1 \rightarrow D_1$, which has a length of 1 and therefore $n^1 = 1$. For the second input source, the shortest input-output causal path is $E_2 \rightarrow R_2 \rightarrow C_2 \rightarrow I \rightarrow D_2$, which has a length of 2, and therefore $n^2 = 2$. Now, let us concentrate on the infinite structure of the global system. The shortest input-output causal path is $E_1 \rightarrow R_1 \rightarrow C_1 \rightarrow D_1$, with a length of 1 and therefore $L_1 = n'_1 = 1$. The two shortest different causal paths are $E_1 \rightarrow R_1 \rightarrow C_1 \rightarrow D_1$ and

$E_2 \to R_2 \to C_2 \to I \to D_2$, with a cumulated length $L_2 = 3$. It results that $n_2' = L_2 - L_1 = 2$. If we compare the set of infinite zero orders of the column subsystems $\{1, 2\}$ with the set of infinite zero orders of the global system $\{1, 2\}$, we observe that they are equal. According to theorem 18, the LTV bond graph model can be decoupled by a static output injection control law. The next step is to determine the output injection control law, i.e. the matrices $K(t)$ and $L(t)$. For this, we must determine first the vectors $C(A - I\frac{d}{dt})^{n^j-1}B^j$ for $\tilde{C}(t)$ and $(A - I\frac{d}{dt})^{n^j}B^j$ for $K(t)$. In table 4.5, the paths and the gains for calculating the vectors $C(A - I\frac{d}{dt})^{n^j-1}B^j$ are presented. For

Table 4.5: I/O causal paths

Path	Length	Gain
$E_1 \to R_1 \to C_1 \to D_1$	1	$\frac{1}{C_1}\frac{1}{R_1}$
$E_2 \to R_2 \to C_2 \to I \to D_2$	2	$\frac{1}{I}\frac{1}{C_2}\frac{1}{R_2}$

the vectors $(A - I\frac{d}{dt})^{n^j}B^j$, we take into consideration the causal paths of length $n^j + 1$ between the dynamic elements in integral causality and the input sources. The results are collected in table 4.6. Using the results from

Table 4.6: Input/Dynamic Elements causal paths

Path	Length	Gain
$E_1 \to R_1 \to C_1 \to R_{C_1} \to C_1$	2	$-\frac{d}{dt}\frac{1}{R_1}$
$E_1 \to R_1 \to C_1 \to R_1 \to C_1$	2	$-\frac{1}{R_1}\frac{1}{C_1}\frac{1}{R_1}$
$E_1 \to R_1 \to C_1 \to I$	2	$\frac{1}{C_1}\frac{1}{R_1}$
$E_2 \to R_2 \to C_2 \to R_2 \to C_2 \to R_2 \to C_2$	3	$\frac{1}{R_2}\frac{1}{C_2}\frac{1}{R_2}\frac{1}{C_2}\frac{1}{R_2}$
$E_2 \to R_2 \to C_2 \to R_2 \to C_2 \to R_{C_2} \to C_2$	3	$\frac{d}{dt}\frac{1}{R_2}\frac{1}{C_2}\frac{1}{R_2}$
$E_2 \to R_2 \to C_2 \to R_{C_2} \to C_2 \to R_2 \to C_2$	3	$\frac{1}{R_2}\frac{1}{C_2}\frac{d}{dt}\frac{1}{R_2}$
$E_2 \to R_2 \to C_2 \to R_{C_2} \to C_2 \to R_{C_2} \to C_2$	3	$\frac{d}{dt}\frac{d}{dt}\frac{1}{R_2}$
$E_2 \to R_2 \to C_2 \to R_2 \to C_2 \to I$	3	$-\frac{1}{C_2}\frac{1}{R_2}\frac{1}{C_2}\frac{1}{R_2}$
$E_2 \to R_2 \to C_2 \to R_{C_2} \to C_2 \to I$	3	$-\frac{1}{C_2}\frac{d}{dt}\frac{1}{R_2}$
$E_2 \to R_2 \to C_2 \to I \to C_2$	3	$-\frac{1}{I}\frac{1}{C_2}\frac{1}{R_2}$
$E_2 \to R_2 \to C_2 \to I \to R_I \to I$	3	$-\frac{d}{dt}\frac{1}{C_2}\frac{1}{R_2}$
$E_2 \to R_2 \to C_2 \to I \to C_1$	3	$-\frac{1}{I}\frac{1}{C_2}\frac{1}{R_2}$

tables 4.5 and 4.6, we obtain:

$$\tilde{C}(t) = \begin{pmatrix} \frac{1}{C_1 R_1} & 0 \\ 0 & \frac{1}{R_2 I C_2} \end{pmatrix} \tag{4.49}$$

$$(A - \frac{d}{dt})^{n^j} B^j = \begin{pmatrix} \frac{1}{C_1 R_1} & -\frac{1}{R_2^2 C_2^2} + \frac{2\dot{R}_2}{R_2^2 C_2} \\ -\frac{1}{R_1^2 C_1} + \frac{\dot{R}_1}{R_1^2} & -\frac{1}{R_2 I C_2} \\ 0 & -\frac{1}{R_2 I C_2} + \frac{1}{R_2^3 C_2^2} - \frac{3\dot{R}_2}{R_2^3 C_2} - \frac{\ddot{R}_2}{R_2^2} + \frac{2\dot{R}_2^2}{R_2^3} \end{pmatrix} \tag{4.50}$$

According to relations (4.27) and (4.28), the decoupling matrices are:

$$K(t) = \begin{pmatrix} -1 & I(\frac{1}{R_2 C_2} - \frac{2\dot{R}_2}{R_2}) \\ C_1(\frac{1}{R_1 C_1} - \frac{\dot{R}_1}{R_1}) & 1 \\ 0 & IC_2(\frac{1}{IC_2} - \frac{1}{R_2^2 C_2^2} + \frac{3\dot{R}_2}{R_2^2 C_2} + \frac{\ddot{R}_2}{R_2} - \frac{2\dot{R}_2^2}{R_2^2}) \end{pmatrix} \tag{4.51}$$

$$L(t) = \begin{pmatrix} R_1 C_1 & 0 \\ 0 & R_2 I C_2 \end{pmatrix} \tag{4.52}$$

Let us consider now the dual bond graph model from figure 4.3. As our

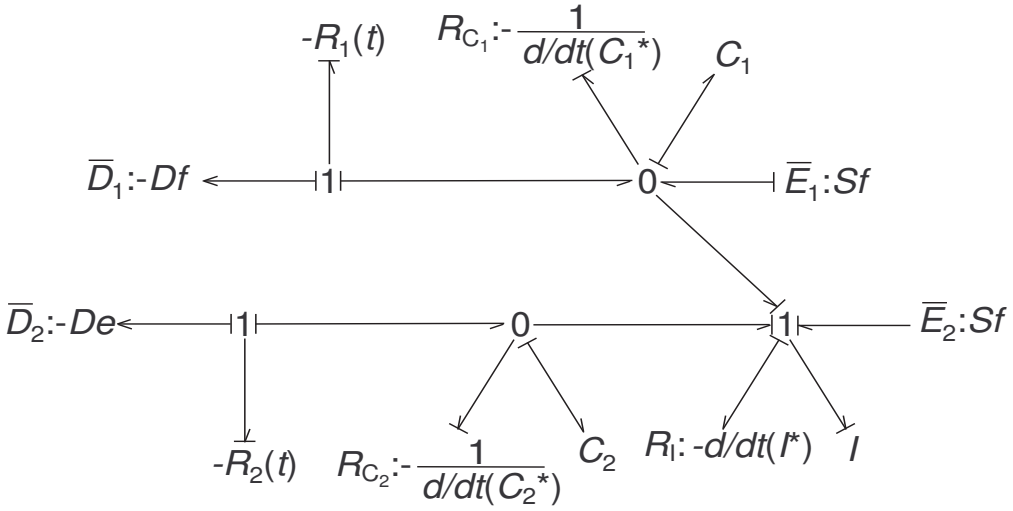

Figure 4.5: OBG of Dual Bond Graph Model

interest is to determine the decoupling state feedback control law, we have to construct first the OBG. In figure 4.5, the OBG of the dual bond graph model is pictured.

The shortest input/output causal path for $\bar{D}_1$ is $\bar{D}_1 \leftarrow R_1 \leftarrow C_1 \leftarrow \bar{E}_1$ of

length 1, therefore $n_1 = 1$. The shortest causal path for $\bar{D}_2$ is $\bar{D}_2 \leftarrow R_2 \leftarrow C_2 \leftarrow I \leftarrow \bar{E}_2$ of length 2 and therefore $n_2 = 2$. The shortest input-output causal path of the system is $\bar{D}_1 \leftarrow R_1 \leftarrow C_1 \leftarrow \bar{E}_1$ and therefore $L_1 = n'_1 = 1$. The two shortest disjoint causal paths are $\bar{D}_1 \leftarrow R_1 \leftarrow C_1 \leftarrow \bar{E}_1$ and $\bar{D}_2 \leftarrow R_2 \leftarrow C_2 \leftarrow I \leftarrow \bar{E}_2$, therefore $L_2 = 3$ and $n'_2 = L_2 - L_1 = 2$. The orders of the infinite zeros of the row sub-systems are $\{1, 2\}$ and the orders of the infinite zeros of the global system are $\{1, 2\}$. According to theorem 17, this model can be decoupled by a regular static state feedback control law.

Control synthesis is based on the computation of the vectors $(A^T + I\frac{d}{dt})^{n_i} c_i^T$ and $B^T(A^T + I\frac{d}{dt})^{n_i - 1} c_i^T$. In tables 4.7 and 4.8, we present each path and its gain.

Using these results, we can conclude that $\tilde{B}(t) = \begin{pmatrix} \frac{1}{C_1}\frac{1}{R_1} & 0 \\ 0 & -\frac{1}{I}\frac{1}{C_2}\frac{1}{R_2} \end{pmatrix}$ and

Table 4.7: I/O causal paths

Path	Length	Gain
$\bar{D}_1 \leftarrow R_1 \leftarrow C_1 \leftarrow \bar{E}_1$	1	$\frac{1}{C_1}\frac{1}{R_1}$
$\bar{D}_2 \leftarrow R_2 \leftarrow C_2 \leftarrow I \leftarrow \bar{E}_2$	2	$-\frac{1}{I}\frac{1}{C_2}\frac{1}{R_2}$

$$(A^T + \tfrac{d}{dt})^{n_i} c_i^T = \begin{pmatrix} \frac{1}{C_1 R_1} & -\frac{1}{R_1^2 C_1} + \frac{\dot{R}_1}{R_1^2} & 0 \\ \frac{1}{R_2^2 C_2^2} - \frac{2\dot{R}_2}{R_2^2 C_2} & \frac{1}{R_2 I C_2} & \frac{1}{R_2 I C_2} - \frac{1}{R_2^3 C_2^2} + \frac{3\dot{R}_2}{R_2^3 C_2} + \frac{\ddot{R}_2}{R_2^2} - \frac{2\dot{R}_2^2}{R_2^3} \end{pmatrix}.$$

This means that, according to relations (4.11) and (4.12), the decoupling matrices are:

$$F(t) = \begin{pmatrix} -1 & C_1(\frac{1}{R_1 C_1} - \frac{\dot{R}_1}{R_1}) & 0 \\ I(\frac{1}{R_2 C_2} - \frac{2\dot{R}_2}{R_2}) & 1 & IC_2(\frac{1}{IC_2} - \frac{1}{R_2^2 C_2^2} + \frac{3\dot{R}_2}{R_2^2 C_2} + \frac{\ddot{R}_2}{R_2} - \frac{2\dot{R}_2^2}{R_2^2}) \end{pmatrix} \tag{4.53}$$

$$G(t) = \begin{pmatrix} R_1 C_1 & 0 \\ 0 & -R_2 I C_2 \end{pmatrix} \tag{4.54}$$

A simple inspection of relations (4.44) and (4.53), as well as (4.45) and (4.54) prove that the relations (4.41) and (4.42) are validated for this example.

Table 4.8: Dynamic element/Output Detector causal paths

Path	Length	Gain
$\bar{D}_1 \leftarrow R_1 \leftarrow C_1 \leftarrow R_{C_1} \leftarrow C_1$	1	$-\frac{d}{dt}\frac{1}{R_1}$
$\bar{D}_1 \leftarrow R_1 \leftarrow C_1 \leftarrow R_1 \leftarrow C_1$	1	$-\frac{1}{R_1}\frac{1}{C_1}\frac{1}{R_1}$
$\bar{D}_1 \leftarrow R_1 \leftarrow C_1 \leftarrow I$	1	$\frac{1}{C_1}\frac{1}{R_1}$
$\bar{D}_2 \leftarrow R_2 \leftarrow C_2 \leftarrow R_2 \leftarrow C_2 \leftarrow R_2 \leftarrow C_2$	2	$-\frac{1}{R_2}\frac{1}{C_2}\frac{1}{R_2}\frac{1}{C_2}\frac{1}{R_2}$
$\bar{D}_2 \leftarrow R_2 \leftarrow C_2 \leftarrow R_2 \leftarrow C_2 \leftarrow R_{C_2} \leftarrow C_2$	2	$-\frac{d}{dt}\frac{1}{R_2}\frac{1}{C_2}\frac{1}{R_2}$
$\bar{D}_2 \leftarrow R_2 \leftarrow C_2 \leftarrow R_{C_2} \leftarrow C_2 \leftarrow R_2 \leftarrow C_2$	2	$-\frac{1}{R_2}\frac{1}{C_2}\frac{d}{dt}\frac{1}{R_2}$
$\bar{D}_2 \leftarrow R_2 \leftarrow C_2 \leftarrow R_{C_2} \leftarrow C_2 \leftarrow R_{C_2} \leftarrow C_2$	2	$-\frac{d}{dt}\frac{d}{dt}\frac{1}{R_2}$
$\bar{D}_2 \leftarrow R_2 \leftarrow C_2 \leftarrow R_2 \leftarrow C_2 \leftarrow I$	2	$\frac{1}{C_2}\frac{1}{R_2}\frac{1}{C_2}\frac{1}{R_2}$
$\bar{D}_2 \leftarrow R_2 \leftarrow C_2 \leftarrow R_{C_2} \leftarrow C_2 \leftarrow I$	2	$\frac{1}{C_2}\frac{d}{dt}\frac{1}{R_2}$
$\bar{D}_2 \leftarrow R_2 \leftarrow C_2 \leftarrow I \leftarrow C_2$	2	$\frac{1}{I}\frac{1}{C_2}\frac{1}{R_2}$
$\bar{D}_2 \leftarrow R_2 \leftarrow C_2 \leftarrow I \leftarrow R_I \leftarrow I$	2	$\frac{d}{dt}\frac{1}{C_2}\frac{1}{R_2}$
$\bar{D}_2 \leftarrow R_2 \leftarrow C_2 \leftarrow I \leftarrow C_1$	2	$\frac{1}{I}\frac{1}{C_2}\frac{1}{R_2}$

4.3 Decoupling Problem with Pole Placement for LTV Models

4.3.1 Geometrical Approach

4.3.1.1 A. (A, B) - invariance and state feedback

The aim of this section is to present a geometrical approach for the decoupling problem with stability of linear systems. In the first part, some geometrical results are recalled and invariant subspaces used in the input-output decoupling problem are defined.

The concept of (A, B)-invariance has been introduced by [61] to solve various decoupling and pole-assignment problems for linear time-invariant multivariable systems. For LTI structured systems, the problem of decoupling with stability was solved by [11]. In [27] the concepts have been generalized for linear time-varying systems. Therefore, we briefly present the results obtained, even though in [27], the problem of input-output decoupling is solved without tackling the stability problem.

Definition 30. *[27] Suppose that* $(A, B) \in \mathbf{A}_p^{n\times n} \times \mathbf{A}_p^{n\times m}$ *and that* ν *is generated by* $V \in \mathbf{A}_p^{n\times k}$*, where* $\mathbf{A}_p$ *is the ring of piecewise real analytic functions. Then* ν *is called meromorphically* (A, B)*-invariant if there exist* $N \in \mathbf{M}_p^{k\times k}$ *and* $M \in \mathbf{M}_p^{n\times k}$*, where* $\mathbf{M}_p$ *is the ring of piecewise meromorphical functions, such that*

$$(\delta I - A)V = VN + BM \tag{4.55}$$

ν *is called* (A, B)*-invariant if (4.55) holds true for some* N *and* M *with entries in* $\mathbf{A}_p$ *instead of* $\mathbf{M}_p$*.*
In terms of state feedback, ν *is an* (A, B)*-invariant subspace if there exists a set* $\mathcal{F}(A, B; \nu)$ *of state feedback matrices* F *such that* $(\delta I - A - BF)\nu \subset \nu$*. Let be* $\mathcal{L}(A, B; kerC)$ *the set of* (A, B)*-invariant subspaces included in the subspace* $kerC$*. This subspace is closed for addition; it thus contains a supremal element.*

Property 31. *[27] The subspace* $\mathcal{L}(A, B; kerC)$ *contains a supremal element denoted* $\nu^* = sup\mathcal{L}(A, B; kerC)$*.*

For control purposes, the orthogonal complement of the subspace ν^* *is used. It is the limit of algorithm (4.56):*

$$\begin{cases} \nu^{0\perp} = 0 \\ \nu^{\mu\perp} = (kerC)^\perp + (\delta I + A^T)((ImB)^\perp \bigcap (\nu^{\mu-1})^\perp) \end{cases} \tag{4.56}$$

Stable dynamics are associated with a second set of (A, B)*-invariant subspaces: stabilizable subspaces.*

Definition 31. ν *is a stabilizable* (A, B)*-invariant subspace if there exists a set of state feedback matrices* $F \in \mathcal{F}(A, B; \nu)$ *verifying equation (4.57).*

$$\sigma(\nu|A + BF|\nu) \subset \mathbb{C}_- \tag{4.57}$$

Theorem 20. *An LTV system can be decoupled by static state feedback if* $\nu^* = \bigcap_{i=1}^m \nu_i^*$*.*

This theorem leads to the procedure for calculating the control law, which is based on the following property.

Property 32. *Let* Σ *be a square LTV system (3.51) which can be decoupled by a regular static state feedback law (4.6). If* $\tilde{B}(t)$ *is its decoupling matrix*

and $\{n_i\}$ *is its row infinite structure, consider* $\{\nu_i^*\}$ *a family of geometric supports, solution of the decoupling problem, then the matrices* $F(t)$ *and* $G(t)$ *are calculated according to equations (4.58).*

$$\begin{cases} h_i(t)\nu_i^*(t) = 0, i = 1, \ldots, m \\ F(t) = -\tilde{B}^{-1}(t)(h_i(t) + ((A^T + \delta I)^{n_i} c_i^T)^T(t))_{i=1,\ldots,m} \\ G(t) = \tilde{B}^{-1}(t) diag(g_i)_{i=1,\ldots,m} \end{cases} \tag{4.58}$$

This property allows the computation of matrices $F(t)$ and $G(t)$ based on a family of subspace solutions of the decoupling problem. The parameters g_i, $i = 1, \ldots, m$ can be freely chosen; they set the static gain of the closed-loop system. The row vectors $h_i(t)$ are a linear combination of the base vectors of the subspace $\nu_i^{*\perp}$. Therefore it introduces in the control law a number of degrees of freedom equal to the dimension of this subspace. The choice of the decoupling subspaces allows one to determine the total number of degree of freedom of the control law.

4.3.1.2 B. (C, A) - invariance and output injection

For solving the decoupling with stability by state feedback problem, a geometrical approach, based on (A, B)-invariance is used. Naturally, for output injection (C, A)-invariance is used.

Definition 32. *[27] Suppose that* $(C, A) \in \mathbf{A}_p^{n\times m} \times \mathbf{A}_p^{n\times n}$ *and that* $\mathcal{S} \in \mathbb{W}_n$ *is generated by* $V \in \mathbf{A}_p^{n\times k}$*. Then* $\mathcal{S}$ *is called meromorphically* (C, A)*-invariant if there exist* $N \in \mathbf{M}_p^{k\times k}$ *and* $M \in \mathbf{M}_p^{n\times k}$ *such that*

$$(A - sI_n)V = VN + MC \tag{4.59}$$

$\mathcal{S}$ is called (C, A)-invariant if (4.59) holds true for some N and M with entries in $\mathbf{A}_p$ instead of $\mathbf{M}_p$.
In terms of output injection, $\mathcal{S}$ is a (C, A)-invariant subspace if there exists a set $\mathcal{K}(C, A; \mathcal{S})$ of output injection matrices K such that $(sI_n - A - KC)\mathcal{S} \subset \mathcal{S}$. Let $\mathcal{L}(kerC, A; ImB)$ be the set of (C, A)- invariant subspaces including the subspace ImB.

Property 33. *[27] The subspace* $\mathcal{L}(kerC, A; ImB)$ *contains a infinimum element denoted* $\mathcal{S}^* = inf\mathcal{L}(kerC, A; ImB)$.

For control purposes, the subspace is the limit of algorithm (4.60):

$$\begin{cases} \mathcal{S}^0 = 0 \\ \mathcal{S}^\mu = (ImB) + (A - sI)((kerC) \bigcap (\mathcal{S}^{\mu-1})) \end{cases} \tag{4.60}$$

Stable dynamics are associated with a second set of (C, A)-invariant subspaces: stabilizable subspaces.

Definition 33. *[27] $\mathcal{S}$ is a stabilizable (C, A)-invariant subspace if there exists a set of output injection matrices $K \in (C, A; \mathcal{S})$ verifying equation:*

$$Re(\sigma(\mathcal{S}|A + KC|\mathcal{S})) < 0 \tag{4.61}$$

Theorem 21. *An LTV system can be decoupled by static output injection if $\mathcal{S}^* = \bigcap_{j=1}^{m} \mathcal{S}_j^*$.*

This theorem leads to the procedure for calculating the control law, which is based on the following property.

Property 34. *Let Σ be a square LTV system (3.51) which can be decoupled by a regular static output injection law. If $\tilde{C}(t)$ is its decoupling matrix and $\{n^j\}$ is its column infinite structure, consider $\mathcal{S}_j^*$ a family of geometric supports, solution of the decoupling problem, then the matrices K and L are calculated according to equations (4.62).*

$$\begin{cases} \mathcal{S}_j^*(t) h_j(t) = 0, j = 1, \ldots, m \\ K(t) = -(h_j(t) + A(t)\tilde{A}(t) - \frac{d}{dt}\tilde{A}(t))\tilde{C}^{-1}(t) \\ L(t) = diag(\lambda_j)_{j=1,\ldots,m}\tilde{C}^{-1}(t) \end{cases} \tag{4.62}$$

This property allows the computation of matrices K and L based on a family of subspace solutions of the decoupling problem. The parameters λ_j, $j = 1, \ldots, m$ can be freely chosen; they set the static gain of the closed-loop system. The column vectors h_j are a linear combination of the base vectors of the subspace $\mathcal{S}_j^*$. Therefore it introduces in the control law a number of degrees of freedom equal to the dimension of this subspace. The choice of the decoupling subspaces allows one to determine the total number of degree of freedom of the control law.

4.3.1.3 Graphical Procedure

In order to solve the equations (4.58) and (4.62) respectively, computation of the base vectors of the subspaces $\nu_i^{*\perp}$ and $\mathcal{S}_j^*$ are needed. The aim of this subsection is to identify a graphical method for calculating these vectors. The following properties are used:

Property 35. $\nu_i^{*\perp} = span\left\{((A^T + \delta I)^j c_i^T)^T(t)\,,\ 0 \leq j \leq n_i - 1\right\}$, *where* $\{n_i\}$ *is the set of row infinite zero orders of the row system* $\Sigma(c_i, A, B)$.

Property 36. $\mathcal{S}_j^* = span\left\{((A - I\frac{d}{dt})^k B^j)(t), 0 \leq k \leq n^j - 1\right\}$ *,where* n^j *is the infinite zero order of the column system* $\Sigma(C, A, B^j)$.

Both for structured systems and for bond graphs, the graphical procedures which were developed at the beginning of the previous section can be used for determining the vectors $((A^T + \delta I)^j c_i^T)^T(t)$ and $((A - I\frac{d}{dt})^k B^j)(t)$.

Structured Systems

Spanning these vectors is easy because the vectors $((A^T + \delta I)^j c_i^T)^T(t)$ can be calculated according to the formula (4.15), where the paths between the i^{th} output vertex and the set of state vertices of length j are taken into consideration. And for the vectors $((A - I\frac{d}{dt})^k B^j)(t)$, the formula (4.29) can be applied, where the causal paths between the j^{th} input source and the set of state variables of length k are taken into consideration. The only difference is that proposition 35 is applied on the OSG and property 36 is applied on the CSG.

Bond Graph Approach

For calculating the vectors $((A^T + \delta I)^j c_i^T)^T(t)$ on a bond graph , we apply property 24 on the OBG, but we consider only the causal paths of length j. Analogously, for vectors $((A - I\frac{d}{dt})^k B^j)(t)$, we use property 30 on the CBG, with the causal paths of length k.

4.3.1.4 Duality between (A, B) and (C, A) Invariance

The two invariant concepts have been discussed in [27] for LTV models. Our interest is with the duality between (A, B) and (C, A) invariance and more specific with the duality between the relations (4.58) and (4.62). The aim

is to obtain formulas (4.41) and (4.42) for the decoupling with partial pole placement.

Theorem 22. *The state feedback control law which decouples with partial pole placement a system Σ is equal to the output injection control law which decouples with partial pole placement the dual system $\bar{\Sigma}$ and viceversa, if the same poles and static gains are assigned.*

Starting from equations (4.58) and (4.62), we can easily observe that the duality holds if the duality between the base vectors of the subspaces $\nu_i^{*\perp}$ and $\mathcal{S}_j^*$ holds. If propositions 35 and 36 are used, then the duality is based on vectors $((A^T + I\frac{d}{dt})^j c_i^T)^T(t)$ and $((A - I\frac{d}{dt})^k B^j)(t)$. In order to prove this duality, the same approach used for proving theorem 16 should be applied.

Remark 20. *The eigenvalues of the matrix A and the eigenvalues of the state matrix of the dual system $\bar{A} = -A^T$ are opposed, therefore if in one case an eigenvalue is stable it is unstable for the dual model.*

The unassigned poles by the state feedback control law or the output injection control law are invariant zeros. Using the duality between the state feedback and the output injection, we can make the following observation:

Remark 21. *The invariant zeros of a bond graph model Σ under the state feedback control are the same as the invariant zeros of the dual bond graph model $\bar{\Sigma}$ under the output injection control law.*

The pole placement problem is not completely solved because it is difficult to determine the explicit expression for the control law graphically on the LTV model. A perspective for determining the complete pole placement control law can be considered by proving that the ν_{stab}^* and S_{stab}^* are dual. But, for the time-being, we have not fully exploited the possibilities of this approach.

4.4 Decoupling and Input-Output Linearization of Nonlinear Systems

The decoupling problem for nonlinear systems has been tackled since the early 1970's. Analytical solutions have been proposed in [53], [21] and [54].

A geometrical approach has been introduced in [28]. Our interest was to offer a graphical approach. Therefore, we focused on extending the LTV procedures to the nonlinear case.
System decoupling for nonlinear models can be done graphically, if we use the variational model (see [36], [39], [38] and [41]). Using the variational model presents two major advantages. Firstly, we can reconstruct the nonlinear control law, after we have determined the control law on the linearized model. Secondly, we can perform the procedures graphically on the structured system representations or on the bond graphs.
This section is split into three parts; in the first part, we define a variational model, in the second part, we solve the decoupling by state feedback problem for nonlinear system and in the third, the decoupling by output injection problem. At the end of this section, we present some examples which illustrate the use of the techniques introduced in this section and in the previous one.

4.4.1 Variational Model

A variational model, also called tangential system, is a linear system which is attached to a nonlinear system.

$$\Sigma_{NL} : \begin{cases} \dot{x} = f(x,u) \\ y = h(x,u) \end{cases} \tag{4.63}$$

Definition 34. *Given a nonlinear system (4.63), a variational (tangential) system is obtained by differentiating like in equation 4.64:*

$$\Sigma_{Var} : \begin{cases} \dot{dx} = \frac{\partial f(x,u)}{\partial x} dx + \frac{\partial f(x,u)}{\partial u} du \\ dy = \frac{\partial h(x,u)}{\partial x} dx + \frac{\partial h(x,u)}{\partial u} du \end{cases} \tag{4.64}$$

If we consider that the variable dx are independent of variable x, then we can consider that the variational model is a linear time-varying system, with the state vector dx. Graphical methods have been proposed for constructing the variational model both for structured systems ([41]) and bond graphs ([2]).

4.4.1.1 Structured Systems

So far, the structured systems had not been used extensively for nonlinear systems. In fact, the graph representation is compatible only with linear systems. Some solutions for the decoupling problem of nonlinear models using the structured systems has been proposed in [32] and [48].
In order to use the structured systems procedures, we have defined the variational structured system, which consist of representing the linear time-varying system (4.64), with the input vertices du, the output vertices dy and the state vertices dx. For a detailed example on the procedure for obtaining the tangential structured system, at the end of this section we have consider the example of a separated excited DC motor.

4.4.1.2 Variational Bond Graph

The variational bond graph is the bond graph model which has the algebraic representation of the tangential system. It is obtained by considering the derivatives of the nonlinear functions associated with the bond graph elements. A short example is provided, considering the nonlinearity of a

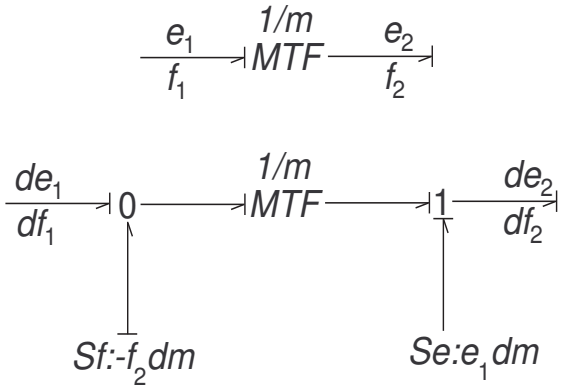

Figure 4.6: Variational Bond Graph of a Nonlinear Modulated Transformer

modulated transformer. On the nonlinear bond graph, the modulated transformer has a nonlinear gain $\begin{cases} e_2 = me_1 \\ f_1 = mf_2 \end{cases}$. Applying the differential operator leads us to $\begin{cases} de_2 = mde_1 + dme_1 \\ df_1 = mdf_2 + dmf_2 \end{cases}$ In figure 4.6 this operation is explained.

Two modulated sources are added so that the equations for 1-junction and 0-junction respectively on the variational bond graph are the same as the ones above. If we consider that dx is the state vector, du the input vector and dy the output vector of the variational bond graph, then the variational bond graph is a linear time-varying model.

4.4.2 State Feedback

The aim of this section is to solve the problem of input-output decoupling by state feedback problem for nonlinear systems.
Given a nonlinear system (4.63), can it be decoupled by a static state feedback control law $u = \alpha(x) + \beta(x, \bar{u})$*, where by decoupled we understand that the* i^{th} *output* y_i *is influenced only by the* i^{th} *input* $\bar{u}_i$*? If so, what are the functions* $\alpha(x)$ *and* $\beta(x, \bar{u})$*?*
Our solution is based on the use of the tangential system.
As the variational system is a time-varying model the procedure described in the previous section can be used to determine whether it can be decoupled or not. Afterwards we continue with the procedure for the control law synthesis for the LTV model. But we do not have to determine the matrices $F(t)$ and $G(t)$. It is sufficient to calculate matrices $\tilde{A}(t)$ and $\tilde{B}(t)$ from equation 4.9 and 4.10 respectivelly. Using this information, the equation for the decoupling of the variational model can be written as:

$$(\tilde{A}A + \delta\tilde{A})dx + \tilde{B}du = d\bar{u} \tag{4.65}$$

Equation (4.65) is a total integral and after integration the expression of the static decoupling law is obtained. Moreover, if we consider the control law which decouples the variational model with pole placement, then the equation (4.66) is obtained, where p_{ij} are the parameters used for the pole placement.

$$\begin{array}{l}(\sum_{j=0}^{n_i-1} p_{ij}((A^T + \delta I)^j c_i^T)^T(t) + \\ ((A^T + \delta I)^{n_i} c_i^T)^T(t))_{i=1,\ldots,m} dx + \tilde{B}du = d\bar{u}\end{array} \tag{4.66}$$

Equation (4.66) is also a total integral and after computations it leads to the synthesis of the decoupling law for the nonlinear model, with pole placement and linearization of the model, if the zero dynamics are stable.

4.4.3 Output Injection

Given a nonlinear system as in equation (4.67), can it be decoupled by a static output injection control law, where by decoupled we understand that the i^{th} output z_i is influenced only by the i^{th} input u_i? If so, what are the functions $k(y)$ and $l(y)$?

$$\begin{cases} \dot{x}(t) = f(x(t), u(t)) + k(y(t)) \\ y(t) = h(x(t), u(t)) \\ z(t) = l(y(t)) \end{cases} \tag{4.67}$$

The solution is based on the use of the variational model, just like in the case of state feedback. As the variational system is a time-varying model the procedure described above can be used to determine whether it can be decoupled or not. Afterwards we continue with the procedure for the control law synthesis for the LTV model by determining the matrices $\tilde{A}$ and $\tilde{C}$ from relations 4.25 and 4.26 respectively.
In the end, equation (4.68) has to be integrated to obtain the decoupled system and equation (4.69) for the linearized and stable system. In order to obtain the functions $k(y)$ and $l(y)$ both equations have to be expressed in format (4.70).

$$\begin{cases} \dot{dx} = (A - A\tilde{A}\tilde{C}^{-1}C + \frac{d}{dt}(\tilde{A})\tilde{C}^{-1}C)dx + Bdu \\ dz = \tilde{C}^{-1}Cdx \end{cases} \tag{4.68}$$

$$\begin{cases} \dot{dx} = ((A - A\tilde{A}\tilde{C}^{-1}C + \frac{d}{dt}(\tilde{A})\tilde{C}^{-1}C) + (\sum_{i=0}^{n^j-1} p_{ij}(A - I\frac{d}{dt})^i B^j)_{j=1,\dots,m})dx + Bdu \\ dz = \tilde{C}^{-1}Cdx \end{cases} \tag{4.69}$$

$$\begin{cases} \dot{x} = f(x, u) + k(h(x, u)) \\ z = l(h(x, u)) \end{cases} \tag{4.70}$$

4.4.4 Application - Nonlinear Structured System

The example which is proposed to present the use of the procedures introduced in this section is a separately excited DC motor(SEDCM). The system

is defined by the following equations:

$$\begin{cases} L_e \frac{dI_e(t)}{dt} + R_e I_e(t) = V_e(t) \\ L_r \frac{dI_r(t)}{dt} + R_r I_r(t) = V_r(t) - K L_e I_e(t)\Omega(t) \\ J \frac{d\Omega(t)}{dt} + f\Omega(t) = K L_e I_e(t) I_r(t) \\ y_1 = I_e(t) \\ y_2 = \Omega(t) \end{cases} \tag{4.71}$$

Let us consider
$x(t) = (I_e(t), I_r(t), \Omega(t))^T = (x_1, x_2, x_3)^T(t)$ as the state vector and $u(t) = (V_e(t), V_r(t))^T = (u_1, u_2)^T(t)$ as the input vector. The system (4.71) is nonlinear, and if we want to decouple this nonlinear system we have to determine the tangential system first. The variational system is:

$$\begin{cases} \dot{dx_1} = -\frac{R_e}{L_e} dx_1 + \frac{1}{L_e} du_1 \\ \dot{dx_2} = -\frac{KL_e}{L_r} x_3 dx_1 - \frac{R_r}{L_r} dx_2 - \frac{KL_e}{L_r} x_1 dx_3 + \frac{1}{L_r} du_2 \\ \dot{dx_3} = \frac{KL_e}{J} x_2 dx_1 + \frac{KL_e}{J} x_1 dx_2 - \frac{f}{J} dx_3 \\ dy_1 = dx_1 \\ dy_2 = dx_3 \end{cases} \tag{4.72}$$

Using the variational graph of the motor we can apply the procedures de-

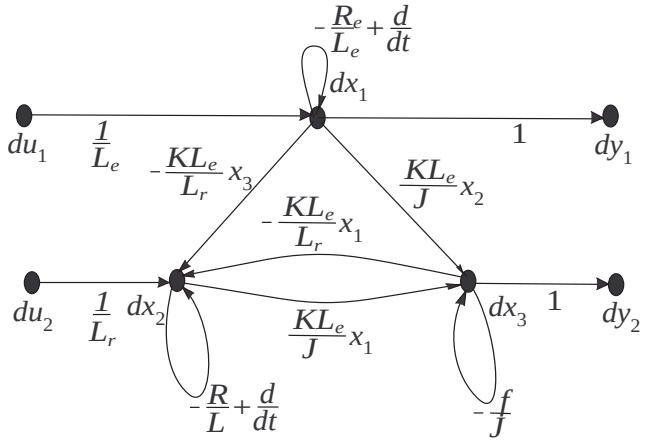

Figure 4.7: OSG of the Variational model for the SEDCM

scribed in the previous sections to determine whether or not the system can be decoupled.

The first step consists in determining the infinite zero orders n_i for each

sub-system $\Sigma(c_i, A, B)$. The shortest path for dy_1 is $du_1 \rightarrow dx_1 \rightarrow dy_1$, which has the length 1 and therefore $n_1 = 1$. Analogously the shortest path for the second output dy_2 is $du_2 \rightarrow dx_2 \rightarrow dx_3 \rightarrow dy_2$ and $n_2 = 2$. Secondly the infinite zero orders of the global model have to be determined. The shortest path is $du_1 \rightarrow dx_1 \rightarrow dy_1$ and has a length of 1, therefore $L_1 = n_1' = 1$. The two shortest different paths are $du_1 \rightarrow dx_1 \rightarrow dy_1$ and dy_2 is $du_2 \rightarrow dx_2 \rightarrow dx_3 \rightarrow dy_2$, therefore $L_2 = 3$ and $n_2' = 2$. The orders of the infinite zeros of the row sub-systems are $\{1, 2\}$ and the orders of the infinite zeros of the global system are $\{1, 2\}$. According to theorem 17, this model can be decoupled by a regular static state feedback control law.
Once the stage of system analysis has been finished, we can proceed to the computation of the matrices $\tilde{A}(t)$ and $\tilde{B}(t)$ and equation (4.66) can be integrated. The last part of the solution was too difficult to be calculated directly; therefore a formal calculus program (MAPLE) was used. The static control law for the decoupling by state feedback was determined; its expression is given in equation (4.73). Similar procedure is developed for input-output linearization.

$$\begin{cases} u_1 = R_e x_1 + L_e v_1 \\ u_2 = K L_1 x_1 x_3 + R_2 x_2 + \frac{L_2 f}{J} x_2 - \frac{L_2 f^2}{K L_1 J} \frac{x_3}{x_1} \\ \qquad -l_2 \frac{x_2}{x_1} v_1 + \frac{L_2 J}{K L_1 x_1} v_2 \end{cases} \tag{4.73}$$

4.4.5 Application - Nonlinear Bond Graph Model

For this application we have chosen a well known example: a two-link robot manipulator (figure 4.8). The inputs of the system are the torques in each

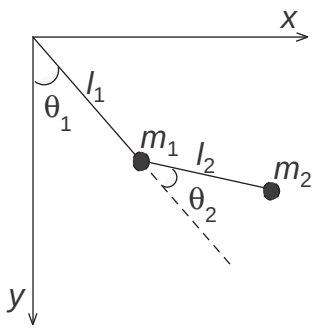

Figure 4.8: Two-link robot manipulator

joint and the outputs are the angles θ. Following the bond graph methodology for creating the bond graph representation, we consider the equations of the velocities on the two axes are:

$$\begin{cases} \dot{x}_1 = l_1\dot{\theta}_1 cos\theta_1 \\ \dot{y}_1 = -l_1\dot{\theta}_1 sin\theta_1 \\ \dot{x}_2 = \dot{x}_1 + l_2(\dot{\theta}_1 + \dot{\theta}_2)cos(\theta_1 + \theta_2) \\ \dot{y}_2 = \dot{y}_1 - l_2(\dot{\theta}_1 + \dot{\theta}_2)sin(\theta_1 + \theta_2) \end{cases} \tag{4.74}$$

The bond graph model on the nonlinear system is presented in figure 4.9, where:

$$\begin{cases} z_1 = cos\theta_1 \\ z_2 = sin\theta_1 \\ z_3 = cos(\theta_1 + \theta_2) \\ z_4 = sin(\theta_1 + \theta_2) \end{cases} \tag{4.75}$$

Obtaining the nonlinear bond graph model is just the first stage of the de-

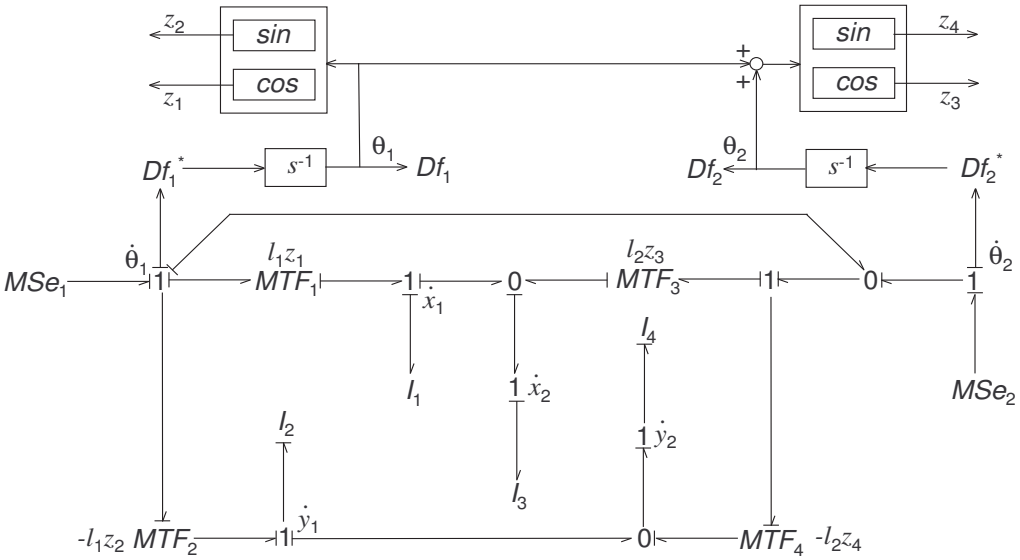

Figure 4.9: Nonlinear Bond Graph model with algebraic equations

coupling procedure. The second stage is to determine the variational bond graph. Using the algorithm presented in section 4.4.1.2, we obtain the linear time-varying bond graph model.

In the following, we perform the procedure of system decoupling by output injection and the procedure for system decoupling with stability by state

feedback for this bond graph model.

The procedure presented in the previous section for decoupling by state feedback for LTV models uses the Observability Bond Graph, while the decoupling by output injection uses the Controllability Bond Graph. But in our variational bond graph the inputs and the outputs share the same junctions and the same causality. This means that beside the sign of the gain of the differential loop, the CBG and the OBG are identical. As all the modulated transformers have time-dependent parameters and all the causal paths pass by at least one transformer, all the dynamic elements in integral causality on the BGI get a differential loop (the dissipative elements R_1 and R_2). which is presented in figure 4.10.

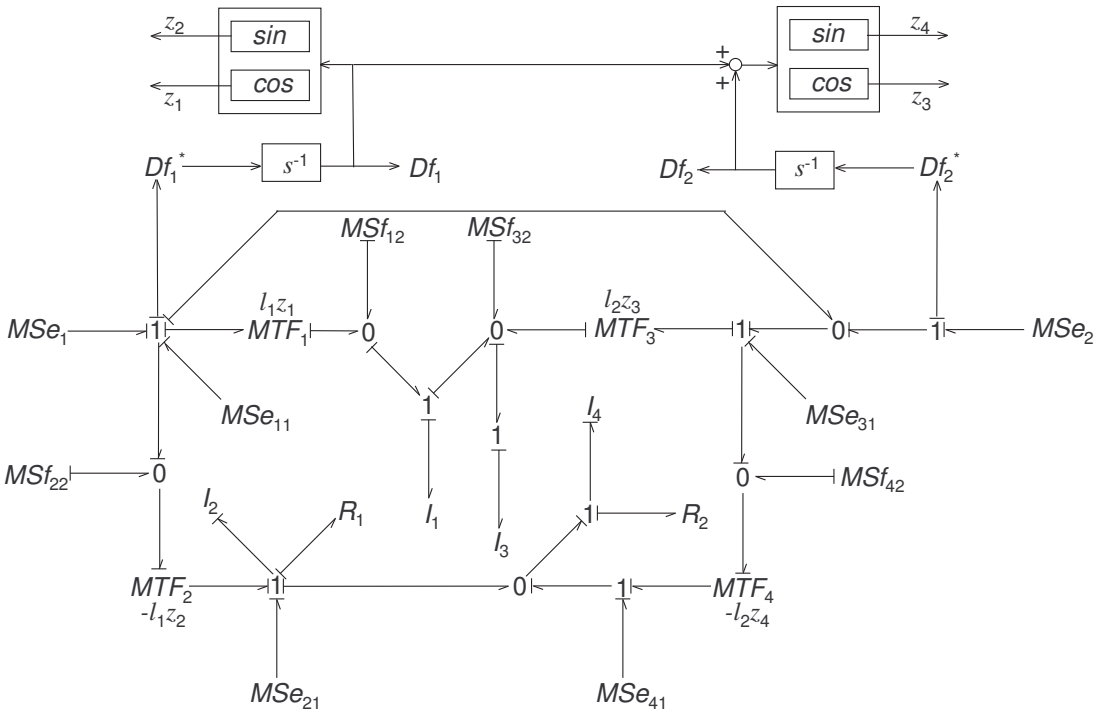

Figure 4.10: Observability Bond Graph model

Output Injection

Using the variational graph of the robot we can apply the procedures described in the previous sections to determine whether or not the system can be decoupled.

For system analysis, we have to determine the infinite zero orders n^i for each

sub-system $\Sigma(C, A, B^j)$. The shortest causal path for MSe_1 is $MSe_1 \rightarrow I_2 \rightarrow Df_1$, which has the length 1 and therefore $n^1 = 1$. Analogously the shortest causal path for the second source MSe_2 is $MSe_2 \rightarrow I_4 \rightarrow Df_2$ and $n_2 = 1$.

Secondly the infinite zero orders of the global model have to be deter-

Table 4.9: Causal paths for decoupling by output injection

Causal Path	Length
$MSe_1 \rightarrow MTF_2 \rightarrow I_2 \rightarrow MTF_2 \rightarrow Df_1$	1
$MSe_1 \rightarrow MTF_2 \rightarrow I_2 \rightarrow MTF_4 \rightarrow Df_2$	1
$MSe_2 \rightarrow MTF_4 \rightarrow I_4 \rightarrow MTF_4 \rightarrow Df_2$	1
$MSe_1 \rightarrow MTF_2 \rightarrow I_2 \rightarrow R_1 \rightarrow I_2$	2
$MSe_1 \rightarrow MTF_2 \rightarrow I_2 \rightarrow MTF_4 \rightarrow MTF_3 \rightarrow I_3 \rightarrow MTF_3 \rightarrow MTF_4 \rightarrow I_4$	2
$MSe_1 \rightarrow MTF_2 \rightarrow I_2 \rightarrow MTF_4 \rightarrow MTF_3 \rightarrow I_3 \rightarrow MTF_3 \rightarrow MTF_4 \rightarrow I_2$	2
$MSe_1 \rightarrow MTF_2 \rightarrow I_2 \rightarrow MTF_2 \rightarrow MTF_1 \rightarrow I_1 \rightarrow MTF_1 \rightarrow MTF_2 \rightarrow I_2$	2
$MSe_1 \rightarrow MTF_2 \rightarrow I_2 \rightarrow MTF_2 \rightarrow MTF_1 \rightarrow I_3 \rightarrow MTF_1 \rightarrow MTF_2 \rightarrow I_2$	2
$MSe_1 \rightarrow MTF_2 \rightarrow I_2 \rightarrow MTF_2 \rightarrow MTF_1 \rightarrow I_3 \rightarrow MTF_3 \rightarrow MTF_4 \rightarrow I_2$	2
$MSe_1 \rightarrow MTF_2 \rightarrow I_2 \rightarrow MTF_2 \rightarrow MTF_1 \rightarrow I_3 \rightarrow MTF_3 \rightarrow MTF_4 \rightarrow I_4$	2
$MSe_2 \rightarrow MTF_4 \rightarrow I_4 \rightarrow R_2 \rightarrow I_4$	2
$MSe_2 \rightarrow MTF_4 \rightarrow I_4 \rightarrow MTF_4 \rightarrow MTF_3 \rightarrow I_3 \rightarrow MTF_3 \rightarrow MTF_4 \rightarrow I_4$	2
$MSe_2 \rightarrow MTF_4 \rightarrow I_4 \rightarrow MTF_4 \rightarrow MTF_3 \rightarrow I_3 \rightarrow MTF_3 \rightarrow MTF_4 \rightarrow I_2$	2
$MSe_2 \rightarrow MTF_4 \rightarrow I_4 \rightarrow MTF_4 \rightarrow MTF_3 \rightarrow I_3 \rightarrow MTF_1 \rightarrow MTF_2 \rightarrow I_2$	2
$MSe_2 \rightarrow MTF_4 \rightarrow I_2 \rightarrow R_1 \rightarrow I_2$	2
$MSe_2 \rightarrow MTF_4 \rightarrow I_2 \rightarrow MTF_4 \rightarrow MTF_3 \rightarrow I_3 \rightarrow MTF_3 \rightarrow MTF_4 \rightarrow I_4$	2
$MSe_2 \rightarrow MTF_4 \rightarrow I_2 \rightarrow MTF_4 \rightarrow MTF_3 \rightarrow I_3 \rightarrow MTF_3 \rightarrow MTF_4 \rightarrow I_2$	2
$MSe_2 \rightarrow MTF_4 \rightarrow I_2 \rightarrow MTF_4 \rightarrow MTF_3 \rightarrow I_3 \rightarrow MTF_1 \rightarrow MTF_2 \rightarrow I_2$	2
$MSe_2 \rightarrow MTF_4 \rightarrow I_2 \rightarrow MTF_2 \rightarrow MTF_1 \rightarrow I_1 \rightarrow MTF_1 \rightarrow MTF_2 \rightarrow I_2$	2
$MSe_2 \rightarrow MTF_4 \rightarrow I_2 \rightarrow MTF_2 \rightarrow MTF_1 \rightarrow I_3 \rightarrow MTF_1 \rightarrow MTF_2 \rightarrow I_2$	2
$MSe_2 \rightarrow MTF_4 \rightarrow I_2 \rightarrow MTF_2 \rightarrow MTF_1 \rightarrow I_1 \rightarrow MTF_3 \rightarrow MTF_4 \rightarrow I_2$	2
$MSe_2 \rightarrow MTF_4 \rightarrow I_2 \rightarrow MTF_2 \rightarrow MTF_1 \rightarrow I_1 \rightarrow MTF_3 \rightarrow MTF_4 \rightarrow I_4$	2

mined. The shortest causal path is $MSe_1 \rightarrow I_2 \rightarrow Df_1$ and has a length of 1, therefore $L_1 = n'_1 = 1$. The two shortest different causal paths are $MSe_1 \rightarrow I_2 \rightarrow Df_1$ and $MSe_2 \rightarrow I_4 \rightarrow Df_2$, therefore $L_2 = 2$ and $n'_2 = 1$. The orders of the infinite zeros of the row sub-systems are $\{1, 1\}$ and the

orders of the infinite zeros of the global system are $\{1, 1\}$. According to theorem 18, this model can be decoupled by a regular static state feedback control law.
Once the stage of system analysis has been finished, we can proceed to the computation of the matrices $\tilde{A}(t)$ and $\tilde{C}(t)$ using the gains of the causal paths from table 4.9. Then equation (4.69) can be integrated. For calculating the output injection control law, we have used a formal calculus program (MAPLE). The solution of this problem takes a lot of space and is not appropriate to be presented here.

State Feedback

Now, we perform the same task, but this time we search for the state feedback control law which decouples the bond graph model with stability.
The first step consists in determining the infinite zero orders n_i for each subsystem $\Sigma(c_i, A, B)$. The shortest path for Df_1 is $MSe_1 \rightarrow I_2 \rightarrow Df_1$, which has the length 1 and therefore $n_1 = 1$. Analogously the shortest causal path for the second output Df_2 is $MSe_2 \rightarrow I_4 \rightarrow Df_2$ and $n_2 = 1$.
Secondly we focus on the infinite zero orders of the global model. The shortest causal path is $MSe_1 \rightarrow I_2 \rightarrow Df_1$ and has a length of 1, therefore $L_1 = n'_1 = 1$. The two shortest different causal paths are $MSe_1 \rightarrow I_2 \rightarrow Df_1$ and $MSe_2 \rightarrow I_4 \rightarrow Df_2$, therefore $L_2 = 2$ and $n'_2 = 1$. The orders of the infinite zeros of the row sub-systems are $\{1, 1\}$ and the orders of the infinite zeros of the global system are $\{1, 1\}$. According to theorem 17, this model can be decoupled by a regular static state feedback control law.
The computation of the matrices $\tilde{A}(t)$ and $\tilde{B}(t)$ using the gains of the causal paths from table 4.10 is proceeded and equation (4.66) can be integrated.
The static control law for the decoupling and linearization, determined with MAPLE, has been introduced in simulation with the program 20sim in which we have modeled this example. In figure 4.11, we present the inputs and the outputs of the system after input-output linearization and assignation of the poles $p_1 = -2$ on the first channel and $p_2 = -5$ on the second channel.

Table 4.10: Causal paths for decoupling by state feedback

Causal Path	Length
$Df_1 \leftarrow MTF_2 \leftarrow I_2 \leftarrow MTF_2 \leftarrow MSe_1$	1
$Df_1 \leftarrow MTF_2 \leftarrow I_2 \leftarrow MTF_4 \leftarrow MSe_2$	1
$Df_2 \leftarrow MTF_4 \leftarrow I_4 \leftarrow MTF_4 \leftarrow MSe_2$	1
$Df_1 \leftarrow MTF_2 \leftarrow I_2 \leftarrow R_1 \leftarrow I_2$	2
$Df_1 \leftarrow MTF_2 \leftarrow I_2 \leftarrow MTF_4 \leftarrow MTF_3 \leftarrow I_3 \leftarrow MTF_3 \leftarrow MTF_4 \leftarrow I_4$	2
$Df_1 \leftarrow MTF_2 \leftarrow I_2 \leftarrow MTF_4 \leftarrow MTF_3 \leftarrow I_3 \leftarrow MTF_3 \leftarrow MTF_4 \leftarrow I_2$	2
$Df_1 \leftarrow MTF_2 \leftarrow I_2 \leftarrow MTF_2 \leftarrow MTF_1 \leftarrow I_1 \leftarrow MTF_1 \leftarrow MTF_2 \leftarrow I_2$	2
$Df_1 \leftarrow MTF_2 \leftarrow I_2 \leftarrow MTF_2 \leftarrow MTF_1 \leftarrow I_3 \leftarrow MTF_1 \leftarrow MTF_2 \leftarrow I_2$	2
$Df_1 \leftarrow MTF_2 \leftarrow I_2 \leftarrow MTF_2 \leftarrow MTF_1 \leftarrow I_3 \leftarrow MTF_3 \leftarrow MTF_4 \leftarrow I_2$	2
$Df_1 \leftarrow MTF_2 \leftarrow I_2 \leftarrow MTF_2 \leftarrow MTF_1 \leftarrow I_3 \leftarrow MTF_3 \leftarrow MTF_4 \leftarrow I_4$	2
$Df_2 \leftarrow MTF_4 \leftarrow I_4 \leftarrow R_2 \leftarrow I_4$	2
$Df_2 \leftarrow MTF_4 \leftarrow I_4 \leftarrow MTF_4 \leftarrow MTF_3 \leftarrow I_3 \leftarrow MTF_3 \leftarrow MTF_4 \leftarrow I_4$	2
$Df_2 \leftarrow MTF_4 \leftarrow I_4 \leftarrow MTF_4 \leftarrow MTF_3 \leftarrow I_3 \leftarrow MTF_3 \leftarrow MTF_4 \leftarrow I_2$	2
$Df_2 \leftarrow MTF_4 \leftarrow I_4 \leftarrow MTF_4 \leftarrow MTF_3 \leftarrow I_3 \leftarrow MTF_1 \leftarrow MTF_2 \leftarrow I_2$	2
$Df_2 \leftarrow MTF_4 \leftarrow I_2 \leftarrow R_1 \leftarrow I_2$	2
$Df_2 \leftarrow MTF_4 \leftarrow I_2 \leftarrow MTF_4 \leftarrow MTF_3 \leftarrow I_3 \leftarrow MTF_3 \leftarrow MTF_4 \leftarrow I_4$	2
$Df_2 \leftarrow MTF_4 \leftarrow I_2 \leftarrow MTF_4 \leftarrow MTF_3 \leftarrow I_3 \leftarrow MTF_3 \leftarrow MTF_4 \leftarrow I_2$	2
$Df_2 \leftarrow MTF_4 \leftarrow I_2 \leftarrow MTF_4 \leftarrow MTF_3 \leftarrow I_3 \leftarrow MTF_1 \leftarrow MTF_2 \leftarrow I_2$	2
$Df_2 \leftarrow MTF_4 \leftarrow I_2 \leftarrow MTF_2 \leftarrow MTF_1 \leftarrow I_1 \leftarrow MTF_1 \leftarrow MTF_2 \leftarrow I_2$	2
$Df_2 \leftarrow MTF_4 \leftarrow I_2 \leftarrow MTF_2 \leftarrow MTF_1 \leftarrow I_3 \leftarrow MTF_1 \leftarrow MTF_2 \leftarrow I_2$	2
$Df_2 \leftarrow MTF_4 \leftarrow I_2 \leftarrow MTF_2 \leftarrow MTF_1 \leftarrow I_1 \leftarrow MTF_3 \leftarrow MTF_4 \leftarrow I_2$	2
$Df_2 \leftarrow MTF_4 \leftarrow I_2 \leftarrow MTF_2 \leftarrow MTF_1 \leftarrow I_1 \leftarrow MTF_3 \leftarrow MTF_4 \leftarrow I_4$	2

4.5 Conclusions

In this chapter, we have presented a study of the concept of duality in control laws for linear time-varying models. We have used the duality between the state feedback and the output injection control laws. As an application for this duality, we have considered the decoupling problem. In table 4.11, we have gathered the graphical procedures which have been developed for the decoupling problem on the structured systems and bond graphs. The decoupling by state feedback problem for LTV systems was numerically solved in [46], but we have extended this approach to output injection using the

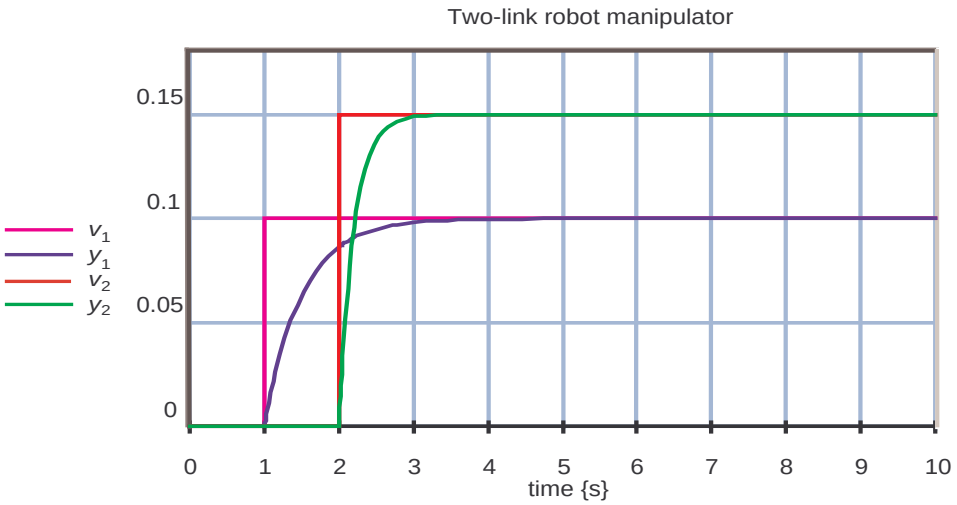

Figure 4.11: Time-response of the decoupled robot system

Table 4.11: Decoupling problem

	SS	Bond graph
Decoupling by SF of LTV systems	finished	finished
Decoupling by OI of LTV systems	finished	finished
Decoupling with pole placement by SF of LTV systems	simple law further developing	simple law further developing
Decoupling with pole placement by OI of LTV systems	simple law further developing	simple law further developing
Decoupling/Linearization by SF of nonlinear systems	finished	finished
Decoupling/Linearization by OI of nonlinear systems	finished	finished

duality between the two control laws. The decoupling with pole placement problem needs further investigations because we have used here the simplest law possible. Further study of the invariant zeros may be considered for a better control law. For nonlinear models, we have used the passage through the variational model in order to obtain a decoupling law. By using the pole placement procedure, we developed a nonlinear control law which linearizes the model.

The study of duality has been focused on three directions:

- Duality between infinite structure.
- Duality between state feedback and output injection.
- Duality between (A, B) and (C, A)-invariance.

Conclusions and Perspectives

In this report, we have proposed a study of the concept of duality in system analysis and control synthesis for linear time-varying models. Graphic procedures, using the structured systems representation and bond graph representation, have been proposed to illustrate the duality between controllability and observability, as well as the duality between state feedback and output injection.

Using the concept of duality defined in [50] with the module theoretical approach, this study defines for structured systems and bond graphs the concept of dual model, using a graphical perspective.

The duality between controllability and observability is well-known to the control community, especially for LTI case. Our approach for dealing with system analysis presents two stages. First, we focused on the computational methods which permit determining graphically the controllability and observability matrices. For this computational procedures, we had to develop some graphic representations which emulate the noncommutative aspects which characterize the LTV systems. The CSG and OSG for structured systems and the CBG and OGB for bond graphs are graphical tools which allow to extend the LTI methods for LTV systems. The second stage concerns graphical procedures for determining the controllability and observability directly on the structured systems and bond graphs. For determining the observability property for LTV bond graph models, the only solution so far is to pass through the dual bond graph and to evaluate the controllability of the dual model.

For the study of the duality between the state feedback and output injection, we have considered a classic problem, the decoupling problem. The decoupling by state feedback is a known problem, but the use of output injection to solve this problem is new, because given the definition of output injection,

its application on physical systems is impossible since we can not directly interfere on the state dynamics of the system. We have proposed graphic methods for both decoupling by state feedback and output injection of LTV models. The extension for the decoupling problem with pole placement came out naturally by extending some LTI methods.

The control synthesis for the decoupling problem has been taken one step further when we tackled the problem for nonlinear systems. The use of the variational model is essential in this case. On one hand for structured systems, nonlinear methods are not so widely spread ([48]). On the other hand, the use of the variational model, which is a LTV system, can be the solution for a graphical procedure for nonlinear systems decoupling.

This study is a development which can be extended into different directions. The duality in bond graph model has been based on some physical notions, the duality between the energy and the co-energy variables. These physical aspects may represent a possible link between the physical representation (Hamiltonian) and mathematical descriptions (state space representation, modules).

Certain aspects which define a dual bond graph model characterize also the adjoint bond graph model which has been developed for synthesis of optimal control. Even though the optimal control procedures for bond graph models concern only LTI models, a possible extension for LTV models can be considered if we develop similar procedure to the dualization procedure introduced in chapter 3.

For system decoupling, we have used the simplest laws, more research are to be made for the study of invariant zeros and the possibility of assigning these modes. The duality between (A, B) and (C, A) invariance needs further developing. We can even consider the duality between the (f, g) and (h, f) invariance for nonlinear systems. This extension for the geometric approach may provide some better decoupling laws, both for linear and nonlinear models.

Another research direction which can be developed using the concept of duality is in surveillance. The duality between captors and actuators may offer some interesting solutions for some supervision problems.

Using the output injection we can consider the synthesis of an observer using graphic procedures. In fact, this theoretical study of the duality in control

laws is just the beginning of an approach which might develop interesting results concerning the observation problems. The state feedback and output injection results can be mixed for obtaining an output feedback solution.

Bibliography

[1] A. Achir, C. Andaloussi, and C. Sueur. Flatness based control of linear time-varying bond graphs. *Proceedings of IFAC World Congress, Prague*, 2005.

[2] A. Achir and C. Sueur. Non commutative ring bond graphs application to flatness. *ICBGM*, 37:59–64, 2005.

[3] C. Andaloussi, Z. Chalh, and C. Sueur. Infinite zero of linear time-varying bond graph models: graphical rules. *Proceedings of the 2006 IEEE ICCA, Munich*, pages 2962–2967, 2006.

[4] G. Basile and G. Marro. *Controlled invariants and conditioned invariants in linear system theory.* Pretince Hall, New Jersey, 1992.

[5] J. M. Bertrand, C. Sueur, and G. Dauphin-Tanguy. Bond graph for modeling and control: structural analysis tools for the design of input-output decoupling state feedbacks. *Proceedings of International Conference on Bond Graph Modeling and Simulation, Phoenix*, pages 103–108, 1997.

[6] S. H. Birkett and P. H. Roe. The mathematical foundations of bond graphs - ii. duality. *Journal of Franklin Institute*, 326:691–708, 1989.

[7] H. Bourles and B. Marinescu. Poles and zeros at infinity of linear time-varying systems. *IEEE Transactions on Automatic Control*, 44:1981–1985, 1999.

[8] P. Brunovsky. A classification for linear controllable systems. *Kybernetika*, 6:173–187, 1970.

[9] Z. Chalh, C. Andaloussi, and C. Sueur. Structural properties of bond graph rings. *ICBGM*, 38:20–26, 2007.

[10] P. M. Cohn. *Free Rings and their Relations*. Academic Press, London, 2^{nd} edition edition, 1985.

[11] C. Commault and J. M. Dion. A comprehensive introduction to the geometric theory of linear multivariable systems. *IEEE Transactions on Education*, 35:92–97, 1992.

[12] G. Dauphin-Tanguy. *Les Bond Graphs*. Hermes Science, Paris, 2000.

[13] E. J. Davison and S. H. Wang. Properties of linear time-invariant multivariable systems subject to arbitrary output and state feedback. *IEEE Transactions on Automatic Control*, 18:24–32, 1973.

[14] E. Delaleau and M. Fliess. Algorithme de structure, filtrations et découplage. *C. R. Acad. Sci. Paris Sér. I*, 315:101–106, 1992.

[15] J. Descusse and J. M. Dion. On the structure at infinity of linear square decoupled systems. *IEEE Transactions on Automatic Control*, 27:971–974, 1982.

[16] J. M. Dion and C. Commault. Smith-mcmillan factorizations at infinity of rational matrix functions and their control interpretation. *System & Control Letters*, 1:312–320, 1982.

[17] J. M. Dion and C. Commault. Feedback decoupling of structured systems. *IEEE Transactions on Automatic Control*, 38:1132–1135, 1993.

[18] J. M. Dion, C. Commault, and J. W. van der Woude. Generic properties of linear structured systems: a survey. *Automatica*, 39:1125–1144, 2003.

[19] P. L. Falb and W. A. Wolovich. On the decoupling of multivariable systems. *Preprints JACC, Philadelphia*, pages 791–796, 1967.

[20] M. Fliess. Some basic structural properties of generalized linear systems. *Systems & Control Letters*, 15:391–396, 1990.

[21] E. Freund. The structure of decoupled nonlinear systems. *Int. Journal Control*, 21:443–450, 1975.

[22] P. A. Fuhrmann. Duality in polynomial models with some applications to geometric control theory. *IEEE Transactions on Automatic Control*, 26:284–295, 1981.

[23] G. Gawthrop. Control system configuration: inversion and bicausal bond graphs. *Proceedings of International Conference on Bond Graph Modeling and Simulation, Phoenix*, pages 97–102, 1997.

[24] E. G. Gilbert. The decoupling of multivariable systems by state feedback. *SIAM Journal of Control and Optimization*, 7:50–63, 1969.

[25] K. Glover and L. M. Silverman. Characterization of structural controllability. *IEEE Transactions on Automatic Control*, 21:931–939, 1976.

[26] M. L. J. Hautus. *The formal Laplace transform for smooth linear systems.* Lecture notes in Economics and Mathemathical systems 131, Springer-Verlag, 1975.

[27] A. Ilchmann. Time-varying control systems: a geometric approach. *IMA Journal of mathematical Control and Information*, 6:411–440, 1989.

[28] A. Isidori, A. J. Krener, C. Gori-Giorgi, and S. Monaco. Nonlinear decoupling viafeedback: a differential geometric approach. *IEEE Transactions on Automatic Control*, 26:331–345, 1981.

[29] T. Kailath. *Linear Systems.* Prentince Hall, Englewood-Cliff, N.J., 1980.

[30] R. E. Kalman, P. L. Falb, and M. A. Arbib. *Topics in Mathematical System Theory.* McGraw-Hill, New York, 1969.

[31] D. Karnopp, D. Margolis, and R. Rosenberg. *System dynamics: a unified approach.* John Wiley & Sons, 1975.

[32] A. Kasinski and J. Levine. *A fast graph theoretic algorithm for the feedback decoupling problem of nonlinear systems. in Mathematical theory of networks and systems, Lecture notes in control and information sciences*, pages 550–562. Elsevier Science Publisher B. V., 1984.

[33] E. R. Kolchin. *Differential algebra and algebraic groups.* Academic press, New York, 1973.

[34] T. Y. Lam. *A first course in Noncommutative Rings*. Springer, New York, 2001.

[35] S. Lichiardopol and C. Sueur. Decoupling of linear time-varying systems with a bond graph approach. *ECMS 2006, Bonn, Germany*, 2006.

[36] S. Lichiardopol and C. Sueur. Decoupling of non linear bond graph models. *Joint CCA, ISIC and CACSD 2006, Munich, Germany*, 2006.

[37] S. Lichiardopol and C. Sueur. Duality of linear systems: a bond graph perspective. *Mathmod 2006, Vienna, Austria*, 2006.

[38] S. Lichiardopol and C. Sueur. Decoupling and input-output linearization of nonlinear bond graph models by output injection. *EEC 2007, Kos, Greece*, 2007.

[39] S. Lichiardopol and C. Sueur. Input-output linearization and decoupling of nonlinear bond graph models. *ICBGM 2007, San Diego, California, USA*, 2007.

[40] S. Lichiardopol and C. Sueur. Linear time-varying structured systems: Part i. graphical representation and analysis. *IFAC SSSC 2007, Iguacu Falls, Brasil*, 2007.

[41] S. Lichiardopol and C. Sueur. Linear time-varying structured systems: Part ii. control synthesis. *IFAC SSSC 2007, Iguacu Falls, Brasil*, 2007.

[42] S. Lichiardopol and C. Sueur. Pole placement and decoupling of lti systems by output injection. a bond graph approach. *IMAACA 2007, Buenos Aires, Argentina*, 2007.

[43] C. T. Lin. Structural controllability. *IEEE Transactions on Automatic Control*, 19:201–208, 1974.

[44] S. A. Morse. Structural invariants of linear multivariable systems. *SIAM J. Control*, 11:446–465, 1973.

[45] H. M. Paynter. *Analysis design of engineering systems*. MIT Press, Cambridge, Massachusetts, 1960.

[46] W. Porter. Decoupling of and inverses for time-varying linear systems. *IEEE Transactions on Automatic Control*, 14:378–380, 1969.

[47] K. J. Reinschke. Graph-theoretic characterisation of structural properties by means of paths and cycle families. *Proceedings of IFAC World Congress, Budapest*, 1984.

[48] K. J. Reinschke. *Multivariable control, a graph-theoretic approach.* Springer, Berlin, 1988.

[49] J. F. Ritt. *Differential Algebra.* American Mathematical Society, New York, 1950.

[50] J. Rudolph. Duality in time-varying linear systems: A module theoretic approach. *Linear Algebra and its Applications*, 245:83–106, 1996.

[51] R. W. Shields and J. B. Pearson. Structural controllability of multi-input linear systems. *IEEE Transactions on Automatic Control*, 21, 1976.

[52] L. M. Silverman and H. E. Meadows. Controllability and observability intime-variable linear systems. *SIAM Journal of Control*, 5:64–73, 1967.

[53] S. N. Singh and W. J. Rugh. Decoupling in a class of nonlinear systems by state variable feedback. *Journal of Dynamic Systems*, pages 323–329, 1972.

[54] P. Sinha. State feedback decoupling of nonlinear systems. *IEEE Transactions on Automatic Control*, 22, 1977.

[55] N. Suda, B. Wan, and I. Ueno. The orders of infinite zeros of structured systems. *Transactions of the Society of Instrumental Control Engineers*, 25, 1989.

[56] C. Sueur and G. Dauphin-Tanguy. Bond-graph approach for structural analysis of mimo linear systems. *Journal of the Franklin Institute*, 328:55–70, 1991.

[57] C. Sueur and G. Dauphin-Tanguy. *Poles and zeros of multivariable linear systems: a bond graph approach. in: Bond Graph for Engineers(P.C. Breedveld and G. Dauphin-Tanguy)*, pages 211–228. Elsevier Science Publisher B. V., 1992.

[58] A. J. van der Schaft. *Duality for linear systems: External and state space characterization of the adjoint system. in Analysis of Controlled Dynamical Systems (B. Bonnard, B. Bride, J.P. Gauthier and I. Kupka)*, pages 393–403. Birkhäuser, Boston, 1991.

[59] J. W. van der Woude. On the structure at inifnity of a structured system. *Linear Algebra and its Applications*, 148:145–169, 1991.

[60] J. van Dijk. *On the role of bond-graph causality in modelling mechatronic systems*. PhD thesis, University of Twente, 1994.

[61] W. M. Wonham and A. Morse. Decoupling and pole assignement in linear multivariable systems: a geometric approach. *SIAM Journal of Control and Optimization*, 8:1–18, 1970.

[62] X. Xia and S. Scavarda. Adjoint system by using the representation of bond graph. *ICBGM*, 35:15–20, 2001.

Appendix A

Appendix

A.1 Some Matrix Definitions

In this appendix, we introduce some definitions which simplify the writing of the modifications which are performed on the dual bond graph. For that, let us consider that on the bond graph model there are n dynamic elements in integral causality, from which q have time-dependent gains, n_R dissipative elements, m input sources and p output detectors.

Definition 35. *We denote by $I_{n\times q}$ the sparse matrix with n rows and q columns, where $I_{n\times q}[i,j] = 1$, if the i^{th} dynamic element in integral causality (DE_i) is time-dependent ($i = 1,\ldots,n$) and the $(n_R + j)^{th}$ dissipative element is the supplementary dissipative element which is added by the dualization procedure for the i^{th} dynamic element which is time-dependent and $I_{n\times q}[i,j] = 0$, otherwise.*

Definition 36. *We denote by $I_{q\times n} = I_{n\times q}^T$.*

Definition 37. *Let $L_d \in \mathbb{R}(t)^{q\times q}$ be a diagonal matrix:*

$$L_d = diag(\frac{dDE_i(t)}{dt}) \tag{A.1}$$

where DE_i is the gain of the i^{th} time-varying dynamic element, $i = 1,\ldots,q$, either $I_i(t)$ or $C_i(t)$.

L_d is a square matrix which contains on the diagonal the gains of the supplementary dissipative elements which have been added by the dualization procedure.

Property 37. $I_{n\times q}L_dI_{q\times n} = \frac{d}{dt}(F^{-1})$

Proof:

Let us first determine the product $I_d = I_{n\times q}L_d$.

$$I_d(i,j) = \sum_{k=1}^{q} I_{n\times q}(i,k)L_d(k,j) \tag{A.2}$$

But L_d is a diagonal matrix, therefore:

$$I_d(i,j) = I_{n\times q}(i,j)L_d(j,j) \tag{A.3}$$

and as the $I_{n\times q}$ is a sparse matrix with unitary values, then $I_d(i,j) = L_d(j,j)$, if $I_{n\times q}(i,j) = 1$, otherwise $I_d(i,j) = 0$.

The product $I_dI_{q\times n}$ is easy to evaluate, because in matrix I_d we have nonzero elements in positions (i,j), which are the same with the positions of nonzero elements from matrix $I_{n\times q}$ and $I_{q\times n}$ is the transpose of matrix $I_{n\times q}$, with nonzero elements in positions (j,i). Therefore the product will present nonzero element only on the diagonal. Moreover, the nonzero elements appear on the rows which correspond to the time-varying elements, according to the definition of matrix $I_{n\times q}$. In conclusion, the product $I_{n\times q}L_dI_{q\times n} = diag(\frac{dDE_i(t)}{dt})$, if the i^{th} dynamic element has a time-varying gain and 0, otherwise. But, knowing that the derivative of a constant is 0, we can extrapolate the writing and simply say that:

$$I_{n\times q}L_dI_{q\times n} = diag(\frac{dDE_i(t)}{dt}) \tag{A.4}$$

On the other hand, $F = diag(\frac{1}{DE_i})$ and its inverse is $F^{-1} = diag(DE_i)$. Therefore

$$\frac{d}{dt}(F^{-1}) = diag(\frac{dDE_i(t)}{dt}) \tag{A.5}$$

From equation (A.4) and (A.5), we obtain that $I_{n\times q}L_dI_{q\times n} = \frac{d}{dt}(F^{-1})$.

A.2 Dualization effects upon the vectorial representation

In this appendix, we present the transformations which are inflicted on the vectorial representation of a bond graph model after the dualization procedure presented in section 3.1.2 is performed.

Remark 22. *In this appendix, we use the same notations which have been proposed in appendix A.1.*

The following modifications occur on the vectorial representation of the dual system bond graph:

- $\bar{S}_{11} = S_{11}$, because the positions of the I and C elements remain unchanged.
- $\bar{S}_{13} = \begin{pmatrix} S_{13} & I_{n\times q} \end{pmatrix}$, because the positions of the dynamic elements and the R elements remain unchanged and the dynamic element with time-varying gains are causally linked with their supplementary dissipative elements by a causal path with the gain 1.
- $\bar{S}_{31} = \begin{pmatrix} S_{31} \\ -I_{q\times n} \end{pmatrix}$, because the positions of the dynamic elements and the R elements remain unchanged and the supplementary dissipative elements are causally linked only with the dynamic element which has generated their presence by a causal path with the gain -1.
- $\bar{S}_{33} = \begin{pmatrix} S_{33} & 0_{n_R\times q} \\ 0_{q\times n_R} & 0_{q\times q} \end{pmatrix}$, because the positions of the R elements remain unchanged and therefore the causal path between them is the same and the supplementary dissipative elements are not linked with any other element beside the time-varying dynamic element which generated them.
- $\bar{S}_{14} = S_{41}^T$, because the inputs and the outputs change places and therefore the causal path that was between the dynamic elements and the outputs is now the causal path between the dynamic elements and the inputs.

- $\bar{S}_{34} = \begin{pmatrix} S_{43}^T \\ 0_{q\times p} \end{pmatrix}$, because the inputs and the outputs change places and therefore the causal path that was between the R elements and the outputs is now the causal path between the R elements and the inputs and the supplementary dissipative elements are not linked with any input sources.

- $\bar{S}_{41} = S_{14}^T$, because the inputs and the outputs change places and therefore the causal path that was between the dynamic elements and the inputs is now the causal path between the dynamic elements and the outputs and the output are reversed.

- $\bar{S}_{43} = \begin{pmatrix} S_{34}^T & I_{m\times q} \end{pmatrix}$, because the inputs and the outputs change places and therefore the causal path that was between the R elements and the inputs is now the causal path between the R elements and the reversed outputs and the supplementary dissipative elements are not linked with any output detectors.

- $\bar{S}_{44} = -S_{44}^T$, because the inputs and the outputs change places and therefore the causal path is the same, the only thing that changes is that the path has different starting and ending points and the output in reversed.

- $\bar{L} = \begin{pmatrix} -L & 0_{n_R\times q} \\ 0_{q\times n_R} & -L_d \end{pmatrix}$, because the value of the R elements is opposite from the one they previously had and we have added the q supplementary dissipative elements.

- $\bar{F} = F$, because the value and the causality of the C and I elements remain unchanged.